ISSN 2413-9432

BIOMEDICAL PHOTONICS

Volume 14, # 4, 2025

In the issue:

BMP

Российская Фотодинамическая Ассоциация

www.pdt-association.com

BIOMEDICAL PHOTONICS

BIOMEDICAL PHOTONICS –
research and practice, peer-reviewed, multidisciplinary journal.
The journal is issued 4 times per year.
The circulation – 1000 copies., on a quarterly basis.

The journal is included into the List of peer-reviewed science press of the State Commission for Academic Degrees and Titles of Russian Federation
The journal is indexed in the international abstract and citation database – Scopus.

The publisher «Agentstvo MORE».
Moscow, Khokhlovskiy lane, 9

Editorial staff:

Chief of the editorial staff	Ivanova-Radkevich V.I.
Science editor professor	Mamontov A.S.
Literary editor	Moiseeva R.N.
Translators	Kalyagina N.A.
Computer design	Kreneva E.I.
Desktop publishing	Shalimova N.M.

The Address of Editorial Office:
Russia, Moscow, 2nd Botkinskiy proezd, 3
Tel. 8 (495) 945–86–60
www: PDT-journal.com
E-mail: PDT-journal@mail.ru

Corresponding to:
125284, Moscow, p/o box 13

Registration certificate ПИ № ФС 77–51995, issued on 29.11.2012 by the Federal Service for Supervision of Communications, Information Technology, and Mass Media of Russia

The subscription index of «Rospechat» agency – 70249

BIOMEDICAL PHOTONICS

BIOMEDICAL PHOTONICS –
научно-практический, рецензируемый,
мультидисциплинарный журнал.
Выходит 4 раза в год.
Тираж – 1000 экз., ежеквартально.

Входит в Перечень ведущих рецензируемых научных журналов ВАК РФ.
Индексируется в международной реферативной базе данных Scopus.

Издательство «Агентство МОРЕ».
Москва, Хохловский пер., д. 9

Редакция:

Зав. редакцией	Иванова-Радкевич В.И.
Научный редактор	проф. Мамонтов А.С.
Литературный редактор	Моисеева Р.Н.
Переводчики	Калягина Н.А.
Компьютерный дизайн	Кренева Е.И.
Компьютерная верстка	Шалимова Н.М.

Адрес редакции:
Россия, Москва, 2-й Боткинский пр., д. 3
Тел. 8 (495) 945–86–60
www: PDT-journal.com
E-mail: PDT-journal@mail.ru

Адрес для корреспонденции:
125284, Москва, а/я 13

Свидетельство о регистрации ПИ
№ ФС 77–51995, выдано 29.11.2012 г.
Федеральной службой по надзору в сфере связи, информационных технологий и массовых коммуникаций (Роскомнадзор)

Индекс по каталогу агентства «Роспечать» – 70249

ORIGINAL ARTICLES

CASE REPORTS

ОРИГИНАЛЬНЫЕ СТАТЬИ

КЛИНИЧЕСКИЕ НАБЛЮДЕНИЯ

ORIGINAL ARTICLES

INVESTIGATIO OF THE pH-DEPENDENT HYDROLYSIS OF A CHLORIN e6 HYDRAZIDE DERIVATIVES AS A POTENTIAL PHOTOSENSITIZER FOR COMBINED ANTICANCER THERAPY

Medvedev D.Y., Grin M.A.
Institute of Fine Chemical Technologies, MIREA – Russian Technological University, Moscow, Russia

Abstract

Oncological diseases represent a global healthcare challenge, and the development of new effective therapeutic strategies remains a pressing task. Chemotherapy and photodynamic therapy (PDT) are key treatment modalities, however, their application is associated with side effects, systemic toxicity, and the development of drug resistance. In recent years, combined approaches, including the use of pH-sensitive delivery systems, have been actively investigated. The present study was dedicated to the investigation of the pH-dependent hydrolysis of a chlorin e6 hydrazide derivative, acting as a potential photosensitizer (PS) for combined anticancer therapy. Hydrazide fragments, due to their lability in the weakly acidic environment of the tumor microenvironment (pH 4.5-6.0), are promising for the creation of targeted drug delivery systems. The decomposition of the hydrazide fragment was studied spectrophotometrically in an acetate buffer (pH 5.0) over 120 minutes. Spectral changes (bathochromic shift, appearance of a maximum at 688 nm) were recorded, indicating the formation of a protonated precursor compound. A linear dependence of product accumulation on time was obtained, characteristic of zero-order reactions. A high coefficient of determination confirmed the adequacy of the obtained model. This approach ensures controlled release of active components and demonstrates the potential of the developed PS for enhancing PDT efficacy and reducing the systemic toxicity of chemotherapy.

Key words: chlorin e6, photodynamic therapy, hydrazide, hydrolysis.

Contacts: Medvedev D.Y., e-mail: dy.medvedev@mail.ru

For citations: Medvedev D.Y., Grin M.A. Investigation of the pH-dependent hydrolysis of a chlorin e6 hydrazide derivative as a potential photosensitizer for combined anticancer therapy, *Biomedical Photonics*, 2025, vol. 14, no. 4, pp. 4–10. doi:10.24931/2413–9432–2025–14-4-4-10

ИССЛЕДОВАНИЕ pH-ЗАВИСИМОГО ГИДРОЛИЗА ГИДРАЗИДНОГО ПРОИЗВОДНОГО ХЛОРИНА e6 КАК ПОТЕНЦИАЛЬНОГО ФОТОСЕНСИБИЛИЗАТОРА ДЛЯ КОМБИНИРОВАННОЙ ПРОТИВООПУХОЛЕВОЙ ТЕРАПИИ

Д.Ю. Медведев, М.А. Грин
Институт тонких химических технологий, РТУ МИРЭА, Москва, Россия

Резюме

Онкологические заболевания представляют собой глобальную проблему здравоохранения, и разработка новых эффективных терапевтических стратегий является актуальной задачей. Химиотерапия и фотодинамическая терапия (ФДТ) являются ключевыми методами лечения, однако их применение сопряжено с побочными эффектами, системной токсичностью и развитием лекарственной устойчивости. В последние годы активно исследуются комбинированные подходы, в том числе с использованием pH-чувствительных систем доставки. Настоящее исследование было посвящено изучению гидролиза гидразидного производного хлорина e6, выступающего в качестве потенциального фотосенсибилизатора (ФС) для комбинированной противоопухолевой терапии. Гидразидные фрагменты, благодаря своей лабильности в слабокислой среде опухолевого микроокружения (pH 4,5-6,0), являются перспективными для создания систем адресной доставки лекарств. Изучение разложения гидразидного фрагмента осуществлялось спектрофотометрически в ацетатном буфере (pH 5,0) в течение 120 мин. Были зафиксированы спектральные изменения (батохромный сдвиг, появление максимума при 688 нм), указывающие на образование протонированного соединения-предшественника. Была продемонстрирована

линейная зависимость накопления продукта от времени, характерная для реакций нулевого порядка. Высокий коэффициент детерминации подтвердил адекватность полученной модели. Данный подход обеспечивает контролируемое высвобождение активных компонентов и демонстрирует потенциал разработанного ФС для повышения эффективности ФДТ и снижения системной токсичности химиотерапии.

Ключевые слова: хлорин е6, фотодинамическая терапия, гидразид, гидролиз.

Контакты: Медведев Д.Ю., e-mail: dy.medvedev@mail.ru

Для цитирования: Медведев Д.Ю., Грин М.А. Исследование pH-зависимого гидролиза гидразидного производного хлорина е6 как потенциального фотосенсибилизатора для комбинированной противоопухолевой терапии // Biomedical Photonics. – 2025. – Т. 14, № 4. – С. 4–10. doi:10.24931/2413–9432–2025–14-4-4-10

Introduction

Oncological diseases are a global health problem, being the second leading cause of death in the world after cardiovascular diseases. According to forecasts, the number of new cases of malignant neoplasms, which reached 20 million in 2022, will increase by 77% to 35 million by 2050 [1]. The etiological profile of oncological diseases is characterized by the complex influence of various behavioral factors, including tobacco smoking, alcohol abuse and obesity, along with the exogenous effects of environmental factors such as atmospheric air pollution [2]. These trends highlight the urgent need for further research in the field of oncology and the development of new treatment strategies.

Among the existing therapeutic methods, chemotherapy and photodynamic therapy (PDT) are of particular interest [3]. Chemotherapy based on the use of cytotoxic drugs is aimed at suppressing the proliferation of tumor cells by disrupting their metabolism or damaging genetic material [4, 5]. Despite the wide range of effects, chemotherapy is associated with a number of serious side effects due to non-selective effects on healthy cells of the body. In addition, the development of drug resistance is one of the main reasons for the ineffectiveness of chemotherapy, requiring a constant search for new drugs and strategies for their use.

One of the most common classes of chemotherapeutic drugs are platinum compounds such as cisplatin, carboplatin, and oxaliplatin, which interact with the DNA of tumor cells and cause their death [6]. These preparations contain platinum in the oxidation state of +2 (Pt(II)) and have a square-planar geometry. Cisplatin, which is the first representative of this class, forms adducts with DNA, disrupting the processes of replication and transcription [7, 8]. Carboplatin, which has less pronounced nephrotoxicity, also interacts with DNA, forming adducts, but its use is limited by myelosuppression [9]. Oxaliplatin containing a diaminocyclohexane ligand has a wide range of activity, but it can cause neurotoxicity [10]. Despite their high efficacy, the use of platinum drugs is associated with problems of resistance and toxicity, which stimulates the development of new approaches, such as the use of Pt(IV) prodrugs and targeting the tumor microenvironment [11, 12].

In recent years, platinum pyridine complexes, which have unique properties and the potential to overcome the limitations of traditional platinum preparations, have been actively investigated [13]. Pyridine ligands coordinating with platinum can affect its reactivity and selectivity [14, 15]. In addition, pyridine complexes can be modified with various substituents to regulate their lipophilicity, charge, and ability to penetrate cell membranes. The use of pyridine complexes as antitumor agents requires further study, but their potential for the development of new effective and selective drugs is beyond doubt.

PDT is a promising method for the treatment of oncological diseases based on the use of photosensitizers (PS) activated by light of a certain wavelength to generate cytotoxic reactive oxygen species (ROS) [16-18]. ROS such as singlet oxygen cause oxidative damage to cellular components, leading to the death of tumor cells. PDT has a number of advantages over traditional treatment methods, including high selectivity of effects on tumor tissues, minimal systemic toxicity, and the possibility of repeated use [19, 20]. However, the main disadvantage of PDT is the insufficient depth of light penetration into tissues, which limits its use for the treatment of deeply localized tumors.

The combined use of chemotherapy and PDT is a promising strategy that allows combining the advantages of each method and overcoming their disadvantages [21, 22]. The synergistic interaction of chemotherapeutic drugs and PDT can lead to an increase in the effectiveness of treatment, reduce toxicity and overcome drug resistance. In particular, the combination of platinum drugs and PDT can increase the selectivity of effects on tumor cells and reduce systemic toxicity due to local activation of PS and the release of the platinum drug in the tumor microenvironment.

One of the promising approaches to increasing the selectivity and effectiveness of chemotherapy and PDT is the use of pH-sensitive delivery systems that ensure the release of drugs in the acidic environment of the tumor microenvironment [23-25]. Tumor cells are characterized by an increased level of glycolysis and lactic acid formation, which leads to a decrease in the pH of the extracellular space of the tumor [26, 27]. The use of pH-sensitive linkers that are cleaved in an acidic environment makes it possible to create conjugates of chemotherapeutic drugs and PS, which release active components only in the tumor microenvironment, minimizing their effect on healthy tissues.

Previously, our scientific group successfully obtained platinum complexes with derivatives of natural chlorines, which have a high chelating ability and promising photophysical properties [28]. Developing the previously obtained results, in this work we focused on the study of the stability of the hydrazide derivative of e6 chlorin in a slightly acidic environment simulating the tumor microenvironment.

Materials and methods

Reagents and equipment

All solvents have been cleaned and prepared according to standard procedures.

ALUGRAM Xtra SIL G/UV254 plates coated with silica gel 60 (0.2 mm) (Germany) were used for analytical chromatography. Preparative chromatography was performed both by the column method on Silica gel 60 (0.0040-0.0063 mm) silica gel (Germany) and using chromatographic plates on a glass substrate measuring 20×20 cm with the same silica gel.

Absorption spectra were recorded on a Shimadzu UV1800 UV/VIS spectrophotometer (Japan) in quartz cuvettes (0.4×1.0 cm) with an optical path length of 1 cm (spectral slit width of 1 nm).

NMR spectra were recorded on a Bruker DPX300 spectrometer (USA) in $CDCl_3$. The residual signals of the ^1H cores were used to calibrate the scale. The experiments were performed using standard Bruker techniques.

Photosensitizer

The synthesis of PS with the structural formula **1** (Fig. 1) was carried out according to the procedure described earlier [28]. Chlorin e6 was obtained from the biomass of blue-green algae *Arthrospira Platensis* by a well-known method [29] and exhaustively modified with methyl esters diazomethane in the acetone/diethyl ether system to obtain the corresponding trimethyl ether. The vinyl group of trimethyl ether of chlorin e6 in the third position of the macrocycle was further oxidized to the formyl function using the Lemieux-Johnson reaction to obtain PS with the structural formula 2. The final step was the introduction of the isoniazid residue through the Schiff base. The product was purified by column chromatography (CH_2Cl_2:CH_3OH, 15:1) and is crystallized from hexane. The yield of compound **1** was 92.2%.

^1H NMR (300 MHz, $CDCl_3$, δ, ppm): 9.71 (s, 1H, 5-H), 9.58 (s, 1H, 10-H), 9.47 (s, 1H, 20-H), 8.94 (s, 1H, 33-NH), 8.80 (s, 2H, 3^6-CH, 3^8-CH), 8.56 (s, 1H, 3^1-CH), 7.75 (d, J = 25.1 Hz, 2H, 3^5-CH, 3^9-CH), 5.34 (dd, J = 36.7 Hz, 19.2 Hz, 2H, 15^1-CH_2), 4.42 (d, J = 9.0 Hz, 2H, 17-H, 18-H), 4.28 (s, 3H, 13^2-$COOCH_3$), 3.83 (s, 3H, 15^2-$COOCH_3$), 3.66 (s, 3H, 17^3-$COOCH_3$), 3.54 (s, 3H, 12^1-CH_3), 3.50 (s, 3H, 7^1-CH_3), 3.14 (d, J = 9.5 Hz, 3H, 2^1-CH_3), 2.70 – 2.11 (m, 6H, 8^1-CH_2, 17^1-CH_2, 17^2-CH_2), 1.74 (s, 3H, 18^1-CH_3), -1.68 (s, 2H, 21-NH, 23-NH).

Mass spectrum (ESI) m/z: $[M+H]^+$ calculated for $[C_{42}H_{44}N_7O_7+H]^+$ – 759.3, found – 760.5.

Acid hydrolysis of compound

The decomposition of the hydrazide fragment was studied spectrophotometrically. Compound **1** at a concentration of 1 mg/mL was incubated in a DMF/acetate buffer system (4:1) at pH 5.0 for 2 h. During the incubation, aliquots were collected at 5-min intervals and diluted to a concentration of 7.5 μmol/L, optimal for subsequent spectrophotometric analysis [30]. Optical density measurements were performed at a wavelength of 688 nm, corresponding to the absorption maximum of the protonated form of precursor compound 2, containing a formyl function at the third position of the macrocycle.

Results and Discussion

Modification of the chlorin macrocycle at position 3 of the tetrapyrrole ring represents a promising approach for improving the physicochemical properties and biological activity of compounds. The advantages of this modification include the ability to introduce various functional groups at the free carboxyl groups at positions 13, 15, and 17. In particular, the introduction of substituents at position 3 allows for effective variation of the hydrophobic/hydrophilic balance of the molecule, which is critical for its distribution in biological systems.

Studies of hydrazide degradation are of significant interest in the context of anticancer drug development, primarily due to their lability in the slightly acidic environment characteristic of the microenvironment of many malignant tumors. Accelerated metabolism in rapidly proliferating tumor cells leads to the accumulation of metabolites such as lactic acid, which lowers the pH of the extracellular space and inside tumor cells to values in the range of 4.5-7.0. Unlike the physiologically neutral environment (pH ~7.4) of healthy tissue, this slightly acidic environment

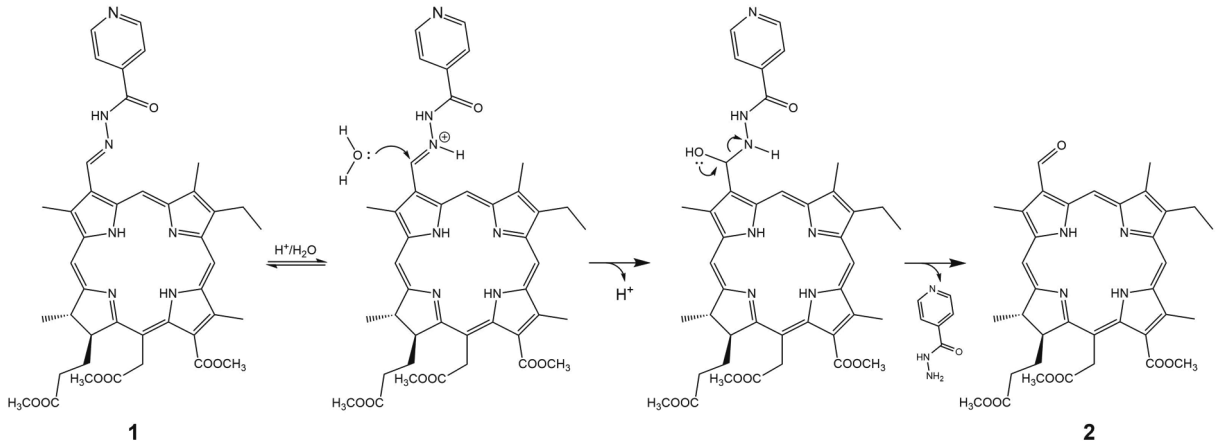

Рис. 1. Предполагаемый механизм кислотного гидролиза гидразидного фрагмента.
Fig. 1. Proposed mechanism of acid hydrolysis of the hydrazide fragment.

promotes rapid hydrolysis of the hydrazide bond. This property makes hydrazides promising for the development of targeted drug delivery systems. Conjugates containing hydrazide moieties can remain stable in the bloodstream but release a therapeutically active substance (e.g., a cytostatic agent or a PS) upon reaching tumor tissue. This mechanism increases the therapeutic efficacy of the drug by targeting it directly to the tumor and reduces systemic toxicity, minimizing side effects on healthy tissue. Studying the conditions of hydrazide hydrolysis, as well as their stability in various pH environments, is key to optimizing the design of new antitumor agents and delivery systems.

The change in spectral characteristics during incubation at pH 5.0 demonstrates chemical transformations of the hydrazide derivative of chlorin e6 (Fig. 1). The initial spectrum of compound **1** (0 min) is characterized by intense absorption bands at 410-450 nm (Soret) and 500-700 nm (Q-bands), typical of chlorin compounds. After 60 minutes of incubation, significant formation of the reaction product was detected: a noticeable bathochromic shift of the absorption bands and the formation of a distinct peak at 688 nm were observed. After 120 minutes of incubation, a further bathochromic shift of these bands is observed, with the emergence of a pronounced absorption maximum at 688 nm. This change in the absorption spectrum indicates the formation of the parent compound in a protonated form containing a formyl function at the third position of the macrocycle, consistent with the mechanism of hydrazide bond hydrolysis.

The decomposition of the hydrazide moiety and the accumulation of the formyl derivative absorbing at 688 nm were studied by analyzing the linear regression dependence of absorbance on time (Fig. 2). The resulting equation, the main parameters of which are presented in Table, demonstrates a high coefficient of

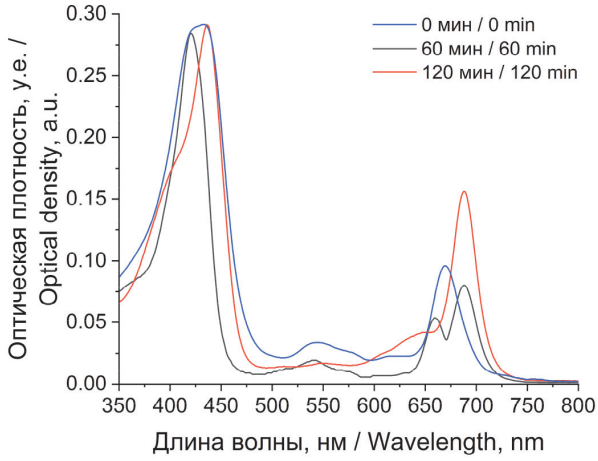

Рис. 2. Спектры поглощения раствора соединения **1** в ацетатном буфере (pH 5,0) при различных временных интервалах инкубации.
Fig. 2. Absorption spectra of compound **1** solution in acetate buffer (pH 5,0) at different incubation time intervals.

Таблица
Параметры линейной регрессии накопления продукта гидролиза во времени

Table
Parameters of linear regression for product accumulation during hydrolysis over time

Уравнение Equation	y = a + b·x
Коэффициент b Coefficient b	0,05 ± 5,32·10^{-4}
Коэффициент a Coefficient a	9,20·10^{-4} ± 7,59·10^{-4}
Остаточная сумма квадратов Residual sum of squares	1,12441
Коэффициент детерминации (R^2) Coefficient of determination (R^2)	0,99844

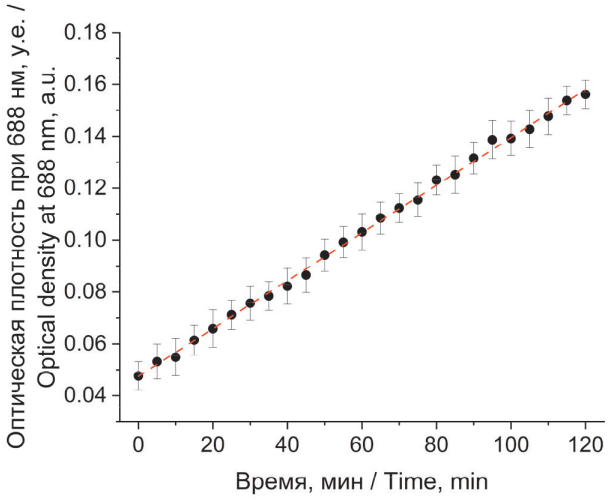

Рис. 3. Динамика накопления продукта реакции во времени.
Fig. 3. Dynamics of reaction product accumulation over time.

determination, indicating a linear fit to the experimental data. The slope of the curve reflects a constant rate of product accumulation, indicating that the process occurs at a steady state over the studied time range.

The observed linear dependence of the reaction product concentration on time is characteristic of zero-order reactions with respect to one or more initial reactants. Alternatively, a variant in which the concentration of the limiting reactant remains constant throughout the experiment is possible. This may be due either to its presence in significant stoichiometric excess or to the presence of an external factor (e.g., a catalyst or reactant source) that ensures its generation or consumption at a constant rate. Consequently, the most probable hypothesis explaining the observed linear dependence of product formation at this stage of the decomposition of the hydrazide fragment is the variant in which the rate of the process is limited by a substance whose concentration is maintained practically unchanged under the experimental conditions.

Conclusion

This study evaluated the pH-dependent hydrolysis of a hydrazide linker conjugated to a chlorin e6 derivative under conditions simulating the slightly acidic environment of a tumor microenvironment. The results demonstrate that the hydrazide can act as a pH-sensitive moiety that can be used in targeted delivery systems, providing controlled release. Thus, the developed PS has significant potential for enhancing the efficacy of photodynamic therapy for cancer and reducing the systemic toxicity of chemotherapy.

This work was supported by the Ministry of Science and Higher Education of the Russian Federation under state contract No. FSFZ-2025-0020.

REFERENCES

1. de Martel C., Georges D., Bray F., Ferlay J., Clifford G.M. Global burden of cancer attributable to infections in 2018: a worldwide incidence analysis. *The Lancet global health*, 2020, vol. 8, pp. e180-e190. doi:10.1016/S2214-109X(19)30488-7.
2. Chen H., Zhang G., Qian Y., Peng Y., Li X., Wang J., Wang J., Hu Y., Xiao H., Zhong Q., Li X., Xie Y., Chen Y., Zhao L., Jing Q., Shan X., Wang Y. Advancements in the Application of the Intersection of Medicine and Engineering in Cancer Research. *Cancer Nexus*, 2025, vol. 1, pp. e70003. doi:10.1002/cnx2.70003.
3. Piña-Sánchez P., Chávez-González A., Ruiz-Tachiquín M., Vadillo E., Monroy-García A., Montesinos J.J., Grajales R., Gutiérrez de la Barrera M., Mayani H. Cancer biology, epidemiology, and treatment in the 21st century: Current status and future challenges from a biomedical perspective. *Cancer Control*, 2021, vol. 28, pp. 10732748211038735. doi:10.1177/10732748211038735.
4. Tilsed C.M., Fisher S.A., Nowak A.K., Lake R.A., Lesterhuis W.J. Cancer chemotherapy: Insights into cellular and tumor microenvironmental mechanisms of action. *Frontiers in oncology*, 2022, vol. 12, pp. 960317. doi:10.3389/fonc.2022.960317.
5. Dasari S., Tchounwou P.B. Cisplatin in cancer therapy: molecular mechanisms of action. *European journal of pharmacology*, 2014, vol. 740, pp. 364-378. doi:10.1016/j.ejphar.2014.07.025.
6. Ali I., Wani W.A., Haque A., Saleem K. Glutamic acid and its derivatives: candidates for rational design of anticancer drugs. *Future medicinal chemistry*, 2013, vol. 5, pp. 961-978. doi:10.4155/fmc.13.62.
7. Mantri Y., Lippard S.J., Baik M.H. Bifunctional binding of cisplatin to DNA: why does cisplatin form 1, 2-intrastrand cross-links with ag but not with GA?. *Journal of the American Chemical Society*, 2007, vol. 129, pp. 5023-5030. doi:10.1021/ja067631z.
8. Eastman A. The mechanism of action of cisplatin: from adducts

ЛИТЕРАТУРА

1. de Martel C., Georges D., Bray F., Ferlay J., Clifford G.M. Global burden of cancer attributable to infections in 2018: a worldwide incidence analysis // The Lancet global health. – 2020. – Vol. 8. – P. e180-e190. doi:10.1016/S2214-109X(19)30488-7.
2. Chen H., Zhang G., Qian Y., Peng Y., Li X., Wang J., Wang J., Hu Y., Xiao H., Zhong Q., Li X., Xie Y., Chen Y., Zhao L., Jing Q., Shan X., Wang Y. Advancements in the Application of the Intersection of Medicine and Engineering in Cancer Research // Cancer Nexus. – 2025. – Vol. 1. – P. e70003. doi:10.1002/cnx2.70003.
3. Piña-Sánchez P., Chávez-González A., Ruiz-Tachiquín M., Vadillo E., Monroy-García A., Montesinos J.J., Grajales R., Gutiérrez de la Barrera M., Mayani H. Cancer biology, epidemiology, and treatment in the 21st century: Current status and future challenges from a biomedical perspective // Cancer Control. – 2021. – Vol. 28. – P. 10732748211038735. doi:10.1177/10732748211038735.
4. Tilsed C.M., Fisher S.A., Nowak A.K., Lake R.A., Lesterhuis W.J. Cancer chemotherapy: Insights into cellular and tumor microenvironmental mechanisms of action // Frontiers in oncology. – 2022. – Vol. 12. – P. 960317. doi:10.3389/fonc.2022.960317.
5. Dasari S., Tchounwou P.B. Cisplatin in cancer therapy: molecular mechanisms of action // European journal of pharmacology. – 2014. – Vol. 740. – P. 364-378. doi:10.1016/j.ejphar.2014.07.025.
6. Ali I., Wani W.A., Haque A., Saleem K. Glutamic acid and its derivatives: candidates for rational design of anticancer drugs // Future medicinal chemistry. – 2013. – Vol. 5. – P. 961-978. doi:10.4155/fmc.13.62.
7. Mantri Y., Lippard S.J., Baik M.H. Bifunctional binding of cisplatin to DNA: why does cisplatin form 1, 2-intrastrand cross-links with ag but not with GA? // Journal of the American Chemical Society. – 2007. – Vol. 129. – P. 5023-5030. doi:10.1021/ja067631z.
8. Eastman A. The mechanism of action of cisplatin: from adducts to

to apoptosis. *Cisplatin: Chemistry and biochemistry of a leading anticancer drug*, 1999, pp. 111-134. doi:10.1002/9783906390420.ch4.

9. Chang X., Bian M., Liu L., Yang J., Yang Z., Wang Z., Lu Y., Liu W. Induction of immunogenic cell death by novel platinum-based anticancer agents. *Pharmacological Research*, 2023, vol. 187, pp. 106556. doi:10.1016/j.phrs.2022.106556.
10. Kiyonari S., Iimori M., Matsuoka K., Watanabe S., Morikawa-Ichinose T., Miura D., Niimi S., Saeki H., Tokunaga E., Oki E., Morita M., Kadomatsu K., Maehara Y., Kitao H. The 1, 2-diaminocyclohexane carrier ligand in oxaliplatin induces p53-dependent transcriptional repression of factors involved in thymidylate biosynthesis. *Molecular cancer therapeutics*, 2015, vol. 14, pp. 2332-2342. doi:10.1158/1535-7163.MCT-14-0748.
11. Johnstone T.C., Suntharalingam K., Lippard S.J. The next generation of platinum drugs: targeted Pt (II) agents, nanoparticle delivery, and Pt (IV) prodrugs. *Chemical reviews*, 2016, vol. 116, pp. 3436-3486. doi:10.1021/acs.chemrev.5b00597.
12. Gandioso A., Shaili E., Massaguer A., Artigas G., González-Cantó A., Woods J.A., Sadler P.J., Marchán V. An integrin-targeted photoactivatable Pt (IV) complex as a selective anticancer pro-drug: synthesis and photoactivation studies. *Chemical Communications*, 2015, vol. 51, pp. 9169-9172. doi:10.1039/c5cc03180j.
13. Kutlu E., Emen F.M., Kismali G., Kınaytürk N.K., Kılıç D., Karacolak A.I., Demirdogen R.E. Pyridine derivative platinum complexes: Synthesis, molecular structure, DFT and initial anticancer activity studies. *Journal of Molecular Structure*, 2021, vol. 1234. pp. 130191. doi:10.1016/j.molstruc.2021.130191.
14. Zorzi D., Laurent A., Pawlik T.M., Lauwers G.Y., Vauthey J.N., Abdalla E.K. Chemotherapy-associated hepatotoxicity and surgery for colorectal liver metastases. *Journal of British Surgery*, 2007, vol. 94, pp. 274-286. doi:10.1002/bjs.5719.
15. Anderegg G., Wanner H. Pyridine derivatives as complexing agents. XIII. The stability of the palladium (II) complexes with pyridine, 2, 2′-bipyridyl, and 1, 10-phenanthroline. *Inorganica chimica acta*, 1986, vol. 113, pp. 101-108. doi:10.1016/S0020-1693(00)82229-X.
16. Dąbrowski J.M., Arnaut L.G. Photodynamic therapy (PDT) of cancer: from local to systemic treatment. *Photochemical & Photobiological Sciences*, 2015, vol. 14, pp. 1765-1780. doi:10.1039/c5pp00132c.
17. Li X., Lovell J.F., Yoon J., Chen X. Clinical development and potential of photothermal and photodynamic therapies for cancer. *Nature reviews Clinical oncology*, 2020, vol. 17, pp. 657-674. doi:10.1038/s41571-020-0410-2.
18. Donohoe C., Senge M.O., Arnaut L.G., Gomes-da-Silva L.C. Cell death in photodynamic therapy: From oxidative stress to anti-tumor immunity. *Biochimica et Biophysica Acta (BBA)-Reviews on Cancer*, 2019, vol. 1872, pp. 188308. doi:10.1016/j.bbcan.2019.07.003.
19. Li X., Lee S., Yoon J. Supramolecular photosensitizers rejuvenate photodynamic therapy. *Chemical Society Reviews*, 2018, vol. 47, pp. 1174-1188. doi:10.1039/c7cs00594f.
20. Kaczorowska A., Malinga-Drozd M., Kałas W., Kopaczyńska M., Wołowiec S., Borowska K. Biotin-containing third generation glucoheptoamidated polyamidoamine dendrimer for 5-aminolevulinic acid delivery system. *International Journal of Molecular Sciences*, 2021, vol. 22, pp. 1982. doi:10.3390/ijms22041982.
21. Dąbrowski J.M., Arnaut L.G. Photodynamic therapy (PDT) of cancer: from local to systemic treatment. *Photochemical & Photobiological Sciences*, 2015, vol. 14, pp. 1765-1780. doi:10.1039/c5pp00132c.
22. Wentrup R., Winkelmann N., Mitroshkin A., Prager M., Voderholzer W., Schachschal G., Jürgensen C., Büning C. Photodynamic therapy plus chemotherapy compared with photodynamic therapy alone in hilar nonresectable cholangiocarcinoma. *Gut and liver*, 2016, vol. 10, pp. 470. doi:10.5009/gnl15175.
23. Li B., Meng Z., Li Q., Huang X., Kang Z., Dong H., Chen J., Sun J., Dong Y., Li J., Jia X., Sessler J.L., Meng Q., Li C. A pH responsive complexation-based drug delivery system for oxaliplatin. *Chemical science*, 2017, vol. 8, pp. 4458-4464. doi:10.1039/c7sc01438d.

apoptosis // Cisplatin: Chemistry and biochemistry of a leading anticancer drug. – 1999. – P. 111-134. doi:10.1002/9783906390420.ch4.

9. Chang X., Bian M., Liu L., Yang J., Yang Z., Wang Z., Lu Y., Liu W. Induction of immunogenic cell death by novel platinum-based anticancer agents // Pharmacological Research. – 2023. – Vol. 187. – P. 106556. doi:10.1016/j.phrs.2022.106556.
10. Kiyonari S., Iimori M., Matsuoka K., Watanabe S., Morikawa-Ichinose T., Miura D., Niimi S., Saeki H., Tokunaga E., Oki E., Morita M., Kadomatsu K., Maehara Y., Kitao H. The 1, 2-diaminocyclohexane carrier ligand in oxaliplatin induces p53-dependent transcriptional repression of factors involved in thymidylate biosynthesis // Molecular cancer therapeutics. – 2015. – Vol. 14. – P. 2332-2342. doi:10.1158/1535-7163.MCT-14-0748.
11. Johnstone T.C., Suntharalingam K., Lippard S.J. The next generation of platinum drugs: targeted Pt (II) agents, nanoparticle delivery, and Pt (IV) prodrugs // Chemical reviews. – 2016. – Vol. 116. – P. 3436-3486. doi:10.1021/acs.chemrev.5b00597.
12. Gandioso A., Shaili E., Massaguer A., Artigas G., González-Cantó A., Woods J.A., Sadler P.J., Marchán V. An integrin-targeted photoactivatable Pt (IV) complex as a selective anticancer pro-drug: synthesis and photoactivation studies // Chemical Communications. – 2015. – Vol. 51. – P. 9169-9172. doi:10.1039/c5cc03180j.
13. Kutlu E., Emen F.M., Kismali G., Kınaytürk N.K., Kılıç D., Karacolak A.I., Demirdogen R.E. Pyridine derivative platinum complexes: Synthesis, molecular structure, DFT and initial anticancer activity studies // Journal of Molecular Structure. – 2021. – Vol. 1234. – P. 130191. doi:10.1016/j.molstruc.2021.130191.
14. Zorzi D., Laurent A., Pawlik T.M., Lauwers G.Y., Vauthey J.N., Abdalla E.K. Chemotherapy-associated hepatotoxicity and surgery for colorectal liver metastases // Journal of British Surgery. – 2007. – Vol. 94. – P. 274-286. doi:10.1002/bjs.5719.
15. Anderegg G., Wanner H. Pyridine derivatives as complexing agents. XIII. The stability of the palladium (II) complexes with pyridine, 2, 2′-bipyridyl, and 1, 10-phenanthroline // Inorganica chimica acta. – 1986. – Vol. 113. – P. 101-108. doi:10.1016/S0020-1693(00)82229-X.
16. Dąbrowski J.M., Arnaut L.G. Photodynamic therapy (PDT) of cancer: from local to systemic treatment // Photochemical & Photobiological Sciences. – 2015. – Vol. 14. – P. 1765-1780. doi:10.1039/c5pp00132c.
17. Li X., Lovell J.F., Yoon J., Chen X. Clinical development and potential of photothermal and photodynamic therapies for cancer // Nature reviews Clinical oncology. – 2020. – Vol. 17. – P. 657-674. doi:10.1038/s41571-020-0410-2.
18. Donohoe C., Senge M.O., Arnaut L.G., Gomes-da-Silva L.C. Cell death in photodynamic therapy: From oxidative stress to anti-tumor immunity // Biochimica et Biophysica Acta (BBA)-Reviews on Cancer. – 2019. – Vol. 1872. – P. 188308. doi:10.1016/j.bbcan.2019.07.003.
19. Li X., Lee S., Yoon J. Supramolecular photosensitizers rejuvenate photodynamic therapy // Chemical Society Reviews. – 2018. – Vol. 47. – P. 1174-1188. doi:10.1039/c7cs00594f.
20. Kaczorowska A., Malinga-Drozd M., Kałas W., Kopaczyńska M., Wołowiec S., Borowska K. Biotin-containing third generation glucoheptoamidated polyamidoamine dendrimer for 5-aminolevulinic acid delivery system // International Journal of Molecular Sciences. – 2021. – Vol. 22. – P. 1982. doi:10.3390/ijms22041982.
21. Dąbrowski J.M., Arnaut L.G. Photodynamic therapy (PDT) of cancer: from local to systemic treatment // Photochemical & Photobiological Sciences. – 2015. – Vol. 14. – P. 1765-1780. doi:10.1039/c5pp00132c.
22. Wentrup R., Winkelmann N., Mitroshkin A., Prager M., Voderholzer W., Schachschal G., Jürgensen C., Büning C. Photodynamic therapy plus chemotherapy compared with photodynamic therapy alone in hilar nonresectable cholangiocarcinoma // Gut and liver. – 2016. – Vol. 10. – P. 470. doi:10.5009/gnl15175.
23. Li B., Meng Z., Li Q., Huang X., Kang Z., Dong H., Chen J., Sun J., Dong Y., Li J., Jia X., Sessler J.L., Meng Q., Li C. A pH responsive complexation-based drug delivery system for oxaliplatin // Chemical science. – 2017. – Vol. 8. – P. 4458-4464. doi:10.1039/c7sc01438d.

24. Liu J., Huang Y., Kumar A., Tan A., Jin S., Mozhi A., Liang X.J. pH-sensitive nano-systems for drug delivery in cancer therapy. *Biotechnology advances*, 2014, vol. 32, pp. 693-710. doi:10.1016/j.biotechadv.2013.11.009.
25. Liu R., Zhang Y., Zhao X., Agarwal A., Mueller L.J., Feng P. pH-responsive nanogated ensemble based on gold-capped mesoporous silica through an acid-labile acetal linker. *Journal of the American Chemical Society*, 2010, vol. 132, pp. 1500-1501. doi:10.1021/ja907838s.
26. Cappellesso F., Mazzone M., Virga F. Acid affairs in anti-tumour immunity. *Cancer cell international*, 2024, vol. 24, pp. 354. doi:10.1186/s12935-024-03520-0.
27. Liberti M.V., Locasale J.W. The Warburg effect: how does it benefit cancer cells?. *Trends in biochemical sciences*, 2016, vol. 41, pp. 211-218. doi:10.1016/j.tibs.2015.12.001.
28. Kirin N.S., Ostroverkhov P.V., Usachev M.N., Birin K.P., Grin M.A. Platinum (II) complexes based on derivatives of natural chlorins with pyridine-containing chelate groups as prototypes of drugs for combination therapy in oncology. *Fine Chemical Technologies*, 2024, vol. 19, pp. 310-326. doi:10.32362/2410-6593-2024-19-4-310-326.
29. Pandit R.P., Thapa Magar T.B., Shrestha R., Lim J., Gurung P., Kim Y.W. Isolation, identification, and biological activities of a new chlorin e6 derivative. *International Journal of Molecular Sciences*, 2024, vol. 25, pp. 7114. doi:10.3390/ijms25137114.
30. Fu R.G., Sun Y., Sheng W.B., Liao D.F. Designing multi-targeted agents: An emerging anticancer drug discovery paradigm. *European journal of medicinal chemistry*, 2017, vol. 136, pp. 195-211. doi:10.1016/j.ejmech.2017.05.016.

24. Liu J., Huang Y., Kumar A., Tan A., Jin S., Mozhi A., Liang X.J. pH-sensitive nano-systems for drug delivery in cancer therapy // Biotechnology advances. – 2014. – Vol. 32. – P. 693-710. doi:10.1016/j.biotechadv.2013.11.009.
25. Liu R., Zhang Y., Zhao X., Agarwal A., Mueller L.J., Feng P. pH-responsive nanogated ensemble based on gold-capped mesoporous silica through an acid-labile acetal linker // Journal of the American Chemical Society. – 2010. – Vol. 132. – P. 1500-1501. doi:10.1021/ja907838s.
26. Cappellesso F., Mazzone M., Virga F. Acid affairs in anti-tumour immunity // Cancer cell international. – 2024. – Vol. 24. – P. 354. doi:10.1186/s12935-024-03520-0.
27. Liberti M.V., Locasale J.W. The Warburg effect: how does it benefit cancer cells? // Trends in biochemical sciences. – 2016. – Vol. 41. – P. 211-218. doi:10.1016/j.tibs.2015.12.001.
28. Kirin N.S., Ostroverkhov P.V., Usachev M.N., Birin K.P., Grin M.A. Platinum (II) complexes based on derivatives of natural chlorins with pyridine-containing chelate groups as prototypes of drugs for combination therapy in oncology // Fine Chemical Technologies. – 2024. – Vol. 19. – P. 310-326. doi:10.32362/2410-6593-2024-19-4-310-326.
29. Pandit R.P., Thapa Magar T.B., Shrestha R., Lim J., Gurung P., Kim Y.W. Isolation, identification, and biological activities of a new chlorin e6 derivative // International Journal of Molecular Sciences. – 2024. – Vol. 25. – P. 7114. doi:10.3390/ijms25137114.
30. Fu R.G., Sun Y., Sheng W.B., Liao D.F. Designing multi-targeted agents: An emerging anticancer drug discovery paradigm // European journal of medicinal chemistry. – 2017. – Vol. 136. – P. 195-211. doi:10.1016/j.ejmech.2017.05.016.

PHOTODYNAMIC THERAPY FOR CILIARY BODY MELANOMA: EXPERIENCE WITH AN ISOLATED TRANSSCLERAL APPROACH

Samkovich E.V.[1], Boiko E.V.[1,2,3], Panova I.E.[1,2,3], Gvazava V.G.[1], Ivanov A.A.[4], Grishacheva T.G.[5], Shevchenko S.B.[6]

[1]Saint Petersburg Branch of the S. Fyodorov National Medical Research Center "Intersectoral Scientific and Technical Complex 'Eye Microsurgery'," Ministry of Health of the Russian Federation, Saint-Petersburg, Russia
[2]North-Western State Medical University named after I.I. Mechnikov, Ministry of Health of the Russian Federation, Saint-Petersburg, Russia
[3]Saint Petersburg State University, Saint-Petersburg, Russia
[4]LLC "Alcom Medica", Saint-Petersburg, Russia
[5]Pavlov First Saint Petersburg State Medical University, Saint-Petersburg, Russia
[6]Institute of Experimental Medicine, Saint-Petersburg, Russia

Abstract

Ciliary body melanoma (CBM) accounts for up to 20% of uveal melanoma cases and presents challenges for organ-preserving treatment due to its peripheral location and proximity to critical ocular structures. This study presents the first clinical results evaluating the efficacy and safety of isolated transscleral photodynamic therapy (TSPDT) with a chlorin e6 photosensitizer in 7 patients with CBM. The procedure was performed using an «ALOD-01» laser system (λ=662 nm) and standardized irradiation parameters (energy density 519.5 J/cm^2, accounting for power loss during scleral transmission). The mean follow-up period was 19.0±5.9 months and demonstrated high local tumor control: complete regression was achieved in 4 patients, and partial regression in 3 patients. A statistically significant reduction in tumor height (from 4.69±2.58 mm to 1.36±1.14 mm; p=0.0062) and basal diameter (from 8.54±3.56 mm to 6.65±3.70 mm; p=0.016) was accompanied by a pronounced vasculo-occlusive effect, manifested as complete tumor avascularity in the majority of patients according to ultrasound with color Doppler Imaging (CDI). Echodenstitometry recorded a statistically significant decrease in mean acoustic density from 35.53±1.26 dB to 28.97±0.83 dB (p=0.0002), which may indicate tumor tissue destruction. No intra– or postoperative complications were recorded throughout the observation period, and a trend towards stable visual acuity was noted. The obtained data suggest that TSPDT is a promising minimally invasive organ-preserving method for treating CBM, requiring further investigation to define its role as either a standalone or combined therapy.

Keywords: uveal melanoma, ciliary body melanoma, choroidal melanoma, ophthalmic oncology, photodynamic therapy, chlorin e6, transscleral photodynamic therapy, photosensitizer.

Contacts: Samkovich E.V., e-mail: e.samkovich@mail.ru

For citations: Samkovich E.V., Boiko E.V., Panova I.E., Gvazava V.G., Ivanov A.A., Grishacheva T.G., Shevchenko S.B. Photodynamic therapy for ciliary body melanoma: experience with an isolated transscleral approach, *Biomedical Photonics*, 2025, vol. 14, no. 4, pp. 11–21. doi: 10.24931/2413–9432–2025–14-4-11-21

ФОТОДИНАМИЧЕСКАЯ ТЕРАПИЯ ПРИ МЕЛАНОМЕ ЦИЛИАРНОГО ТЕЛА: ОПЫТ ИЗОЛИРОВАННОГО ТРАНССКЛЕРАЛЬНОГО ПОДХОДА

Е.В. Самкович[1], Э.В. Бойко[1,2,3], И.Е. Панова[1,2,3], В.Г. Гвазава[1], А.А. Иванов[4], Т.Г. Гришачева[5], С.Б. Шевченко[6]

[1]Санкт-Петербургский филиал МНТК «Микрохирургия глаза», Санкт-Петербург, Россия
[2]Северо-Западный государственный медицинский университет имени И. И. Мечникова, Санкт-Петербург, Россия
[3]Санкт-Петербургский государственный университет, Санкт-Петербург, Россия
[4]ООО «Алком Медика», Санкт-Петербург, Россия
[5]Первый Санкт-Петербургский Государственный Медицинский Университет им. ак. И. П. Павлова, Санкт-Петербург, Россия
[6]Институт Экспериментальной Медицины, Санкт-Петербург, Россия

Резюме

Меланома цилиарного тела (МЦТ) составляет до 20% случаев увеальной меланомы и представляет сложности для органосохранного лечения ввиду периферической локализации и близости к критическим структурам глаза. В настоящем исследовании представлены первые клинические результаты оценки эффективности и безопасности изолированной транссклеральной фотодинамической терапии (ТСФДТ) с фотосенсибилизатором (ФС) хлорин е6 у 7 пациентов с МЦТ. Процедура выполнена с использованием лазерной установки «АЛОД-01» (λ=662 нм) и унифицированных параметров воздействия (плотность энергии 519,5 Дж/см^2 с учетом потерь мощности при прохождении излучения через склеру). Динамическое наблюдение в среднем в течение 19,0±5,9 мес показало высокий локальный контроль над опухолью: полный регресс был достигнут у 4 пациентов, частичный – у 3 пациентов. Статистически значимое уменьшение высоты опухоли (с 4,69±2,58 мм до 1,36±1,14 мм; p=0,0062) и диаметра ее основания (с 8,54±3,56 мм до 6,65±3,70 мм; p=0,016) сочеталось с выраженным васкуло-окклюзивным эффектом, проявляющимся в полной аваскуляризации опухоли у большинства пациентов по данным ультразвукового исследования (УЗИ) в режиме цветового допплеровского картирования (УЗДГ). Эходенситометрия зафиксировала статистически значимое снижение средней акустической плотности с 35,53±1,26 дБ до 28,97±0,83 дБ (p=0,0002), что может свидетельствовать о деструкции опухолевой ткани. На протяжении всего периода наблюдения не зафиксировано интра– или послеоперационных осложнений, отмечена тенденция к сохранению стабильной остроты зрения. Полученные данные позволяют рассматривать ТСФДТ как перспективный минимально инвазивный органосохраняющий метод лечения МЦТ, требующий дальнейшего изучения для определения его роли в качестве изолированной или комбинированной терапии.

Ключевые слова. Увеальная меланома, меланома цилиарного тела, меланома хориоидеи, офтальмоонкология, фотодинамическая терапия, хлорин е6, транссклеральная фотодинамическая терапия, фотосенсибилизатор.

Контакты: Самкович Е.В., e-mail: e.samkovich@mail.ru

Для цитирования: Самкович Е.В., Бойко Э.В., Панова И.Е., Гвазава В.Г., Иванов А.А., Гришачева Т.Г., Шевченко С.Б. Фотодинамическая терапия при меланоме цилиарного тела: опыт изолированного транссклерального подхода // Biomedical Photonics. – 2025. –Т. 14, № 4. – С. 11–21. doi: 10.24931/2413–9432–2025–14-4-11-21

Introduction

Melanoma of the ciliary body (CBM) accounts for up to 20% of all cases of uveal melanoma [1,2]. This localization presents significant difficulties for organ-preserving treatment, due to its anatomical location in close proximity to the lens and drainage system of the eye [1-6]. Peripheral localization and "hidden" growth cause a late diagnosis of this process, and also create significant difficulties in choosing the optimal treatment tactics [2,3,6]. Currently, local surgical resection (block excision) and various types of radiation therapy are in the arsenal of organ-preserving methods for CBM [2,4-10]. However, each of these approaches has certain limitations. Thus, block excision is technically difficult, involves the risk of intra- and postoperative complications, including suprachoroidal hemorrhage, detachment of the choroid and retina, and requires the highest qualification of the surgeon [2,6,7]. Radiation treatment methods such as Ru-106/Rh-106 brachytherapy and proton therapy show high efficacy in local tumor control [5,9,10]. At the same time, in the treatment of CBM, they may be associated with a higher incidence of post-radiation complications compared with post-equatorial tumors, which is due to the inevitable irradiation of critical structures of the anterior part of the eyeball [5, 10-12]. An additional difficulty in brachytherapy is the precise positioning of the ophthalmoapplicator in the area of the ciliary body.

Photodynamic therapy (PDT) has been actively studied in recent years as a minimally invasive organ-preserving approach for uveal melanoma [13-20]. The clinical validity of the use in melanoma is confirmed by the presence of officially registered indications for chlorin photosensitizers (PS), such as photolon / fotoran. The greatest experience has been gained with the use of transpupillary PDT (TPPDT), the effectiveness of which, as shown in a number of studies, depends on the initial size of the tumor, as well as the degree of its vascularization and pigmentation [15,16,18-20]. At the same time, the field of application of TPPDT is limited to neoplasms of the posterior pole of the eye, accessible for irradiation through transparent optical media [18-20]. In this regard, transcleral PDT (TSPDT), which provides direct laser radiation to the base of the tumor through the scleral membrane, is a promising alternative to overcome this anatomical limitation [13,21,22]. The possibility of using this approach has been confirmed in previous experimental studies, which have shown the ability of laser radiation with a wavelength of 660 nm to effectively and safely penetrate the sclera [22]. In addition, selective photochemical damage to the choroidal vascular network has been proven [21]. However, there is no data in the literature on the clinical use of TSPDT for the treatment of ocular vascular melanoma. The present study presents the first clinical results evaluating the efficacy and safety of isolated TSPDT with PS chlorin e6 in the treatment of CBM.

Materials and methods

The study included 7 patients (7 eyes) with CBM who were treated with isolated TSPDT in the period from 2022 to 2024. The inclusion criteria were: tumor thickness up to 9 mm, base diameter up to 15 mm, absence of signs of extrascleral spread and tumor growth in the corner of the anterior chamber, absence of complications.

Ethical aspects

The research protocol was approved by the local Ethics committee of the Federal State Budgetary Budgetary Institution "IEM" (No. 4/24 dated 10/24/2024).

All patients underwent a comprehensive clinical and instrumental examination, which included visometry with an assessment of best corrected visual acuity (BCVA), biomicroscopy, ophthalmoscopy with a non-contact lens, Maklakov tonometry and ultrasound biomicroscopy (UBM). Ultrasound was performed on a Philips Affinity 50 multifunction scanner (Philips Ultrasound, USA) with an L15-7io sensor to evaluate the metric parameters of the tumor, the characteristics of intracellular blood flow using color Doppler mapping (CDM) and densitometric characteristics of tumor tissue (echodensitometry) with quantitative determination of acoustic density in decibels (dB) with the construction of and analysis of amplitude histograms under standardized conditions. To stage the process and exclude metastatic lesions, multispiral computed tomography (MSCT) of the chest organs, magnetic resonance imaging (MRI) of the abdominal cavity with contrast, and MRI of the brain were performed.

The distribution of patients by stage, size, blood flow characteristics, and acoustic density of the tumor is shown in Table 1.

As the data in Table 1 show, the patients in the study were mainly women (n=6), whose average age was 68.7±15.8 years. All tumors belonged to stage II according to the AJCC classification of the 8th edition (IIA n=4), (IIB n=3). According to the degree of pigmentation, strongly pigmented tumors prevailed (n=4). At the time of diagnosis, the vast majority of neoplasms (n=5) had a hypervascular type of blood flow, while 6 patients had several vessels feeding the tumor. The average acoustic density of the tumor tissue before treatment was 35.53±1.26 dB (26.34-44.42). The average follow-up period was 19.0±5.9 months.

The TSPDT procedure was performed under anesthesia, 3 hours before the laser exposure, chlorin-type PS based on chlorin e6 (photolon/fotoran) was administered intravenously at a dose of 1.0 mg/kg body weight. After conjunctival access and transpupillary diaphanoscopy, transcleral laser irradiation of the tumor base was performed using an ALOD-01 laser (λ=662 nm, Alcom Medica, Russia) and specialized transcleral tip probes to accurately mark the tumor boundaries.

The technical parameters of the exposure were unified: radiation power 0.17 W, power density 0.866 W/cm^2, energy density 519.5 J/cm^2 with an

Таблица 1
Клинико-инструментальные характеристики пациентов с меланомой цилиарного тела до лечения (n=7)

Table 1
Clinical and instrumental characteristics of patients with ciliary body melanoma before treatment (n=7)

Параметр Parameter	Значение Value
Возраст, лет Age, years	68,7±15,8 (37-82)
Женский пол, n Female gender, n	6
Мужской пол, n Male gender, n	1
Срок наблюдения, мес Observation period, months	19,0±5,89 (12-30)
Стадия AJCC, n **AJCC stage, n**	
IIA	4
IIB	3
Пигментация, n **Pigmentation, n**	
Выраженная Significant	4
Умеренная Mild	2
Беспигментная Non-pigmented	1
Васкуляризация исходная, n Initial vascularization, n	
Гиперваскулярная Hypervascular	5
Гиповаскулярная Hypovascular	2
Количество питающих опухоль сосудов, n **Number of vessels feeding the tumor, n**	
Один сосуд One vessel	1
Несколько сосудов Several vessels	6
Средняя акустическая плотность, дБ **Average acoustic density, dB**	35,53±1,26 (26,34-44,42)

exposure duration of 600 seconds (10 minutes) in the field. These parameters were proportionally doubled, taking into account the transmittance of the sclera to provide the necessary therapeutic dose in the tumor area. The exposure was carried out concentrically from the center to the periphery with the overlap of fields on 10-15% of the area.

The effectiveness of treatment was assessed in dynamics after 1, 3, 6, 9, 12 months and further annually, which was based on changes in the nature of intracellular blood flow, densitometric characteristics (acoustic density) and metric parameters of the tumor. The response to treatment was assessed according to the RECIST 1.1 criteria (2009): complete regression (absence of elevation according to color Doppler Imaging (CDI) and blood flow according to CDM), partial regression (decrease in tumor height >30% from the initial one), stabilization (change in height within ±30%) and progression (increase in height >30%). The dynamics of maximum corrected visual acuity and intra- and postoperative complications were also evaluated.

Statistical data processing was carried out using the SPSS 28.0 program. Quantitative data were checked for the normality of the distribution using the Shapiro-Wilk test. The arithmetic mean and standard deviation (M±SD) for parameters with a normal distribution and the median with an interquartile range [Me (Q1; Q3)] for parameters with a distribution other than normal were used for the description. To compare the indicators before and after treatment, the Student's t-test was used for paired samples. Fischer's exact test was used to analyze categorical data. The differences were considered statistically significant at $p < 0.05$.

Таблица 2
Клинико-инструментальная динамика опухолевых, ультразвуковых, денситометрических, допплерографических и функциональных параметров до и после проведения изолированной ТСФДТ

Table 2
Clinical and instrumental dynamics of tumor, ultrasound, densitometric, Doppler and functional parameters before and after isolated TSPDT

Параметр Parameter	До лечения Before treatment	После лечения After treatment	Δ (Изменение) Δ (Change)	p-value
Высота опухоли, мм **Tumor height, mm**	4,69±2,58	1,36±1,14	-3,33±2,41	0,0062
[min-max]	*[2,4 – 8,8]*	*[0,0 – 3,0]*	*[-8,3 – -1,0]*	
Диаметр основания, мм **Base diameter, mm**	8,54±3,56	6,65±3,70	-1,89±1,64	0,016
[min-max]	*[5,0 – 14,0]*	*[2,0 – 11,4]*	*[-3,05 – +0,1]*	
МКОЗ **Best-corrected visual acuity**	0,60±0,34	0,71±0,26	+0,11±0,25	0,25
[min-max]	*[0,03 – 1,0]*	*[0,4 – 1,0]*	*[-0,4 – +0,45]*	
Васкуляризация, n (%) **Vascularization, n (%)**				
Гиперваскулярная Hypervascular	5	1		
Гиповаскулярная Hypovascular	2	1		
Аваскулярная Avascular	0	**5**		
Средняя акустическая плотность, дБ **Average acoustic density, dB**	35,53±1,26	28,97±0,83	-6,56±1,12	0,0002
[min-max]	*[26,34 – 44,42]*	*[19,4 – 34,97]*	*[-12,02 – -2,45]*	
Результат лечения, n (%) **Treatment outcome, n (%)**				
Полный регресс Complete regression	-	4		
Частичный регресс Partial regression	-	3		

Results

The clinical and instrumental dynamics of tumor, ultrasound, densitometric, Dopplerographic, and functional parameters before and after treatment are presented in Table 2.

Clinical and instrumental dynamics of tumor, ultrasound, densitometric, Doppler and functional parameters before and after isolated TSPDT.

Given that the key mechanism of action of PDT is primary vascular occlusive effect, the analysis of the results was primarily aimed at assessing changes in intracellular blood flow. As the results presented in Table 2 show, the most pronounced and early changes were recorded in the nature of intracellular vascularization. Thus, if hypervascularization was observed in 5 patients before treatment, then after TSPDT, all patients in this group showed complete tumor avascularization, which may indicate thrombosis of the vessels feeding the tumor. One patient retained the hypovascular type of blood flow, and only one patient showed signs of moderate hypervascularization.

Next, the dynamics of the densitometric characteristics of the tumor was analyzed. Statistical analysis demonstrated a significant decrease in the average acoustic density of tumor tissue from 35.53±1.26 dB to 28.97±0.83 dB (Δ=-6.56±1.12 dB; p=0.0002), which may indirectly indicate a change in the structural characteristics of the tumor, possibly associated with a direct cytotoxic effect and destruction of tumor tissue.

The next step was to assess the reduction in tumor size, which is a natural consequence of the cessation of its blood supply. The analysis showed a statistically significant decrease in tumor height: from 4.69±2.58 mm to 1.36±1.14 mm (Δ = -3.33±2.41 mm; p=0.0062). The diameter of the tumor base also significantly decreased: from 8.54±3.56 mm to 6.65±3.70 mm (Δ = -1.89± 1.64 mm; p = 0.016).

According to the criteria of treatment effectiveness RECIST 1.1 (2009), complete regression was achieved in 4 patients, partial regression in 3 patients. There were no cases of stabilization or progression of the disease, which indicates 100% local control of the tumor during the follow-up period.

When assessing functional outcomes, the changes in BCVA did not reach statistical significance, but a tendency to increase was found (from 0.60±0.34 to 0.71±0.26; Δ = +0.11±0.25; p=0.25). The peripheral localization of tumors of the ciliary body in most cases provided initially high visual acuity, which remained at the same level and tended to improve after treatment. It is important to note that during the entire follow-up period, no intra- or postoperative complications related to the TSPDT were recorded.

The results obtained are confirmed by the following clinical observation. Patient E., 58 years old, was sent to the St. Petersburg branch of S. Fyodorov Eye Microsurgery Federal State Institution of the Ministry of Health of the Russian Federation for consultation with an ophthalmologist with suspected neoplasm of the ciliary body of the right eye. The patient noted a decrease in vision in his right eye during the last 4 months. According to the MRI data of orbits with contrast in the inner segment, a solid formation was determined in the projection of the ciliary body. 0,7*0,6*0,8 cm with a cystic component (0.4 * 0.6 cm), closely adjacent to the lens, intensively accumulating contrast. The patient signed an informed consent for a diagnostic examination. According to the results of a standard ophthalmological examination, including biometry, visometry, tonometry, perimetry, biomicroscopy, biomicroophthalmoscopy, it was found that visual acuity was OD = 0.25 sph – 2.0 cyl -1.0 Dax 25 = 0.5; OS = 0.95 sph +0.25 cyl -0.5 D ax 100 = 1.0; intraocular pressure according to pneumotonometry at OD was 19 mmHg, at OS was 16 mmHg. Biomicroscopy of the right eye revealed an enlarged episcleral vessel at 9 o'clock, islet deposits of pigment on the iris from 3 to 5 o'clock, a moderately pigmented pro-inflammatory neoplasm adjacent to the lens was detected behind the pupillary edge from 2 to 5 o'clock, increased lens opacity in the contact zone. Gonioscopy from 2 to 5 o'clock revealed partial closure of the anterior chamber angle by the iris, pigment on the iris with a local round area of hyperpigmentation measuring 1 mm. Ophthalmoscopically the optic nerve disc was pale pink, the borders were clear, in the macular zone there were no features, at the extreme periphery in the upper-inner segment (mainly the inner) a protruding, pigmented neoplasm of a round shape was determined.

The patient underwent additional instrumental examinations: ultrasound, including CDI with color Doppler mapping of the reflected Doppler signal and spectral Doppler imaging on a PHILIPS Affinity 50 multifunctional scanner (Philips Ultrasound, USA) with an L15-7io high-frequency broadband linear transducer in the operating frequency range of 15 to 7 MHz; ultrasound microscopy (UBM) on an Aviso device with a 25 MHz linear transducer; and photo monitoring. The clinical and instrumental examination data are presented in Fig. 1.

According to ultrasound of the right eye (Fig. 1), in the upper-inner segment in the projection of the ciliary body, a rounded neoplasm with a height of up to 8.8 mm, a diameter of up to 7.4 mm, and an uneven structure with a cyst-like cavity in the thickness were detected. In the CDM mode, multiple color streams were mapped in the projection of a tumor with medium-speed, low-resistance blood flow. During echodensitometry, the average acoustic density of the tumor tissue was 37.4±1.8 dB. According to UBM, in the upper-inner quadrant, a

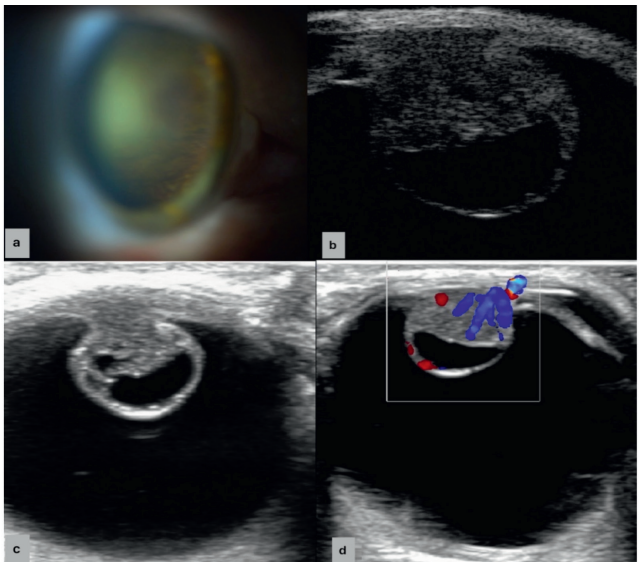

Рис. 1. Диагностические характеристики меланомы цилиарного тела до лечения:
a – пигментированное образование, прилегающее к хрусталику;
b – УБМ проминирующего образования;
c – серошкальное ультразвуковое сканирование;
d – ЦДК внутриопухолевого кровотока.
Fig. 1. Diagnostic characteristics of ciliary body melanoma before treatment:
a – pigmented mass adjacent to the lens;
b – ultrasound biomicroscopy of protruding mass;
c – grayscale ultrasound scanning;
d – color Doppler mapping of intratumoral blood flow.

protruding neoplasm with a height of up to 8.8 mm was visualized in the area of the ciliary body.

To assess the extraocular prevalence of the process, an MRI examination of the abdominal cavity and brain organs, and an MSCT of the lungs were performed. According to the results of additional studies, there are no pathological changes.

Based on the data of a comprehensive clinical and instrumental examination, the patient was diagnosed with T2bN0M0 stage IIB ciliary body melanoma.

Taking into account the size, abundant vascularization and localization of the tumor, the patient was offered treatment in the amount of TSPDT. A voluntary informed consent for treatment has been signed.

On the next day after the TSPDT, ophthalmoscopically, a pronounced reaction was noted in the form of whiteness and swelling of the tumor surface. According to CDI, signs of thrombosis of intracellular vessels were observed (Fig. 2). Echodensitometry data showed an initial decrease in acoustic density to 34.1±2.1 dB.

After treatment, dynamic monitoring was continued. At a follow-up examination 2 months after TSPDT, positive dynamics was noted in the form of partial regression of the tumor according to ultrasound (Fig. 3b) - the height of the tumor decreased to 3.3 mm, the

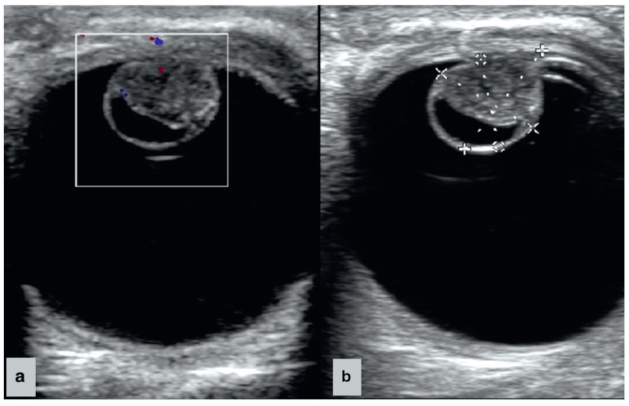

Рис. 2. Ранние изменения после ТСФДТ (1 сут):
a – признаки тромбоза внутриопухолевых сосудов при ЦДК;
b – серошкальное ультразвуковое сканирование.
Fig. 2. Early changes after TSPDT (day 1):
a – signs of intratumoral vessel thrombosis on color Doppler mapping;
b – grayscale ultrasound scanning.

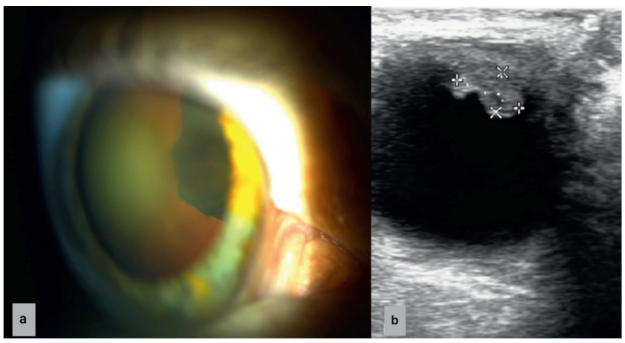

Рис. 3. Динамика состояния через 2 мес после ТСФДТ:
a – биомикроскопия глаза с признаками регресса опухоли;
b – серошкальное ультразвуковое сканирование, демонстрирующее уменьшение размеров опухоли.
Fig. 3. Dynamics at 2 months after TSPDT:
a – biomicroscopy of the eye with signs of tumor regression;
b – grayscale ultrasound scanning demonstrating reduction in tumor size.

diameter of the base decreased to 5.5 mm, according to CDI, blood flow in the tumor was not mapped, and the average acoustic density significantly decreased to 29.2 ±1.5 dB, Biomicroscopically, a decrease in tumor size was noted (Fig. 3a).

Six months after treatment, positive dynamics were noted in the form of tumor regression up to 90%. According to ultrasound data, a decrease in size to 1.1*2.6 mm was observed in the seroscale scanning mode (Fig. 4b), blood flow in the tumor thickness was not mapped during ultrasound with CDM (Fig. 4c), echodensitometry recorded a further decrease in density to 22.6±1.1 dB, biomicroscopically a significant decrease in tumor size was noted (Fig. 4a).

During follow-up examinations 9 months after treatment, the condition is without dynamics. According to ultrasound data in the seroscale scan

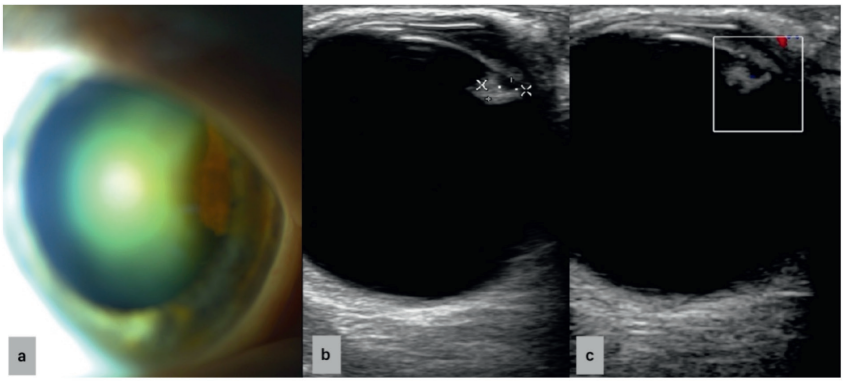

Рис. 4. Динамика состояния через 6 мес после ТСФДТ:
a – биомикроскопия глаза со значительным регрессом опухоли;
b – серошкальное ультразвуковое сканирование, показывающее уменьшение размеров опухоли;
c – ЦДК, подтверждающее аваскулярность опухоли.
Fig. 4. Dynamics at 6 months after TSPDT:
a – biomicroscopy of the eye with significant tumor regression;
b – grayscale ultrasound scanning showing reduction in tumor size;
c – color Doppler mapping confirming tumor avascularity.

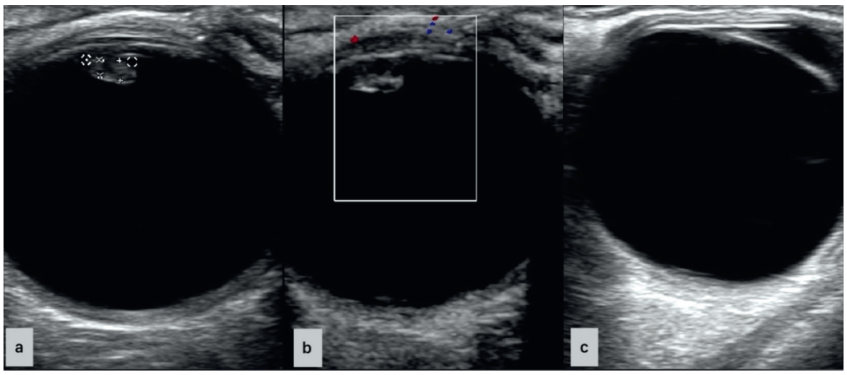

Рис. 5. Отдаленные результаты ТСФДТ:
a – серошкальное ультразвуковое сканирование через 9 мес после лечения;
b – цветовое допплеровское картирование через 9 мес после лечения, аваскулярно;
c – серошкальное ультразвуковое сканирование через 12 мес после лечения, подтверждающее полный регресс опухоли.
Fig. 5. Long-term results of TSPDT:
a – grayscale ultrasound scanning at 9 months after treatment;
b – color Doppler mapping at 9 months after treatment, avascular;
c – grayscale ultrasound scanning at 12 months after treatment, confirming complete tumor regression.

mode, the tumor size was 1.1*2.6 mm (Fig. 5a), in the CDM mode the neoplasm was avascular (Fig. 5b). The acoustic density of the residual tumor tissue was 19.7±0.9 dB. 12 months after the TSPDT, a complete regression of the tumor was achieved, according to ultrasound, the tumor was not visualized (Fig. 5c).

Discussion

TSPDT is an innovative approach in the treatment of intraocular tumors. The key advantage of the technique is the ability of radiation to overcome the scleral membrane with minimal losses and selectively affect the tumor from its base, which is achieved due to the optical properties of the sclera and choroid, which contribute to uniform distribution of energy in the deep layers of the eyeball [14, 22, 23]. The present study presents the first clinical results of the application of this approach for the isolated treatment of melanoma of the choroid of the eyeball.

In the presented series of cases, local tumor control was achieved in all patients during the follow-up period: complete regression was noted in 4 and partial regression in 3 patients with an average follow-up period of 19.0±5.9 months. An important aspect is the absence of cases of local disease progression during follow-up. In cases with insufficient regression dynamics at control examinations within 1-3 months, a timely transition to brachytherapy was used, which excluded wait-and-see tactics. Achieving complete regression in more than half of the patients allows to consider this technology as a potential option for isolated treatment. However, the absence of complete regression in some patients requires further dynamic monitoring and, if necessary, consideration of additional treatment.

The selectivity of PDT, based on the selective accumulation of PS in pathological tissues, minimizes damage to healthy structures of the eye [15, 24-27]. This fact explains the absence of decreased visual acuity and complications characteristic of radiation therapy in the study – post-radiation cataracts, neuroretinopathy, and neovascular glaucoma, which are especially common when tumors of the anterior eye are irradiated and significantly limit the functional results of treatment [5, 11, 12, 13].

The main mechanism of the antitumor effect of PDT is the combined effect on the vessels of the microcirculatory bed of the tumor (vascular occlusive effect) and on tumor cells (direct cytotoxic effect) [15,24,25,28,29]. Complete avascularization of the tumor focus in most patients, which was observed from early follow-up, confirms the pronounced vascular-destroying effect of the method and is consistent with the literature data on tumor vessel thrombosis as a key mechanism of PDT [14-17,19-23].

An important result of this study, consistent with the data on the direct cytotoxic effect, was the objective confirmation of the destruction of tumor tissue using echodensitometry [30, 31]. A statistically significant decrease in the average acoustic density recorded in dynamics (from 35.53±1.26 dB to 28.97±0.83 dB; p=0.0002) may indicate the development of structural changes in the tumor tissue, presumably associated with necrotic processes, which is also consistent with the data obtained in the presented clinical case. The revealed changes, first of vascularization, and then of acoustic density, naturally contribute to the subsequent regression of the neoplasm.

Tissue pigmentation creates significant limitations for PDT in oncological practice, since melanin absorbs light energy, reducing the depth of radiation penetration and therapeutic effectiveness [18, 32, 33]. In the presented study, the combination of red spectrum radiation (660 nm) with transcleral access minimizes the impact of these limitations. The key advantage of the technique is the direct supply of light to the base of the tumor, partially bypassing the pigment barrier, in contrast to the transpupillary approach, where melanin shields the radiation at the top of the tumor [19-21]. In this series of cases, this approach made it possible to achieve regression even with pronounced pigmented neoplasms.

The depth of penetration and the efficiency of radiation delivery remain important aspects of PDT in the treatment of intraocular neoplasms, since light in PDT procedures is subject to scattering and absorption when passing through biological tissues, including the sclera. The wavelength range used to activate PS is 405-900 nm, while the penetration depth significantly depends on the optical properties of the specific wavelength and absorption spectrum of the drug [20, 25]. In this study, PS chlorin e6 was used, which belongs to the second generation of drugs [15, 16, 25, 34, 35]. Unlike first–generation porphyrins operating in the range of 400-630 nm and providing a penetration depth of up to 1-3 mm, chlorin e6 is activated by 660 nm radiation and provides a significantly greater penetration depth of at least 3.5-4.4 mm, as well as reduced absorption by the main tissue chromophores – melanin and hemoglobin [15, 32, 33, 36, 37]. The results obtained in the presented study are consistent with the data on a sufficient depth of radiation penetration in this spectral range.

The main limitation of this study is the small number of patients in the sample and the relatively short follow-up period, which makes it impossible to draw definitive conclusions about long-term outcomes and the frequency of local relapses. The obtained preliminary data, on the one hand, demonstrate the possibility of using TSPDT as an isolated method in individual patients. On the other hand, given the multicomponent approach adopted in oncology and the fact that brachytherapy remains the "gold standard" for the treatment of ocular vascular melanoma, it is currently advisable to consider the TSPDT method primarily as a component of combination therapy. It should be emphasized that this treatment method does not claim to be a universal solution for all patients with CBM. The demonstrated efficacy was achieved within the selected cohort, which determines the relatively narrow indications for its use as an isolated treatment. The key conditions for success are careful patient selection and strict postoperative monitoring, which allows timely assessment of the response and decision on the need for additional intervention.

Further development of the method is associated with several directions. Firstly, TSPDT can be used to treat small tumors of peripheral localization with hypervascular type of blood flow. Secondly, its use as part of a combined approach seems to be the most reasonable, for example, as a neoadjuvant step before brachytherapy or protonotherapy.

The results obtained, in particular, a significant reduction in the size, vascularization, and acoustic density of the tumor after TSPDT, suggest that such tactics may create prerequisites for reducing the radiation dose during subsequent brachytherapy, which can potentially offset the risks of radiation complications. The method may also be used in adjuvant mode. In addition, a promising direction is the combination of TSPDT with other methods, including TPPDT, for a two-way effect on the tumor.

Conclusion

The study shows that isolated TSPDT with PS based on chlorin e6 can be considered as a promising and safe method of organ-preserving treatment of CBM. Within the selected cohort of patients, the method allowed to achieve a high frequency of local control. In addition to a statistically significant reduction in tumor size and a pronounced vascular occlusive effect, an objective confirmation of the destruction of tumor tissue by echodensitometry was a significant result, which may reflect the direct cytotoxic effect of the method. An important aspect is the preservation of stable visual function and the absence of complications. Given the preliminary nature of the data, the results obtained determine the need for further research to clarify the role of TSPDT in the treatment of vascular melanoma, clarifying the prospects for its use as an isolated method or, most likely, a component of combined treatment.

This work was supported by the Russian Science Foundation grant No. 24-75-00047, https://rscf.ru/project/24-75-00047/

REFERENCES

1. Klinicheskie rekomendacii «Uveal'naja melanoma», 2020; Accessed January 07, 2022. https://oncology-association.ru/wp-content/uploads/2020/09/uvealnaja_melanoma.pdf
2. Brovkina A.F. Local treatment of choroidal melanoma: possibilities and limitations. *Russian Annals of Ophthalmology,* 2018, vol. 134, №4, pp. 52-60. (In Russ.) doi: 10.17116/oftalma201813404152.
3. Saakyan S.V., Tsygankov A.Y., Amiryan A.G. Vital prognosis in patients with ciliochorioidal melanoma. *Head and Neck,* 2016, vol. 1-2, pp. 20-23 (In Russ).
4. Grishina E.E., Kim I.D., Izotova E.N. Episcleral spread of ciliochoroidal melanoma following surgeries: a case report. *Russian Journal of Clinical Ophthalmology,* 2023, vol. 23, №2, pp. 107-110 (In Russ). doi: 10.32364/2311-7729-2023-23-2-107-110.
5. Panova I.E., Vorob'ov N.A., Samkovich E. V., Bykhovskii A.A., Martynova N.I., Svistunova E.M. Proton therapy for uveal melanoma (preliminary results). *Fyodorov Journal of Ophthalmic Surgery,* 2023, vol. 3S, pp. 90–101 (In Russ). doi: 10.25276/0235-4160-2023-3S-90-101.
6. Saakyan S.V., Chentsova E.V., Andreyeva T.A. Functional outcomes in patients with tumors of the iridociliary zone after block excision combined with simultaneous and postponed cataract extraction. *Russian Ophthalmological Journal,* 2010, vol. 3, № 1, pp. 23-28 (In Russ).
7. Lee S.M., Kim M. Surgical treatment of uveal melanoma: Exoresection versus endoresection. *Taiwan J. Ophthalmol.,* 2025, vol. 6,15, №1, pp. 34-44. doi: 10.4103/tjo.TJO-D-24-00131.
8. Romano M.R., Ferrara M., Feo A., Merico A., Angi M. Optimizing Surgical Performance and Safety in Endoresection of Uveal Melanoma. *Retina,* 2025 Jun, vol. 1, 45, №6, pp. 1230-1235. doi: 10.1097/IAE.0000000000004273.
9. Banou L., Tsani Z., Arvanitogiannis K., Pavlaki M., Dastiridou A., Androudi S. Radiotherapy in Uveal Melanoma: A Review of Ocular Complications // *Curr. Oncol.,* 2023 Jul, vol. 3, 30, №7, pp. 6374-6396. doi: 10.3390/curroncol30070470.
10. Fleury E., Pignol J.P., Kiliç E., Milder M., van Rij C., Naus N., Yavuzyigitoglu S., den Toom W., Zolnay A., Spruijt K., van Vulpen M., Trnková P., Hoogeman M. Comparison of stereotactic radiotherapy and protons for uveal melanoma patients. *Phys. Imaging Radiat. Oncol.,* 2024 Jun, vol. 26, 31, p. 100605. doi: 10.1016/j.phro.2024.100605.
11. Panova I.E., Bikhovsky A.A., Samkovich E.V., Svistunova E.M. Glucocorticosteroids and Postradiation Macular Edema: Rationale for Choice of Therapy and Efficacy of Use. *Ophthalmology in Russia,* 2024, vol. 21, №3, pp. 533-539 (In Russ.) doi: 10.18008/1816-5095-2024-3-533-539.
12. Panova I.E., Svictunova E.M., Vorobyov N.A., Samkovich E.V., Martynova N.I., Bykhovsky A.A. Neovascular glaucoma as a complication of proton therapy for uveal melanoma. *Russian Journal of Clinical Ophthalmology,* 2024, vol. 21, № 4, pp. 185-192 (In Russ). doi: 10.32364/2311-7729-2024-24-4-4.
13. Saakian S.V., Amirian A.G., Valsky V.V., Mironova I.S. Plaque radiotherapy for anterior uveal melanomas. *Russian Annals of Ophthalmology,* 2015, vol. 131, №2, pp. 5-12 (In Russ). doi: 10.17116/oftalma201513125-11.
14. Boiko E.V., Samkovich E.V., Panova I.E., Svistunova E.M., Ivanov A.A., Bikhovsky A.A. Hybrid photodynamic therapy as part of combined treatment for uveal melanoma (preliminary results). *Ophthalmology in Russia,* 2024, vol. 21, №4, pp. 755–763 (In Russ). doi: 10.18008/1816-5095-2024-4-755-763.
15. Belyj J.A., Tereshhenko A.V., Volodin P.L., Kaplan M.A. Fotodinamicheskaja terapija s fotosensibilizatorom Fotoditazin v oftal'mologii. *Kaluga: MNTK "Mikrohirurgija glaza",* 2008 (In Russ).
16. Zhyliayeva K.P., Demeshko P.D., Navumenka L.V., Krasny S.A., Tzerkovsky D.A., Zherko I.Yu. Photodynamic therapy of primary and recurrent forms of weakly pigment choroidal melanoma. *Biomedical Photonics,* 2022, vol. 11, №3, pp. 17-23 (In Russ). doi: 10.24931/2413-9432-2022-11-3-17-23.

ЛИТЕРАТУРА

1. Клинические рекомендации «Увеальная меланома». 2020. Ссылка активна на 07.01.2023. https://oncology-association.ru/wp-content/uploads/2020/09/uvealnaja_melanoma.pdf
2. Бровкина А.Ф. Локальное лечение меланом хориоидеи: возможности и ограничения // Вестник офтальмологии. – 2018. – Т. 134. № 4. – С. 52-60. doi: 10.17116/oftalma201813404152.
3. Саакян С.В., Цыганков А.Ю., Амирян А.Г. Витальный прогноз у пациентов с цилиохориоидальной локализацией увеальной меланомы // Голова и шея. Российское издание. Журнал Общероссийской общественной организации Федерация специалистов по лечению заболеваний головы и шеи. – 2016. – Т. 1-2. – С. 20-23.
4. Гришина Е.Е., Ким И.Д., Изотова Е.Н. Эписклеральное распространение цилиохориоидальной меланомы после оперативных вмешательств: клиническое наблюдение // РМЖ. Клиническая офтальмология. – 2023. – Т. 23. № 2. – С. 107-110. doi: 10.32364/2311-7729-2023-23-2-107-110.
5. Панова И.Е., Воробьев Н.А., Самкович Е.В., Свистунова Е.М., Мартынова Н.И., Быховский А.А. Протонотерапия увеальной меланомы (предварительные результаты) // Офтальмохирургия. – 2023. – Т. 3s. – С. 90-101. doi: 10.25276/0235-4160-2023-3s-90-101.
6. Саакян С.В., Ченцова Е.В., Андреева Е.А. Функциональные исходы у больных с опухолями иридоцилиарной зоны после блокэксцизий с одномоментной и отсроченной экстракцией катаракты // Российский офтальмологический журнал. – 2010. – Т. 3. № 1. – С. 23-28.
7. Lee S.M., Kim M. Surgical treatment of uveal melanoma: Exoresection versus endoresection // Taiwan J. Ophthalmol. – 2025. – Vol. 6.15. №1. – P. 34-44. doi: 10.4103/tjo.TJO-D-24-00131.
8. Romano M.R., Ferrara M., Feo A., Merico A., Angi M. Optimizing Surgical Performance and Safety in Endoresection of Uveal Melanoma // Retina. – 2025. – Vol. 1.45. №6. – P. 1230-1235. doi: 10.1097/IAE.0000000000004273.
9. Banou L., Tsani Z., Arvanitogiannis K., Pavlaki M., Dastiridou A., Androudi S. Radiotherapy in Uveal Melanoma: A Review of Ocular Complications // Curr Oncol. – 2023 Jul. – Vol. 3.30. №7. – P. 6374-6396. doi: 10.3390/curroncol30070470.
10. Fleury E., Pignol J.P., Kiliç E., Milder M., van Rij C., Naus N., Yavuzyigitoglu S., den Toom W., Zolnay A., Spruijt K., van Vulpen M., Trnková P., Hoogeman M. Comparison of stereotactic radiotherapy and protons for uveal melanoma patients // Phys. Imaging Radiat. Oncol. – 2024. – Vol. 26.31. – P. 100605. doi: 10.1016/j.phro.2024.100605.
11. Панова И.Е., Быховский А.А., Самкович Е.В., Свистунова Е.М. Глюкокортикостероиды и постлучевой макулярный отек: обоснование выбора терапии и эффективность применения // Офтальмология. – 2024. – Т. 21. №3. – С. 533-539. doi: 10.18008/1816-5095-2024-3-533-539.
12. Панова И.Е., Свистунова Е.М., Воробьев Н.А., Самкович Е.В., Мартынова Н.И., Быховский А.А. Неоваскулярная глаукома как осложнение протонной терапии увеальной меланомы // Клиническая офтальмология. – 2024. – Т. 24. №4. – С.185-192. doi: 10.32364/2311-7729-2024-24-4-4.
13. Саакян С.В., Амирян А.Г., Вальский В.В., Миронова И.С. Брахитерапия увеальной меланомы передней локализации // Вестник офтальмологии. – 2015. – Т. 131. №2. – С. 5-12. doi: 10.17116/oftalma201513125-11.
14. Бойко Э.В., Самкович Е.В., Панова И.Е., Свистунова Е.М., Иванов А.А., Быховский А.А. Гибридная фотодинамическая терапия как компонент комбинированного лечения увеальной меланомы (предварительные результаты) // Офтальмология. – 2024. – Т. 21. №4. – С. 755-763. doi: 10.18008/1816-5095-2024-4-755-763.
15. Белый Ю.А., Терещенко А.В., Володин П.Л., Каплан М.А. Фотодинамическая терапия с фотосенсибилизатором «Фотодитазин» в офтальмологии // Под ред. проф. Х.П. Тахчиди. – Калуга. – 2008.
16. Жиляева Е.П., Демешко П.Д., Науменко Л.В., Красный С.А., Церковский Д.А., Жерко И.Ю. Фотодинамическая терапия первич-

17. Samkovich E.V., Panova I.E., Boiko E.V., Svistunova E.M., Bykhovskii A.A. Photodynamic therapy in the combined treatment of choroidal melanoma. *Fyodorov Journal of Ophthalmic Surgery,* 2024, vol. 139, №2, pp. 99–108 (In Russ). doi: 10.25276/0235-4160-2024-2-99-108.
18. Yordi S., Soto H., Bowen R.C., Singh A.D. Photodynamic therapy for choroidal melanoma: What is the response rate? *Surv Ophthalmol,* 2021 Jul-Aug, vol. 66, №4, pp. 552-559. doi: 10.1016/j.survophthal.2020.09.006.
19. Navumenka L.V., Zhyliayeva E.P. Transpupillary Photodynamic Therapy of the Uveal Melanoma. *Ophthalmology. Eastern Europe,* 2020, vol. 10, №4, pp. 489–500. doi: 10.34883/PI.2020.10.4.021.
20. Bely Yu.A., Tereshchenko A.V., Volodin P.L. Transpupillary photodynamic therapy of medium-sized choroidal melanoma with the drug «Photoditazine» (clinical case). *Refractive surgery and ophthalmology,* 2008, vol. 8, №1, pp. 22–26 (In Russ).
21. Panova I.E., Boiko E.V., Samkovich E.V., Gvazava V.G. Isolated Transpupillary Photodynamic Therapy in Local Treatment of Choroidal Melanoma. *Ophthalmology in Russia,* 2025, vol.22, №1, pp. 159-168 (In Russ). doi: 10.18008/1816-5095-2025-1-159-168.
22. Boiko E.V., Samkovich E.V., Panova I.E., Shevchenko S.B., Vorobyev S.L., Kalashnikova E.S., Masian E.A., Gvazava V.G. Transscleral Photodynamic Therapy with a Chlorin e6 Photosensitizer in a Rabbit Experimental Model of an Intraocular Mass Lesion: TS-PDT in experimental ocular mass lesion model. *Journal of Lasers in Medical Sciences,* 2025, vol. 16, p. e26. Retrieved from https://journals.sbmu.ac.ir/jlms/article/view/47901.
23. Samkovich E.V., Boiko E.V., Panova I.E., Vorobiev S.L., Bikhovsky A.A., Masian E.A. Experimental and morphological justification of approaches to hybrid photodynamic therapy of uveal melanoma. *Voprosy Onkologii = Problems in Oncology,* 2025, vol. 71, № 2, pp. 325-333 (In Russ). doi: 10.37469/0507-3758-2025-71-2-325-333.
24. Li X., Lovell J.F., Yoon J., Chen X. Clinical development and potential of photothermal and photodynamic therapies for cancer. *Nat Rev Clin Oncol,* 2020, vol. 17, №11, pp.657-674. doi: 10.1038/s41571-020-0410-2.
25. Grin M., Suvorov N., Ostroverkhov P., Pogorilyy V., Kirin N., Popov A., Sazonova A., Filonenko A. Advantages of combined photodynamic therapy in the treatment of oncological diseases. *Biophysical Reviews,* 2022, vol. 14, № 4, pp. 941-963. doi: 10.1007/s12551-022-00962-6.
26. Lim H.S. Reduction of thermal damage in photodynamic therapy by laser irradiation techniques. *J. Biomed. Opt.,* 2012, vol. 17, №12, p. 128001. doi: 10.1117/1.JBO.17.12.128001.
27. Blasi M.A., Pagliara M.M., Lanza A., Sammarco M.G., Caputo C.G., Grimaldi G., Scupola A. Photodynamic Therapy in Ocular Oncology. *Biomedicines,* 2018, vol. 6, №1, p. 17. doi: 10.3390/biomedicines6010017.
28. Zhou Z., Song J., Nie L., Chen X. Reactive oxygen species generating systems meeting challenges of photodynamic cancer therapy. *Chem Soc Rev,* 2016, vol. 21, 45, №23, pp. 6597-6626. doi: 10.1039/c6cs00271d.
29. Stranadko E.F., Baranov A.V., Duvansky V.A., Lobakov A.I., Morokhotov V.A., Riabov M.V. Photodynamic therapy of cancer of large duodenal papilla and extrahepatic bile ducts. *Biomedical Photonics,* 2020, vol. 9, №2, pp. 18-28. doi: 10.24931/2413-9432-2020-9-2-18-28.
30. Panova I.E., Samkovich E.V., Nechiporenko P.A. Doppler ultrasound in the assessment of blood supply to choroidal melanoma: parallels with contrast angiography and histography. *Russian Annals of Ophthalmology,* 2023, vol. 139, №1, pp. 27-34 (In Russ). doi: 10.17116/oftalma202313901127.
31. Patent 2745691 C1 Russian Federation, IPC A61B 8/10, A61F 9/00. Method for assessing the vascularization of choroidal melanoma based on its acoustic density: no. 2020125755: filed 03.08.2020: publ. 30.03.2021 / E. V. Boiko, I. E. Panova, E. V. Samkovich; applicant Federal State Autonomous Institution "National Medical Research Center "Interbranch Scientific and Technical Complex "Eye Microsurgery" named after

ных и рецидивных слабопигментных форм меланомы сосудистой оболочки глаза // Biomedical Photonics. – 2022. – Т. 11. №3. – С. 17-23. doi: 10.24931/2413-9432-2022-11-3-17-23.
17. Самкович Е.В., Панова И.Е., Бойко Э.В., Свистунова Е.М., Быховский А.А. Фотодинамическая терапия в комбинированном лечении меланомы хориоидеи // Офтальмохирургия. – 2024. – Т.139 №2. – С. 99–108. doi: 10.25276/0235-4160-2024-2-99-108.
18. Yordi S., Soto H., Bowen R.C., Singh A.D. Photodynamic therapy for choroidal melanoma: What is the response rate? // Surv Ophthalmol. – 2021. – Vol. 66. №4. – P. 552-559. doi: 10.1016/j.survophthal.2020.09.006.
19. Науменко Л.В., Жиляева Е.П. Транспупиллярная фотодинамическая терапия меланомы сосудистой оболочки глаза // Офтальмология. Восточная Европа. – 2020. – Т. 10. №4. – С. 489–500. doi: 10.34883/PI.2020.10.4.021.
20. Белый Ю.А., Терещенко А.В., Володин П.Л. Транспупиллярная фотодинамическая терапия меланомы хориоидеи средних размеров с препаратом «Фотодитазин» (клинический случай) // Рефракционная хирургия и офтальмология. – 2008. – Т. 8. №1. – С. 22–26.
21. Панова И.Е., Бойко Э.В., Самкович Е.В., Гвазава В.Г. Изолированная транспупиллярная фотодинамическая терапия в локальном лечении меланомы хориоидеи // Офтальмология. – 2025. – Т. 22. №1. – С. 159-168. doi: 10.18008/1816-5095-2025-1-159-168.
22. Boiko E.V., Samkovich E.V., Panova I.E., Shevchenko S.B., Vorobyev S.L., Kalashnikova E.S., Masian E.A., Gvazava V.G. Transscleral Photodynamic Therapy with a Chlorin e6 Photosensitizer in a Rabbit Experimental Model of an Intraocular Mass Lesion: TS-PDT in experimental ocular mass lesion model // Journal of Lasers in Medical Sciences. – 2025. – Vol. 16. – P. e26. Retrieved from https://journals.sbmu.ac.ir/jlms/article/view/47901
23. Самкович Е.В., Бойко И.Е., Панова И.Е., Воробьев С.Л., Быховский А.А., Масиан Е.А. Экспериментально-морфологическое обоснование подходов к гибридной фотодинамической терапии увеальной меланомы // Вопросы онкологии. – 2025. – Т. 71. № 2. – С. 325-333. doi: 10.37469/0507-3758-2025-71-2-325-333.
24. Li X., Lovell J.F., Yoon J., Chen X. Clinical development and potential of photothermal and photodynamic therapies for cancer // Nat. Rev. Clin. Oncol. – 2020. – Vol. 17. №11. – P. 657-674. doi: 10.1038/s41571-020-0410-2.
25. Grin M., Suvorov N., Ostroverkhov P., Pogorilyy V., Kirin N., Popov A., Sazonova A., Filonenko A. Advantages of combined photodynamic therapy in the treatment of oncological diseases // Biophysical Reviews. – 2022. – Vol. 14. № 4. – P. 941-963. doi: 10.1007/s12551-022-00962-6.
26. Lim H.S. Reduction of thermal damage in photodynamic therapy by laser irradiation techniques // J. Biomed. Opt. – 2012. – Vol. 17. №12. – P. 128001. doi: 10.1117/1.JBO.17.12.128001.
27. Blasi M.A., Pagliara M.M., Lanza A., Sammarco M.G., Caputo C.G., Grimaldi G., Scupola A. Photodynamic Therapy in Ocular Oncology // Biomedicines. – 2018. – Vol. 6. №1. – P. 17. doi: 10.3390/biomedicines6010017.
28. Zhou Z., Song J., Nie L., Chen X. Reactive oxygen species generating systems meeting challenges of photodynamic cancer therapy // Chem. Soc. Rev. – 2016. – Vol. 21;45. №23. – P. 6597-6626. doi: 10.1039/c6cs00271d.
29. Странадко Е.Ф., Баранов А.В., Дуванский В.А., Лобаков А.И., Морохотов В.А., Рябов М.В. Фотодинамическая терапия рака большого дуоденального сосочка и внепечёночных желчных протоков // Biomedical Photonics. – 2020. – Т. 9. №2. – С. 18-28. doi: 10.24931/2413-9432-2020-9-2-18-28.
30. Панова И.Е., Самкович Е.В., Нечипоренко П.А. Ультразвуковая допплерография в оценке кровоснабжения меланомы хориоидеи: параллели с контрастной ангиографией и гистографией // Вестник офтальмологии. – 2023. – Т. 139 №1. – С. 27-34. doi: 10.17116/oftalma202313901127.
31. Патент № 2745691 C1 Российская Федерация, МПК A61B 8/10, A61F 9/00. Способ оценки васкуляризации меланомы хориоидеи по её акустической плотности: № 2020125755: заявл. 03.08.2020: опубл. 30.03.2021 / Э. В. Бойко, И. Е. Панова, Е. В. Самкович; заявитель Федеральное государственное автономное учреждение "Национальный медицинский исследовательский центр "Межотраслевой научно-технический ком-

Academician S.N. Fedorov" of the Ministry of Health of the Russian Federation.
32. Quirk B.J., Brandal G., Donlon S., Vera J.C., Mang T.S., Foy A.B., Lew S.M., Girotti A.V., Jogal S., LaViolette P.S., Connely J.M., Whelan H.T. Photodynamic therapy (PDT) for malignant brain tumors--where do we stand? *Photodiagnosis Photodyn. Ther.,* 2015, vol. 12, №3, pp. 530-44. doi: 10.1016/j.pdpdt.2015.04.009.
33. Ferreira J., Menezes P.F.C., Sibata C.H., Allison R.R., Zucoloto S., Castro e Silva J.R.O. et al. Can efficiency of the photosensitizer be predicted by its photostability in solution? *Laser Phys,* 2009, p. 1-7. doi: 10.1590/S1516-80342009000100003.
34. Kwiatkowski S., Knap B., Przystupski D., Saczko J., Kędzierska E., Knap-Czop K. et al. Photodynamic therapy – mechanisms, photosensitizers and combinations. *Biomed. Pharmacother.,* 2018, vol. 106, pp. 1098-1107. doi: 10.1016/j.biopha.2018.07.049.
35. Filonenko E.V. Clinical implementation and scientific development of photodynamic therapy in Russia in 2010-2020. *Biomedical Photonics,* 2021, vol.10, №4, pp.4-22 (In Russ). doi: 10.24931/2413-9432-2021-9-4-4-22.
36. Dereski M.O., Chopp M., Garcia J.H., Hetzel F.W. Depth measurements and histopathological characterization of photodynamic therapy generated normal brain necrosis as a function of incident optical energy dose. *Photochem. Photobiol.,* 1991 Jul, vol. 54, №1, pp. 109-12. doi: 10.1111/j.1751-1097.1991.tb01992.x.
37. Muller P.J., Wilson B.C. An update on the penetration depth of 630 nm light in normal and malignant human brain tissue in vivo. *Phys. Med. Biol.,* 1986 Nov, vol. 31, №11, pp. 1295-7. doi: 10.1088/0031-9155/31/11/012.

плекс "Микрохирургия глаза" имени академика С.Н. Федорова" Министерства здравоохранения Российской Федерации. – EDN ZRGJXS.
32. Quirk B.J., Brandal G., Donlon S., Vera J.C., Mang T.S., Foy A.B., Lew S.M., Girotti A.V., Jogal S., LaViolette P.S., Connely J.M., Whelan H.T. Photodynamic therapy (PDT) for malignant brain tumors--where do we stand? // Photodiagnosis Photodyn. Ther. – 2015 Sep. – Vol. 12. №3. – P. 530-44. doi: 10.1016/j.pdpdt.2015.04.009.
33. Ferreira J., Menezes P.F.C., Sibata C.H., Allison R.R., Zucoloto S., Castro e Silva J.R.O. et al. Can efficiency of the photosensitizer be predicted by its photostability in solution? // Laser Phys. – 2009. – P. 1—7. doi: 10.1590/S1516-80342009000100003.
34. Kwiatkowski S., Knap B., Przystupski D., Saczko J., Kędzierska E., Knap-Czop K. et al. Photodynamic therapy – mechanisms, photosensitizers and combinations // Biomed Pharmacother. – 2018. – Vol. 106. – P. 1098-1107. doi: 10.1016/j.biopha.2018.07.049.
35. Филоненко Е.В. Клиническое внедрение и научное развитие фотодинамической терапии в России в 2010-2020 гг. // Biomedical Photonics. – 2021. – Т. 10. №4. – С. 4-22. doi: 10.24931/2413-9432-2021-9-4-4-22.
36. Dereski M.O., Chopp M., Garcia J.H., Hetzel F.W. Depth measurements and histopathological characterization of photodynamic therapy generated normal brain necrosis as a function of incident optical energy dose // Photochem. Photobiol. – 1991. – Vol. 54. №1. – P. 109-12. doi: 10.1111/j.1751-1097.1991.tb01992.x. PMID: 1835100.
37. Muller P.J., Wilson B.C. An update on the penetration depth of 630 nm light in normal and malignant human brain tissue in vivo // Phys. Med. Biol. – 1986. – Vol. 31. №11. – P. 1295-7. doi: 10.1088/0031-9155/31/11/012.

ORIGINAL ARTICLES

SEARCH FOR CORRELATIONS IN RAMAN, DIFFUSE REFLECTANCE, AND FLUORESCENCE SPECTROSCOPY DATA FROM INTRACRANIAL TUMORS

Ospanov A.[1], Romanishkin I.D.[2], Savelieva T.A.[1,2], Shugay S.V.[3], Kosyrkova A.V.[3], Pavlova G.V.[3,4], Pronin I.N.[3], Loschenov V.B.[1,2]
[1]National Research Nuclear University MEPhI (Moscow Engineering Physics Institute), Moscow, Russia
[2]Prokhorov General Physics Institute of Russian Academy of Sciences, Moscow, Russia
[3]N.N. Burdenko National Medical Research Center of Neurosurgery, Moscow, Russia
[4]Institute of Higher Nervous Activity and Neurophysiology of the Russian Academy of Sciences, Moscow, Russia

Abstract

The task of developing a decision support system in neurooncology based on optical-spectral analysis of intracranial tumor tissue is associated with several challenges inherent in working with biomedical data. These include the high dimensionality of the feature vector with a relatively small sample size, data gaps, and sample imbalances due to the varying frequencies of various diagnoses. Analysis of correlations between features of the tumors under study will allow both the restoration of data gaps and their augmentation (artificial expansion of the training dataset by creating modified versions of existing examples). This paper presents an analysis of the dependence of various optical-spectral characteristics on the tumor cell/tissue content in the sample and the cross-correlations between various features.

Key words: glial tumor, optical spectroscopy, Raman scattering, diffuse reflectance, fluorescence.

Contacts: Ospanov A., e-mail: ospanovanuar99@gmail.com

For citations: Ospanov A., Romanishkin I.D., Savelieva T.A., Shugay S.V., Kosyrkova A.V., Pavlova G.V., Pronin I.N., Loschenov V.B. Search for correlations in raman, diffuse reflectance, and fluorescence spectroscopy data from intracranial tumors, *Biomedical Photonics*, 2025, vol. 14, no. 4, pp. 22–33. doi:10.24931/2413–9432–2025–14-4-22-33

ПОИСК КОРРЕЛЯЦИЙ В ДАННЫХ СПЕКТРОСКОПИИ КОМБИНАЦИОННОГО РАССЕЯНИЯ, ДИФФУЗНОГО ОТРАЖЕНИЯ И ФЛУОРЕСЦЕНЦИИ ТКАНЕЙ ВНУТРИЧЕРЕПНЫХ ОПУХОЛЕЙ

А. Оспанов[1], И.Д. Романишкин[2], Т.А. Савельева[1,2], С.В. Шугай[3], А.В. Косырькова[3], Г.В. Павлова[3,4], И.Н. Пронин[3], В.Б. Лощенов[1,2]
[1]Национальный исследовательский ядерный университет «МИФИ» (Московский инженерно-физический институт), Москва, Россия
[2]Институт общей физики им. А.М. Прохорова Российской академии наук, Москва, Россия
[3]Национальный медицинский исследовательский центр нейрохирургии имени академика Н. Н. Бурденко, Москва, Россия
[4]Институт высшей нервной деятельности и нейрофизиологии Российской академии наук, Москва, Россия

Резюме

Задача построения системы поддержки принятия решений в нейроонкологии на основе оптико-спектрального анализа тканей внутричерепных опухолей сопряжена с некоторыми сложностями, свойственными работе с биомедицинскими данными. Среди них – высокая размерность вектора признаков при относительно малом объеме выборки, пропуски в данных, а также несбалансирован-

ность выборок из-за разной частоты встречаемости различных диагнозов. Анализ корреляций между признаками исследуемых опухолей позволит выполнять как восстановление пропусков в данных, так и их аугментацию (искусственное расширение обучающего набора данных путём создания модифицированных версий имеющихся примеров). В данной работе представлен анализ зависимости различных оптико-спектральных характеристик от содержания опухолевых клеток/ткани в образце и взаимных корреляций между различными признаками.

Ключевые слова: глиальная опухоль, оптическая спектроскопия, комбинационное рассеяние, диффузное отражение, флуоресценция.

Контакты: Оспанов А., e-mail: ospanovanuar99@gmail.com

Для цитирования: Оспанов А., Романишкин И.Д., Савельева Т.А., Шугай С.В., Косырькова А.В., Павлова Г.В., Пронин И.Н., Лощенов В.Б. Поиск корреляций в данных спектроскопии комбинационного рассеяния, диффузного отражения и флуоресценции тканей внутричерепных опухолей // Biomedical Photonics. – 2025. – Т. 14, № 4. – С. 22–33. doi: 10.24931/2413-9432-2025-14-4-22-33

Introduction

Determining the boundaries of intracranial tumors is a central problem in neuro-oncology today. The magnetic resonance imaging (MRI) is limited as intraoperative tools, and ultrasound does not provide information on tumor metabolic parameters. Therefore, intraoperative optical neuroimaging [1-3] and laser spectroscopy [4,5] have become increasingly important.

Fluorescence spectroscopy techniques are highly dependent on the photosensitizer concentration in the tissue being examined. If the photosensitizer has not accumulated in sufficient quantities in the tissue, fluorescence analysis may be uninformative. Raman spectroscopy (RS) can be a useful complement to fluorescence diagnostic methods. RS does not require photosensitizer accumulation. However, due to the specific features of Raman spectra, namely, the large number of significant peaks and lower signal intensity compared to fluorescence, Raman spectra require more complex signal preprocessing and statistical analysis of the results [6].

Machine learning methods can be used to preprocess and analyze measurement results, particularly Raman spectra. A brief overview of simple machine learning methods for preprocessing data obtained from IR and Raman spectra is provided in [7]. Dimensionality reduction algorithms are one such method. It is the process of reducing the size of a feature vector. A set of features can be a dataset with hundreds of columns or an array of points that form a large sphere in three-dimensional space. As the number of features increases, the number of dimensions also increases proportionally. The more features describe one object, the more objects in the sample we need to ensure that all combinations of feature values are well represented.

Machine learning algorithms can also be used for data analysis, which can be divided into supervised and unsupervised learning. Unsupervised learning works on unlabeled data, without human intervention. An example of an unsupervised learning approach is data clustering. Supervised learning is a method in which a model learns to solve problems based on examples with known answers.

In [6], dimensionality reduction and clustering algorithms were considered for data obtained using fluorescence, diffuse reflectance, and Raman scattering from intracranial tumor biopsies. It shows that an algorithm without training on unlabeled data can distinguish meningeal and glial tumors with good accuracy. The use of more advanced algorithms will make it possible to distinguish between the types and stages of tumors.

Machine learning methods for spectroscopy have become widespread. In [8], neural network algorithms were applied to data obtained using surface-enhanced Raman scattering for pathogen recognition. An excellent example of data classification using machine learning is the work [9], where for classification random forest algorithms and the gradient boosting tree method were used. The objects of classification were Raman spectroscopy data obtained from fresh specimens of glial tumors, which overlaps with the objects studied in our article. Analysis of the application of machine learning methods to spectrally resolved data in neurooncology [10,11] shows that they can be successfully applied to the classification of intracranial tumors, which is what we aim to achieve.

However, we would like to move from classical machine learning methods to neural network-based ones, but the number of experimental specimens we've analyzed to date is insufficient. Samples for different diagnoses vary significantly in the number of specimens they contain. To overcome these limitations in the application of neural network algorithms, we propose expanding groups with small numbers of objects with artificial data – in other words, data augmentation. To successfully implement augmentation, as well as to study the relationships between measured data, we decided to conduct a correlation analysis of the available data, which is the focus of this article.

Interesting application of correlation analysis is presented in the work [12], in which the authors examine brain gliomas and calculate correlation coefficients to validate a previously studied machine learning algorithm that sequentially generates a cellularity prediction map.

Materials and methods

Biological specimens

In total (after removing outliers), more than 250 fresh tissue samples from intracranial brain tumors (hereinafter referred to as biopsies) were examined. Of these, the following were diagnosed:

- Meningioma – 66 specimens (38 – grade I, 21 – grade II, 7 – grade III);
- Glioblastoma – 112 specimens;
- Oligodendrogliomas – 32 specimens (4 with unknown grade; 8 – grade II; 20 – grade III);
- Astrocytomas – 41 specimens (12 with unknown grade; 1 – grade I; 2 – grade II; 26 – grade III).

Experimental stand for spectral analysis

A He-Ne laser (632.8 nm wavelength) and a diode laser (405 nm wavelength) were used to excite the fluorescence signal in biological samples. LESA-01-BIOSPEC spectrometers with optical edge filters attenuating the excitation light (632.8 and 405 nm) at the spectrometer input to the fluorescence signal level were used to record the fluorescence spectra. An optical fiber was used to deliver the laser signal. A halogen lamp and a LESA-01-BIOSPEC spectrometer were used as a white light source to record diffuse reflectance. Raman spectra were measured using a Raman-HR-TEC-785 spectrometer (StellarNet, USA; spectral range 200–2750 cm^{-1}, resolution 4 cm^{-1}), a Ramulaser-785 laser source (StellarNet, USA; 785 nm), and a fiber-optic confocal probe for delivering laser radiation and a Raman signal. The laser peak width is 0.2 nm; power up to 500 mW. Spectral measurements were performed in a darkened room.

Sample collection protocol

The sampling protocol was presented in the following steps:

1. Transfer of brain tumor fragments (biopsy specimens) removed by the surgeon during surgery (cleaned of extrinsic material and placed in saline) to the cryopreservation laboratory for preliminary tissue characterization prior to freezing. Prior to spectroscopic measurements, the specimen is kept at 4°C (specimens were measured no later than 4 hours later).
2. Selection of one to three fragments of 2-5 mm in diameter from the available tumor material. If a fragment is larger than the dimensions described above, it is divided into parts, as larger fragments may have inhomogeneous structure.
3. Darkening the room and measuring the background signal (baseline) of the Raman spectrometer for subsequent software exclusion.
4. Calibration of fluorescence spectrometers (LESA with filters at 405 and 632.8 nm) by wavelengths using 3 lasers: 405, 532, 632.8 nm.
5. The fluorescence spectra of protoporphyrin IX (Pp IX) and the autofluorescence spectra are measured using the LESA-01-BIOSPEC spectrometer (Biospec, Russia) using a common algorithm: the appropriate laser (632.8 nm or 405 nm) is turned on, the distal end of the light guide is brought into soft contact with the sample, and several spectra from different points on each sample are recorded (approximately six measurements). The exposure time is 100 ms.
6. Measurement of diffuse reflectance spectra is performed using a LESA-01-BIOSPEC spectrometer (with a halogen lamp as a white light source) and includes measurement of the baseline, the reference signal in the reflectance mode from a white sample (barium sulfate), measurement of spectra from an object in the diffuse reflectance mode (with the distal end of the light guide in soft contact with the sample, several (about 6) measurements are made for each sample).
7. Measurements of Raman spectra are performed with an exposure of 30 s, 10 measurements from each sample (the power of the 785 nm laser is 150 mW).
8. After measurements, the sample is placed in formalin and given to a morphologist for histological examination.

The process of sampling and recording optical spectra was carried out in the Department of Cryopreservation and Molecular Genetic Analysis of the N.N. Burdenko National Medical Research Center of Neurosurgery.

Spectrum processing

Uno software (Biospec, Russia) was used to process fluorescence and diffuse reflectance spectra. Processing of Raman spectra and subsequent analysis of both fluorescence, diffuse reflectance, and Raman spectra were performed using specialized software developed in Python within the Jupiter Notebook environment.

Components of feature vector were extracted from fluorescence, diffuse reflectance, and Raman spectra. A matrix was formed from the feature vectors of the specimens, which is used for data analysis (in this case, for correlation analysis).

From fluorescence excited by a 632.8 nm laser, backscatter (diffuse reflectance) of laser radiation and Pp IX fluorescence were extracted as features.

From fluorescence excited by a 405 nm laser, diffuse reflectance (diffuse reflectance) of laser radiation and the fluorescence of FAD and porphyrins were extracted. The contribution of diffuse reflectance of broadband radiation to the feature vector is represented by hemoglobin absorption, its oxygen saturation, and the scattering coefficient.

The largest number of feature vector components were taken from the Raman spectra. When choosing which data from the Raman spectra to take as features, the authors relied on the work [7] and also searched for biochemical components that showed the presence of statistically significant differences between the groups [13]. The following biochemical components were taken from the Raman spectra as features: cholesterol; phospholipid; lipids; carotenoids; heme/hemoglobin; oxygenated heme/hemoglobin; proteins; phenylalanine.

Explanation of legenda on Figures for feature vector components are given in Table.

A more detailed description of the methodology is given in our previous works [14,15].

Correlation analysis

Correlation analysis is a statistical method for determining the relationship between two sets of variables (in this case, features in feature vector). The key parameter of this method is the correlation coefficient, which indicates the type of relationship. The correlation coefficient can take values from –1 to 1. Values close to –1 indicate an inverse relationship between the variables, values close to 1 indicate a direct relationship, and values close to 0 indicate no relationship. A very important parameter related to the correlation coefficient is its statistical significance. It allows one to assess the validity of the conclusion

Таблица
Список основных оптико-спектральных параметров и их условных обозначений
Table
List of main optical-spectral parameters and their symbols

Условное обозначение Legend	Оптико-спектральные параметры Optical-spectral parameters
backscatter_633	Обратное рассеяние от 632,8 нм лазера Diffuse reflectance of 632.8 nm laser light
fluo_633	Флуоресценция от 632,8 нм лазера (ассоциированная с протопорфирином IX) Fluorescence excited with 633 nm laser light (associated with Pp IX)
backsca_405	Обратное рассеяние от 405 нм лазера Diffuse reflectance of 405 nm laser light
fluo_405_fad	Флуоресценция флавинов, преимущественно ФАД (флавинадениндинуклеотида) от 405 нм лазера Fluorescence excited with 405 nm laser light (associated with flavins, mainly FAD)
fluo_405_porph	Флуоресценция от 405 нм лазера (ассоциированная с протопорфирином IX) Fluorescence excited with 405 nm laser light (associated with Pp IX)
hemoglobin	Поглощение гемоглобина, определяемый по спектру диффузного отражения от белого источника Hemoglobin calculated from diffuse reflectance spectra
scattering	Коэффициент рассеяния, определяемый по спектру диффузного отражения от белого источника Scattering coefficient calculated from diffuse reflectance spectra
r_cholesterol	Комбинационное рассеяние от холестеринов Raman scattering from cholesterol
r_phospholipid	Комбинационное рассеяние от фосфолипидов Raman scattering from phospholipid
r_lipid	Комбинационное рассеяние от липидов Raman scattering from lipids
r_carothenoid	Комбинационное рассеяние от каротиноидов Raman scattering from carotenoids
r_heme	Комбинационное рассеяние от гема Raman scattering from heme
r_oxy_heme	Комбинационное рассеяние оксигинированного гема Raman scattering of oxygenated heme
r_protein	Комбинационное рассеяние от белков Raman scattering from proteins
r_phenylalanine	Комбинационное рассеяние от фенилаланина Raman scattering from phenylalanine

regarding the presence of a correlation relationship obtained using the correlation coefficient. The lower the significance value, the stronger the correlation relationship described by the correlation coefficient.

In this study, the Spearman rank correlation coefficient was used. This coefficient was chosen because the authors currently have a small amount of data. The Spearman rank correlation coefficient is calculated using formula (1):

$$\rho = \frac{\sum_{i=1}^{n}(x_i - \bar{x})(y_i - \bar{y})}{\sqrt{\sum_{i=1}^{n}(x_i - \bar{x})^2 (y_i - \bar{y})^2}}, \quad (1)$$

where n – number of observations; $\bar{x}$ и $\bar{y}$ – average values.

The statistical significance of the correlation coefficient (1) is determined using the Student's t-test according to the formula (2):

$$t = \frac{\rho\sqrt{(n-2)}}{\sqrt{(1-\rho^2)}}. \quad (2)$$

Calculations of correlation coefficients and their statistical significance were performed using Python programming language and the Jupiter Notebook programming environment. Correlation coefficients were calculated for all feature vectors with each other, as well as correlations between feature vectors and the tumor percentage (percentage of tumor cells) of the biopsy specimen. Fig. 1 shows a generalized diagram of the analysis of biomaterial and its spectral characteristics for the purpose of automating classification, which shows the place that the topic of this article has in this concept.

Results and discussion

Correlation of features with the percentage of tumor in the sample

In order to analyze the physiological correlates of the spectral characteristics of tumors, we carried out a study of the relationship between all known characteristics of the samples, such as features obtained from the pathological report (tumor type glioma/meningioma/oligodenroglioma, tumor grade, percentage of tumor in the sample) and from spectral analysis (presence of various biochemical components and optical characteristics).

The results of the pathomorphological examination allow us to analyze the correlations between the measured optical-spectral characteristics and the content of tumor or necrotic cells/tissue in the sample. Since classification results depend significantly on the percentage of tumor in the sample at which we classify it as a tumor, and the percentage of necrotic tissue at which we classify it as necrosis, we conducted studies of the threshold values for various characteristics.

Fig. 2 shows the summary results of the detected dependencies, which allowed us to identify so-called "healthy tissue correlates," that is, spectral characteristics that are higher in normal tissue, and "tumor tissue correlates," that is, parameters that are higher in tumor and necrotic tissue. A non-monotonous relationship with the percentage of tumor in the sample was also found for lipids and phospholipids, which was the subject of a separate study, described below.

We included carotenoids (r_carothenoid) and oxygenated hemoglobin (r_oxy_heme) among the healthy tissue correlates (Fig. 3a). The carotenoid

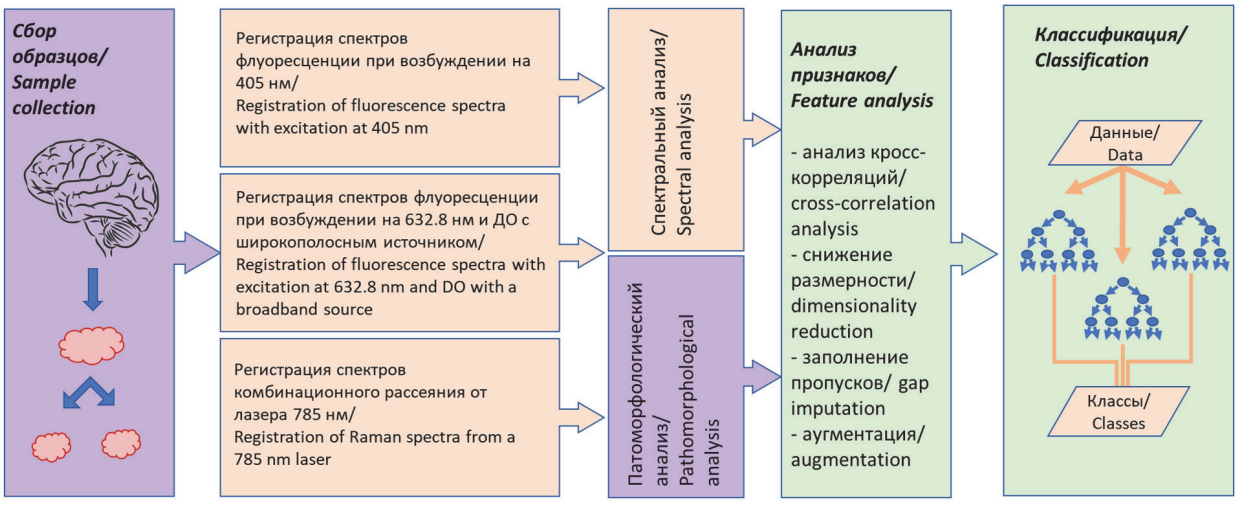

Рис. 1. Схема анализа образцов и данных при построении модели классификации внутричерепных опухолей по данным оптической спектроскопии.
Fig. 1. Scheme of sample and data analysis when constructing a model for classifying intracranial tumors based on optical spectroscopy data.

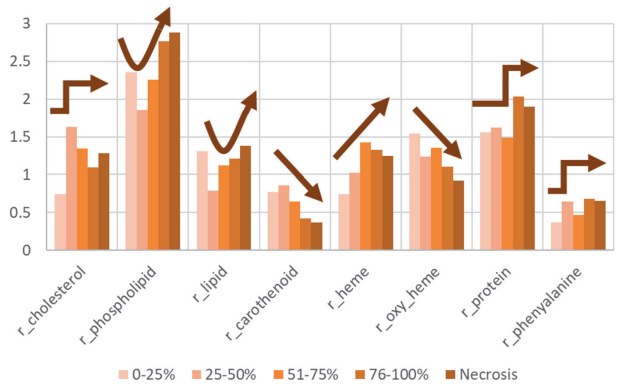

Рис. 2. Зависимость оптико-спектральных характеристик КР от содержания опухолевых тканей в образце.
Fig. 2. Dependence of optical-spectral characteristics from Raman spectra on the content of tumor tissue in the sample.

and oxygenated hemoglobin content in the samples inversely correlated with the percentage of tumor tissue in the sample, since carotenoids are a component of the antioxidant defense system in normal tissues, while tumor tissues are hypoxic. Previous studies have shown that carotenoid concentrations in plasma are inversely proportional to cancer risk in epidemiological and experimental studies. Carotenoids are specifically distributed in different lymphocyte subtypes. Zhou et al. [16] observed a clear decrease in the intensity of the 1157 and 1521 cm^{-1} peaks with an increase in the degree of malignancy of gliomas. Hypoxia also correlates with the degree of tumor malignancy [17].

When it comes to tumor tissue correlates, hemoglobin (r_heme) is, of course, the primary one. Blood volume correlates with the level of vascularization and the degree of malignancy in gliomas [18,19], and the density of microvessels in gliomas can be an independent prognostic factor [20, 21]. This is precisely the nature of the dependence on the tumorigenicity of the sample that we observe with a significance level of 1% for heme, determined using Raman spectroscopy (Fig. 3b).

In Fig. 3, we also see that cholesterol (r_cholesterol) increased with increasing tumor tissue content in the sample. However, the data spread was so wide that the significance level of differences between groups for this parameter was 18%. Tumor tissues were also characterized by higher protein content (r_protein). It should be noted that forming these groups required partitioning with different tumorigenicity thresholds:

- Cholesterol levels in specimens with 26% or more tumor tissues (including necrosis) are significantly higher than in specimens with 0–25% tumor tissues;

- Heme levels in specimens with 51% or more tumor tissues (including necrosis) are significantly higher than in specimens with 0–50% tumor tissues;
- Protein levels in specimens with 76% or more tumor tissues (including necrosis) are significantly higher than in specimens with 0–75% tumor tissues.

This suggests the need for a finer division of specimens into classes for some characteristics, as well as a continuous change in these characteristics in general.

Correlations between spectral features

Correlation coefficients for features were examined to identify relationships between them. For each pair of features, Spearman's rank correlation coefficients and

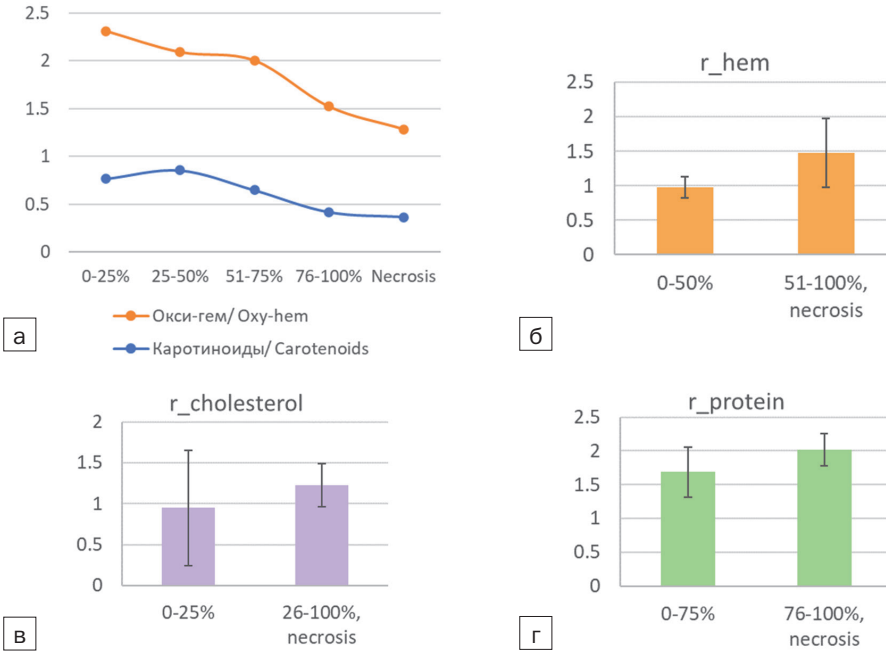

Рис. 3. Корреляты здоровых и опухолевых тканей (включая ткани с некротическими включениями).
Fig. 3. Correlates of healthy and tumor tissues (including tissues with necrosis).

statistical significance for each correlation coefficient were calculated. As a criterion of interest, as well as a certain statistical significance of the correlation between features, we took the threshold value of the rank correlation coefficient by modulus of 0.7 or higher, and the value of statistical significance of 0.05 or less. Feature vectors satisfying the above condition are called feature vectors satisfying the criterion of interest. Fig. 5-9 show graphs of the dependencies of feature vectors satisfying the criterion of interest with correlation coefficients and with the statistical significance of the correlation coefficients. A comparison was also made of the spectral features determined from the diffuse reflectance and Raman spectra, which showed a non-monotonic dependence on the content of tumor tissue in the sample.

Correlation of diffuse reflectance and Raman scattering features

In our previous study [15], we compared light scattering in tumors recorded intraoperatively and during studies in biobank. Similar patterns were demonstrated, with a minimum for the perifocal zone in intraoperative studies, which we compared with the light scattering minimum for samples containing 26–50% tumor tissue during data analysis in biobank. We explained this nontrivial behavior of the parameter by the gradual degradation of normal white matter during tumor development, which competes in its effect with the growth of tumor cell content. Light scattering in tissues occurs due to fluctuations in the refractive index of the medium. The main source of these fluctuations are lipids in cell membranes, which is especially relevant for the white matter of the brain, which comprises 50% of the myelin sheaths of nerve tracts. In this study, we compared these diffuse reflectance data with the results of lipid and phospholipid analysis, which, as shown in Fig. 2 and 4, also demonstrate a local minimum for the same samples. A study of the lipid and phospholipid content in tumor samples using Raman spectra revealed the same "saddle-shaped" dependence on the tumor percentage of the samples (Fig. 4).

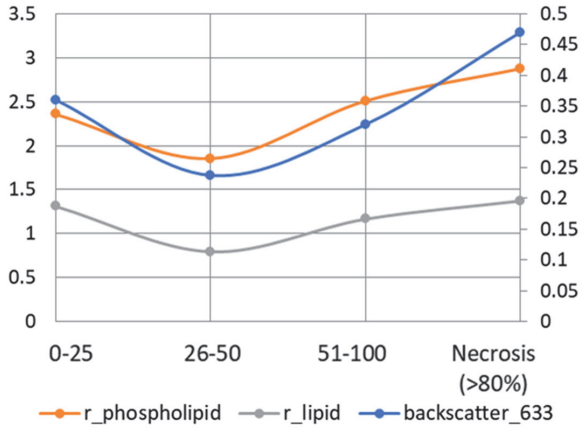

Рис. 4. Корреляция сигнала диффузного отражения и содержания липидов и фосфолипидов.
Fig. 4. Correlation of diffuse reflectance signal and content of lipid and phospholipid.

Meningiomas

66 samples diagnosed with meningioma were examined and analyzed in total. Of these, 38 were grade I meningiomas, 21 were grade II meningiomas, and 7 were grade III meningiomas.

Fig. 5 shows two dependences of features that meet the criteria of interest for grade I meningioma. A positive correlation is observed between the fluorescence of Pp IX (fluo_405_porph) and FAD (fluo_405_fad) upon excitation by laser radiation with a wavelength of 405 nm (Fig. 5a). In Fig. 5b, a direct correlation is observed between the Raman scattering of proteins (r_protein) and phospholipids (r_phospholipid). According to work [22], phospholipids in Raman spectra are most strongly manifested in the white matter of the brain, stronger in normal tissue, weaker in a tumor, but stronger in necrotic tissue than in a tumor. If we look at Fig. 2 in this article, we will see just such a non-monotonic dependence of the expression of the presence of phospholipids on the percentage of tumor in the sample with a local minimum falling approximately in the range of 25–50%. Moreover, the protein presence index demonstrates a fairly significant increase when moving to samples with a tumor prevalence of more than 50%. According to surface-enhanced Raman spectroscopy data [23], the presence of proteins is higher, including in glioblastomas.

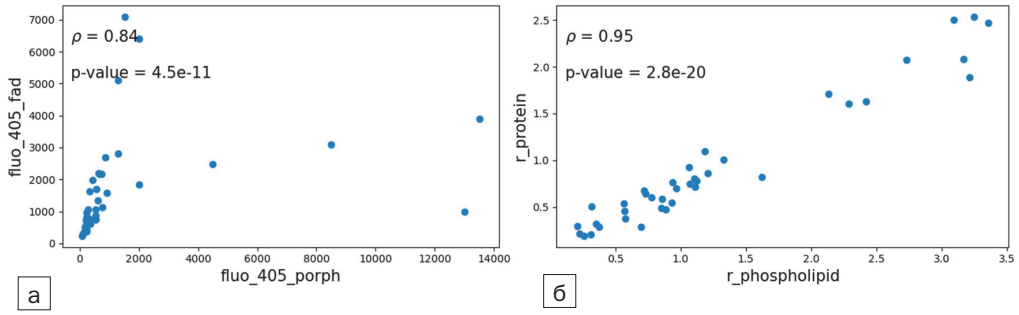

Рис. 5. Графики зависимости компонент вектора признаков, удовлетворяющих критерию интереса для менингиом I степени.
Fig. 5. Graphs of the dependence of the components of the feature vector satisfying the criterion of interest for grade I meningiomas.

Fig. 6a shows a correlation between PP IX (fluo_405_porph) and FAD (fluo_405_fad) similar to Fig. 5a. Work [24] showed that free FAD is present to a greater extent in grade II meningioma than protein-bound FAD, and it is more concentrated in grade II meningioma than grade I, while control samples show a higher frequency of protein-bound FAD and a decrease in the concentration of free FAD. In [25], fluorescence analysis was performed using a modified surgical microscope. Data were obtained on flavin fluorescence in the 500–580 nm range and the integrated fluorescence spectrum in the 430–740 nm range in freshly removed samples of various brain tumors: low- and high-grade gliomas, meningiomas, and metastases. It was shown that the fluorescence of protein-bound flavin mononucleotide (FMN) in brain tumors increased with a shift in metabolism toward a more glycolytic mode. These metrics were characteristic of various tumors and demonstrated the potential for their use in machine learning-based classification of brain tumors. The increased accumulation of Pp IX within tumor cells is likely due to the difference in cell proliferation between tumor and healthy tissues. In particular, porphobilinogen deaminase activity increases during replication [26]. Another enzyme with altered activity in tumor cells is ferrochelatase, whose reduced expression has been demonstrated in many tissues and tumors, including glioblastoma [27, 28]. This condition promotes a longer presence of Pp IX inside the cells, which may also be associated with the intensity of their fluorescence [29, 30]. Thus, the fluorescence correlation in this case appears to be consistent, and we can extend this pattern to all types of tumors analyzed in this work.

Glial tumors

A total of 185 glial tumors were examined. Of these: glioblastomas – 112; oligodendrogliomas – 28 (grade II – 8; grade III v 20; unknown grade – 4); astrocytomas – 41 (grade I – 1; grade II – 2; grade III – 26, unknown grade – 12).

Fig. 7 shows the cross-correlations of parameters for oligodendrogliomas, demonstrating the maximum relationship between the features. Among these, maximum values of the correlation coefficient are between the fluorescence of Pp IX (fluo_405_porph) and FAD (fluo_405_fad) upon excitation with a 405 nm laser (ρ = 0.97) and between the indices of protein (r_protein) and phospholipid (r_phospholipid) presence, calculated from Raman spectra (ρ = 0.98).

General considerations regarding these relationships were discussed above in the section on meningiomas. The high correlation between phospholipids (r_phospholipid) and heme (r_heme) appears quite

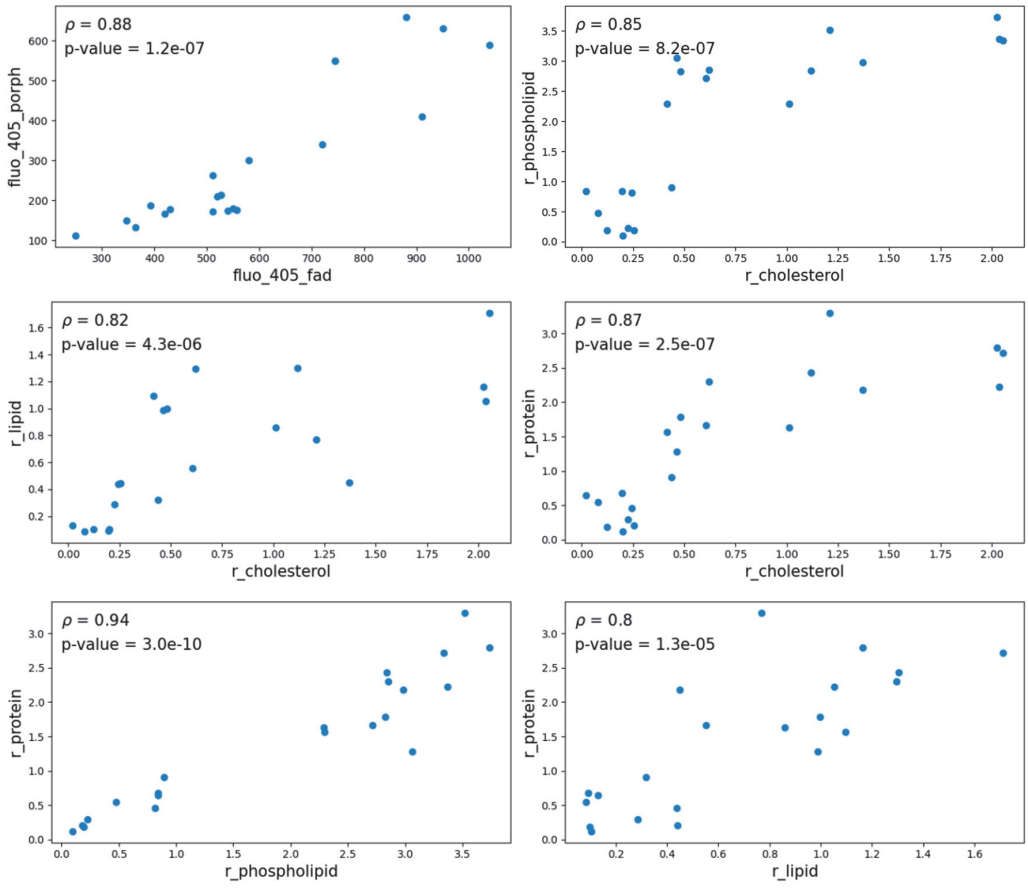

Рис. 6. Графики зависимости векторов признаков, удовлетворяющие критерию интереса для менингиомы II степени.
Fig. 6. Graphs of the dependence of feature vectors satisfying the criterion of interest for grade II meningioma.

expected, as we already identified heme as a correlate of tumor tissue, and the increasing expression of phospholipid spectral lines with increasing tumor tissue content of the samples, starting from 50%, also allows us to consider them in this way. However, the non-monotonic dependence of the phospholipid signal on the tumor tissue content means that higher values can also be observed at lower, "healthy," heme concentrations, which is reflected in the corresponding diagram in Fig. 7 by the wide scatter.

Moreover, the high correlation of phospholipids with oxygenated heme appears secondary to the previous case, as it is due to the generally higher hemoglobin content in tumor tissues. Furthermore, we see very high variability in oxygenated hemoglobin with high phospholipid content for two reasons: it could be healthy tissue, which has a higher phospholipid content and a higher hemoglobin saturation level; or it could be a tumor, which is more hypoxic, but has a higher overall heme content, meaning a higher absolute value of oxygenated hemoglobin. The correlation of such features as heme and proteins, as well as lipids and phospholipids, does not require additional explanation. Phenylalanine, despite the fact that it shows high values of correlation coefficients with many parameters, demonstrates a tendency towards clustering of values. According to [22, 23], the phenylalanine Raman signal is higher in glioblastoma, astrocytoma, and necrosis than in normal tumors, stronger in necrosis than in tumors, elevated in high-grade tumors, and slightly elevated after radiation therapy. Fig. 2 in our work shows that its relationship with tumorigenesis is ambiguous. Further research will likely be required to evaluate its role.

For anaplastic astrocytoma, we can see a high correlation, already demonstrated previously for

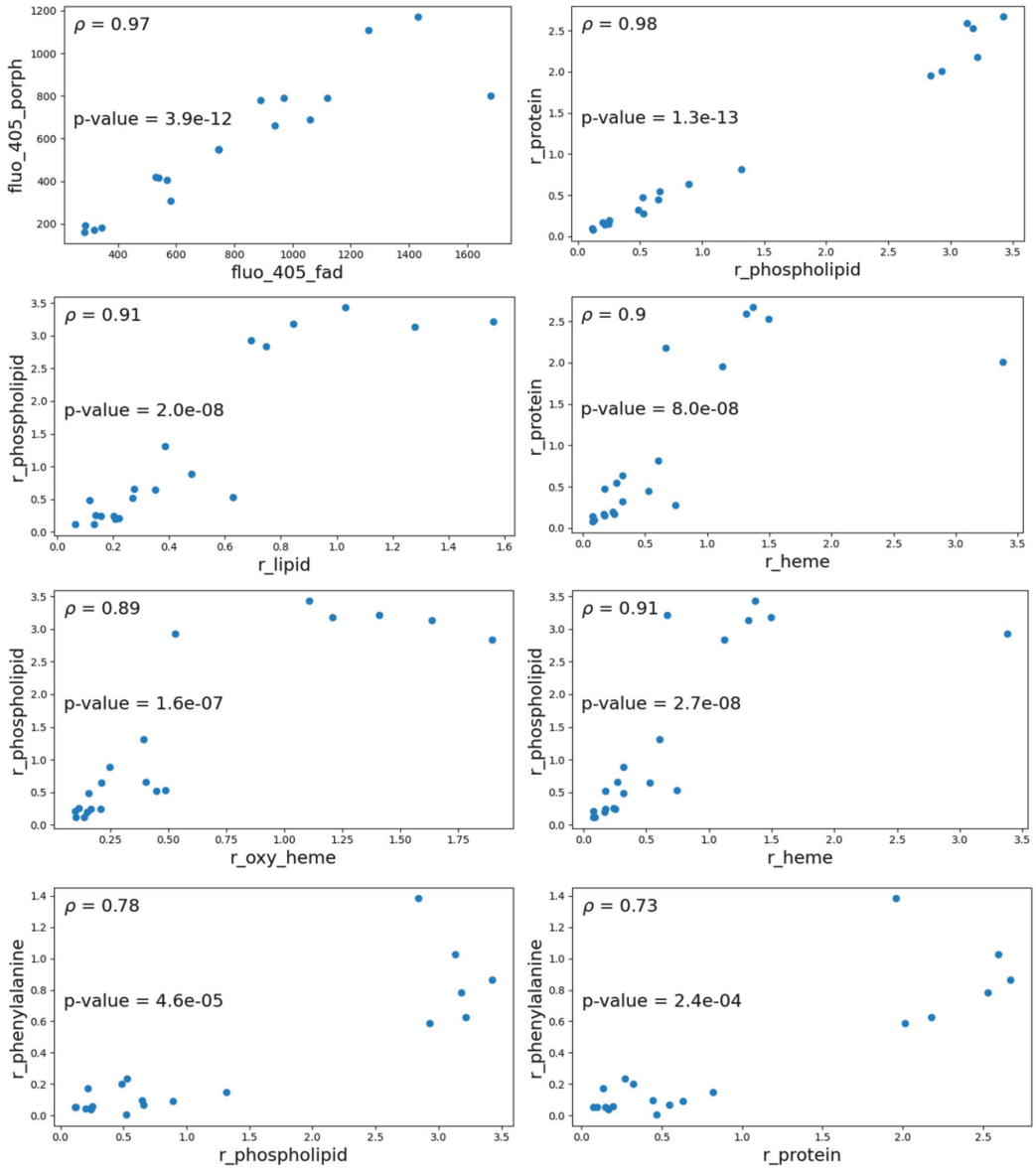

Рис. 7. Графики взаимных корреляций отдельных компонент вектора признаков, удовлетворяющие критерию интереса для олигодендроглиомы III степени.
Fig. 7. Graphs of mutual correlations of individual components of the feature vector satisfying the criterion of interest for oligodendroglioma grade III.

other tumors and explained above (Fig. 8). Analysis of glioblastomas (Fig. 9) reveals a predictably high data variability across all parameters, as this is a highly heterogeneous tumor. However, we can identify fairly strong correlations between proteins and phospholipids, as discussed above, proteins and heme, both total and oxygenated (apparently due to heme being a prosthetic group of the protein molecule), lipids and phospholipids, and between heme and phenylalanine.

Conclusions

An analysis of correlations between the features of the intracranial tumors studied, calculated based on fluorescence, diffuse reflectance, and spontaneous Raman spectra, and the tumor tissue content in the specimens, allowed us to identify spectral correlates of healthy tissues, such as carotenoids and oxygenated heme, as well as tumor tissue correlates, such as heme, cholesterol, and proteins. An analysis of cross-correlations between spectral features revealed a relationship between the autofluorescence of FAD and Pp IX, as well as phospholipids and proteins. This analysis, combined with data of tumor tissue content, explains the greater scatter of results with higher phospholipid content. Other features showed significant correlations, usually due to a common chemical nature.

This work was supported by the Ministry of Science and Higher Education of the Russian Federation (the Federal Scientific-technical program for genetic technologies development for 2019–2030), agreement №075-15-2025-559

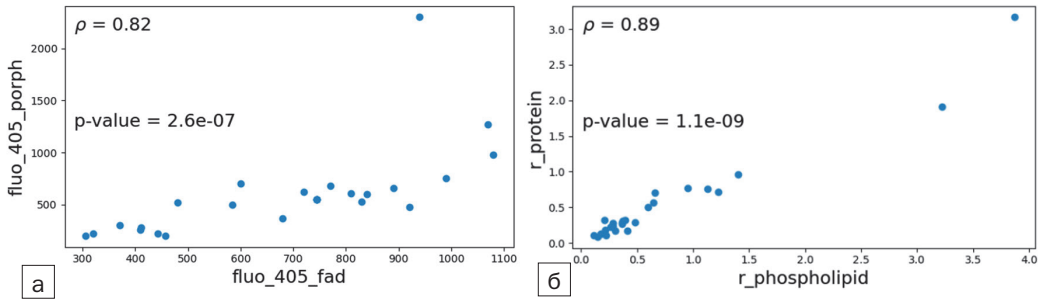

Рис. 8. Графики зависимости признаков, удовлетворяющие критерию интереса для астроцитомы III степени.
Fig. 8. Graphs of the dependence of features satisfying the criterion of interest for astrocytoma grade III.

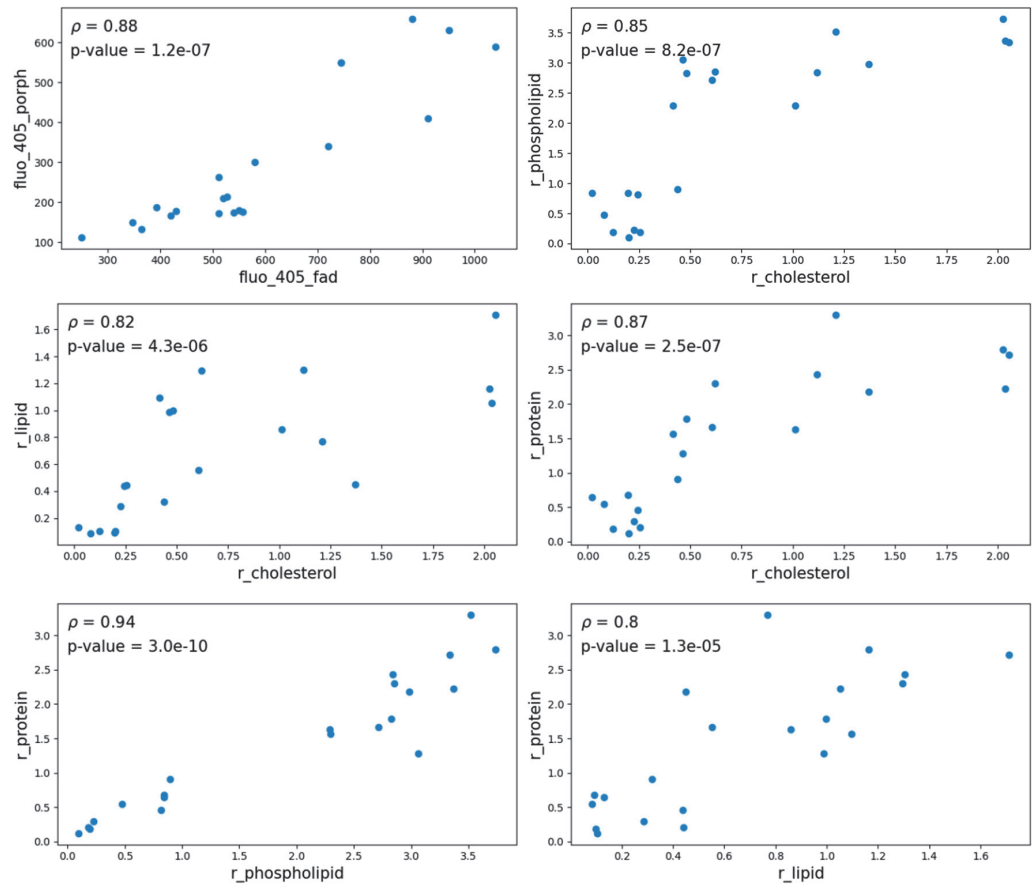

Рис. 9. Графики зависимости векторов признаков, удовлетворяющие критерию интереса для глиобластом.
Fig. 9. Graphs of the dependence of feature vectors satisfying the criterion of interest for glioblastomas

REFERENCES

1. Bailey D., Zacharia B.E. Intraoperative imaging techniques to improve tumor detection in the surgical management of gliomas // Adv. Cancer Res. – 2025. – vol. 166, pp. 103–135. doi: 10.1016/bs.acr.2025.05.001
2. Rynda A.Yu., Olyushin V.E., Rostovtsev D.M., et al. Results of microsurgical resection of glioblastomas under endoscopic and fluorescent control // Biomedical Photonics. – 2024. – vol. 13. – pp. 20-30. doi: 10.24931/2413-9432-2024-13-3-20-30
3. Goryaynov S.A., Okhlopkov V.A., Golbin D.A., et al. Fluorescence Diagnosis in Neurooncology: Retrospective Analysis of 653 Cases // Front. Oncol. – 2019. – vol. 9. – pp. 830. doi: 10.3389/fonc.2019.00830
4. Potapov AA, Goriaïnov SA, Loshchenov VB, et al. Intraoperative combined spectroscopy (optical biopsy) of cerebral gliomas. Burdenko's Journal of Neurosurgery. – 2013. – vol. 77. – pp. 3-10.
5. Stupak E.V., Glotov V.M., Askandaryan A.S. et al. Raman Spectroscopy in the Diagnosis of Brain Gliomas: A Literature Review // Cureus. – 2025. – vol. 17 – pp. – e79165. doi: 10.7759/cureus.79165.
6. Ospanov A., Romanishkin I., Savelieva T. et al. Optical Differentiation of Brain Tumors Based on Raman Spectroscopy and Cluster Analysis Methods // Int. J. Mol. Sci. – 2023. – vol. 24. – pp. 14432. doi: 10.3390/ijms241914432
7. Gautam, R., Vanga, S., Ariese, F. et al. Review of multidimensional data processing approaches for Raman and infrared spectroscopy // EPJ Techn Instrum. – 2015. – vol. 2. doi: 10.1140/epjti/s40485-015-0018-6
8. Lee J, Huh J. Pathogen Recognition via Surface-Enhanced Raman Scattering: Self-Supervised Learning and Transfer Learning approaches // ChemRxiv. – 2025. – doi:10.26434/chemrxiv-2025-cmr8g.
9. Riva M., Sciortino T., Secoli R. et al. Glioma biopsies Classification Using Raman Spectroscopy and Machine Learning Models on Fresh Tissue Samples // Cancers (Basel). – 2021. – vol. 13. – pp. 1073. doi: 10.3390/cancers13051073.
10. Savelieva T., Romanishkin I., Ospanov A. et al. Machine Learning and Artificial Intelligence Systems Based on the Optical Spectral Analysis in Neuro-Oncology // Photonics. – 2025. – vol. 12. – pp. 37. doi: 10.3390/photonics12010037.
11. Savelieva T.A., Romanishkin I.D., Ospanov A. et al. Machine learning methods for spectrally-resolved imaging analysis in neuro-oncology. Biomedical Photonics // 2024. – vol. 13. – pp. 40-54. doi: 10.24931/2413-9432-2024-13-4-40-54.
12. Nocera G., Sanvito F., Yao J. et al. Independent histological validation of MR-derived radio-pathomic maps of tumor cell density using image-guided biopsies in human brain tumors // J Neurooncol. – 2025. doi: 10.1007/s11060-025-05105-x.
13. Romanishkin I., Savelieva T., Kosyrkova A. et al. Differentiation of glioblastoma tissues using spontaneous Raman scattering with dimensionality reduction and data classification // Front Oncol. – 2022. – vol. 12. – pp. 944210. doi: 10.3389/fonc.2022.944210.
14. Romanishkin I.D., Savelieva T.A., Ospanov A. et al. Classification of intracranial tumors based on optical-spectral analysis // Biomedical Photonics. – 2023. – vol. 12. – pp. 4-10. doi: 10.24931/2413-9432-2023-12-3-4-10.
15. Romanishkin I.D., Savelieva T.A., Ospanov A. et al. Comparison of optical-spectral characteristics of glioblastoma at intraoperative diagnosis and ex vivo optical biopsy // Biomedical Photonics. – 2024. – vol. 13. – pp. 4-12. doi: 10.24931/2413-9432-2024-13-4-4-12.
16. Zhou Y, Liu C.-H., Wu B. et al. Optical biopsy identification and grading of gliomas using label-free visible resonance Raman spectroscopy // Journal of Biomedical Optics. – 2019. – vol. 24. – pp. 095001 doi: 10.1117/1.JBO.24.9.095001.
17. Evans S.M., Judy K.D., Dunphy I. et al., Hypoxia Is Important in the Biology and Aggression of Human Glial Brain Tumors. // Clin Cancer Res. – 2004. – vol.10. – pp. 8177 doi: 10.1158/1078-0432.CCR-04-1081
18. Takano S., Yoshii Y., Kondo S. et al. Concentration of vascular endothelial growth factor in the serum and tumor tissue of brain tumor patients. // Cancer Res. – 1996. – vol. 56. – pp. 2185-2190.

ЛИТЕРАТУРА

1. Bailey D., Zacharia B.E. Intraoperative imaging techniques to improve tumor detection in the surgical management of gliomas // Adv. Cancer Res. – 2025. – Vol. 166. – P. 103–135. doi: 10.1016/bs.acr.2025.05.001.
2. Рында А.Ю., Олюшин Д.М., Ростовцев Д.М. и др. Результаты микрохирургической резекции глиобластом под эндоскопическим и флуоресцентным контролем // Biomedical Photonics. – 2024. – Vol. 13. – P. 20-30. doi: 10.24931/2413-9432-2024-13-3-20-30.
3. Goryaynov S.A., Okhlopkov V.A., Golbin D.A., et al. Fluorescence Diagnosis in Neurooncology: Retrospective Analysis of 653 Cases // Front. Oncol. – 2019. – Vol. 9. – P. 830. doi: 10.3389/fonc.2019.00830.
4. Потапов А.А., Горяйнов С.А., Лощенов В.Б., и др. Интраоперационная комбинированная спектроскопия (оптическая биопсия) глиом головного мозга // Журнал «Вопросы нейрохирургии» имени Н.Н. Бурденко. – 2013. – Vol. 77. – № 2. – P. 3-10.
5. Stupak E.V., Glotov V.M., Askandaryan A.S. et al. Raman Spectroscopy in the Diagnosis of Brain Gliomas: A Literature Review // Cureus. – 2025. – Vol. 17 – P. – e79165. doi: 10.7759/cureus.79165.
6. Ospanov A., Romanishkin I., Savelieva T. et al. Optical Differentiation of Brain Tumors Based on Raman Spectroscopy and Cluster Analysis Methods // Int. J. Mol. Sci. – 2023. – Vol. 24. – P. 14432. doi: 10.3390/ijms241914432.
7. Gautam, R., Vanga, S., Ariese, F. et al. Review of multidimensional data processing approaches for Raman and infrared spectroscopy // EPJ Techn Instrum. – 2015. – Vol. 2. doi: 10.1140/epjti/s40485-015-0018-6.
8. Lee J, Huh J. Pathogen Recognition via Surface-Enhanced Raman Scattering: Self-Supervised Learning and Transfer Learning approaches // ChemRxiv. – 2025. – doi: 10.26434/chemrxiv-2025-cmr8g.
9. Riva M., Sciortino T., Secoli R. et al. Glioma *biopsies* Classification Using Raman Spectroscopy and Machine Learning Models on Fresh Tissue Samples // Cancers (Basel). – 2021. – Vol. 13. – P. 1073. doi: 10.3390/cancers13051073.
10. Savelieva T., Romanishkin I., Ospanov A. et al. Machine Learning and Artificial Intelligence Systems Based on the Optical Spectral Analysis in Neuro-Oncology // Photonics. – 2025. – Vol. 12. – P. 37. doi: 10.3390/photonics12010037
11. Савельева Т.А., Романишкин И.Д., Оспанов А. и др. Методы машинного обучения для анализа спектрально-разрешенных изображений в нейроонкологии. Biomedical Photonics // 2024. – Vol. 13. – P. 40-54. doi: 10.24931/2413-9432-2024-13-4-40-54.
12. Nocera G., Sanvito F., Yao J. et al. Independent histological validation of MR-derived radio-pathomic maps of tumor cell density using image-guided biopsies in human brain tumors // J Neurooncol. – 2025. doi: 10.1007/s11060-025-05105-x.
13. Romanishkin I., Savelieva T., Kosyrkova A. et al. Differentiation of glioblastoma tissues using spontaneous Raman scattering with dimensionality reduction and data classification // Front Oncol. – 2022. – Vol. 12. – 944210. doi: 10.3389/fonc.2022.944210.
14. Романишкин И.Д., Савельева Т.А., Оспанов А. и др. Классификация внутричерепных опухолей на основе оптико-спектрального анализа // Biomedical Photonics. – 2023. – Vol. 12. – P. 4-10. doi: 10.24931/2413-9432-2023-12-3-4-10
15. Романишкин И.Д., Савельева Т.А., Оспанов А. и др. Сравнение оптико-спектральных характеристик глиобластомы при интраоперационной диагностике и оптической биопсии ex vivo // Biomedical Photonics. – 2024. – Vol. 13. – P. 4-12. doi: 10.24931/2413-9432-2024-13-4-4-12
16. Zhou Y., Liu C.-H., Wu B. et al. Optical biopsy identification and grading of gliomas using label-free visible resonance Raman spectroscopy // Journal of Biomedical Optics. – 2019. – Vol. 24. – P. 095001. doi: 10.1117/1.JBO.24.9.095001.
17. Evans S.M., Judy K.D., Dunphy I. et al., Hypoxia Is Important in the Biology and Aggression of Human Glial Brain Tumors. // Clin Cancer Res. – 2004. – Vol.10. – 8177 doi: 10.1158/1078-0432.CCR-04-1081.
18. Takano S., Yoshii Y., Kondo S. et al. Concentration of vascular endothelial growth factor in the serum and tumor tissue of brain tumor patients. // Cancer Res. – 1996. – Vol. 56. – P. 2185-2190.

19. Takahashi J.A., Fukumoto M., Igarashi K. et al. Correlation of basic fibroblast growth factor expression levels with the degree of malignancy and vascularity in human gliomas. // J Neurosurg. – 1992. – vol. 76. – pp. 792-798.
20. Scatliff J.H., Radcliffe W.B., Pittman H.H., Park C.H. Vascular structure of glioblastomas. // Am J Roentgenol Radium Ther Nucl Med. – 1969. – vol. 105. – pp. 795-805
21. Weidner N. Tumoural vascularity as a prognostic factor in cancer patients: the evidence continues to grow. // J Pathol. – 1998. – vol. 184. – pp. 119-22.
22. Brusatori M., Auner G., Noh T., et al. Intraoperative Raman Spectroscopy // Neurosurg Clin N Am. – 2017. – vol. 28. – pp. 633-652. doi: 10.1016/j.nec.2017.05.014.
23. Aydin O., Altas M., Kahraman M. et al. Differentiation of healthy brain tissue and tumors using surface enhanced Raman scattering // Appl Spectrosc. – 2009. – Vol. 63. – pp. 1095–100
24. Mehidine H., Refregiers M., Jamme F. et al. Molecular changes tracking through multiscale fluorescence microscopy differentiate Meningioma grades and non-tumoral brain tissues // Sci Rep. – 2021. – vol. 11. – pp. 3816. doi: 10.1038/s41598-020-78678-4.
25. Reichert D., Wadiura L.I., Erkkilae M.T., et al. Flavin fluorescence lifetime and autofluorescence optical redox ratio for improved visualization and classification of brain tumors // Front Oncol. – 2023. – vol. 20. – pp. 1105648. doi: 10.3389/fonc.2023.1105648.
26. Mazurek M., Szczepanek D., Orzyłowska A., Rola R. Analysis of Factors Affecting 5-ALA Fluorescence Intensity in Visualizing Glial Tumor Cells—Literature Review // International Journal of Molecular Sciences. – 2022. – vol. 23. – pp. 926. doi: 10.3390/ijms23020926.
27. Kemmner W., Wan K., Rüttinger S. et al. Silencing of human ferrochelatase causes abundant protoporphyrin-IX accumulation in colon cancer // FASEB J. – 2008. – vol. 22. – pp. 500–509.
28. Kim S., Kim J.E., Kim Y.H. et al. Glutaminase 2 expression is associated with regional heterogeneity of 5-aminolevulinic acid fluorescence in glioblastoma // Sci. Rep. – 2017. – vol. 7. – pp. 12221.
29. Utsuki S., Oka, H., Fujii K. Intraoperative Photodynamic Diagnosis of Brain Tumors Using 5-Aminolevulinic Acid // In Diagnostic Techniques and Surgical Management of Brain Tumors; Abujamra, A.L., Ed.; InTech: Rijeka, Croatia, 2011. – pp. 227–244
30. Ohgari Y., Nakayasu Y., Kitajima S. et al. Mechanisms involved in δ-aminolevulinic acid (ALA)-induced photosensitivity of tumor cells: Relation of ferrochelatase and uptake of ALA to the accumulation of protoporphyrin // Biochem. Pharmacol. – 2005. – vol. 71. – pp. 42–49.

19. Takahashi J.A., Fukumoto M., Igarashi K. et al. Correlation of basic fibroblast growth factor expression levels with the degree of malignancy and vascularity in human gliomas. // J Neurosurg. – 1992. – Vol. 76. – P. 792-798.
20. Scatliff J.H., Radcliffe W.B., Pittman H.H., Park C.H. Vascular structure of glioblastomas. // Am J Roentgenol Radium Ther Nucl Med. – 1969. – Vol. 105. – P. 795-805.
21. Weidner N. Tumoural vascularity as a prognostic factor in cancer patients: the evidence continues to grow. // J Pathol. – 1998. – Vol. 184. – P. 119-22.
22. Brusatori M., Auner G., Noh T., et al. Intraoperative Raman Spectroscopy // Neurosurg Clin N Am. – 2017. – Vol. 28. – P. 633-652. doi: 10.1016/j.nec.2017.05.014.
23. Aydin O., Altas M., Kahraman M. et al. Differentiation of healthy brain tissue and tumors using surface enhanced Raman scattering // Appl Spectrosc. – 2009. –Vol. 63. – P. 1095–100.
24. Mehidine H., Refregiers M., Jamme F. et al. Molecular changes tracking through multiscale fluorescence microscopy differentiate Meningioma grades and non-tumoral brain tissues // Sci Rep. – 2021. – Vol. 11. – P. 381. doi: 10.1038/s41598-020-78678-4.
25. Reichert D., Wadiura L.I., Erkkilae M.T., et al. Flavin fluorescence lifetime and autofluorescence optical redox ratio for improved visualization and classification of brain tumors // Front Oncol. – 2023. – Vol. 20. – P. 1105648. doi: 10.3389/fonc.2023.1105648.
26. Mazurek M., Szczepanek D., Orzyłowska A., Rola R. Analysis of Factors Affecting 5-ALA Fluorescence Intensity in Visualizing Glial Tumor Cells—Literature Review // International Journal of Molecular Sciences. – 2022. – Vol. 23. – P. 926. doi: 10.3390/ijms23020926
27. Kemmner W., Wan K., Rüttinger S. et al. Silencing of human ferrochelatase causes abundant protoporphyrin-IX accumulation in colon cancer // FASEB J. – 2008. – Vol. 22. – P. 500–509,
28. Kim S., Kim J.E., Kim Y.H. et al. Glutaminase 2 expression is associated with regional heterogeneity of 5-aminolevulinic acid fluorescence in glioblastoma // Sci. Rep. – 2017. – Vol. 7. – P. 12221.
29. Utsuki S., Oka, H., Fujii K. Intraoperative Photodynamic Diagnosis of Brain Tumors Using 5-Aminolevulinic Acid // In Diagnostic Techniques and Surgical Management of Brain Tumors; Abujamra, A.L., Ed.; InTech: Rijeka, Croatia, 2011. – P. 227–244
30. Ohgari Y., Nakayasu Y., Kitajima S. et al. Mechanisms involved in δ-aminolevulinic acid (ALA)-induced photosensitivity of tumor cells: Relation of ferrochelatase and uptake of ALA to the accumulation of protoporphyrin // Biochem. Pharmacol. – 2005. – Vol. 71. – P. 42–49.

ORIGINAL ARTICLES

THE EFFECTIVENESS OF INTRAOPERATIVE PHOTODYNAMIC THERAPY IN THE COMPLEX TREATMENT OF STAGE III AND IV NEPHROBLASTOMA IN CHILDREN

Rostovtsev N.M.[1,2], **Polyakov V.G.**[3], **Kuzmina N. E.**[1,2], **Neizvestnykh E.A.**[1,2], **Kuzmina A.V.**[2]
[1]Chelyabinsk Regional Children's Clinical Hospital, Chelyabinsk, Russia
[2]South-Urals State Medical University, Chelyabinsk, Russia
[3]National Medical Research Center of Oncology named after N. N. Blokhin, Moscow, Russia

Abstract

Nowadays, the problem of malignant neoplasms management remains a priority task. To achieve further progress in cancer treatment, it is necessary to focus on existing but still undervalued methods. One of these approaches is photodynamic therapy (PDT), which can be used in combination with surgery as well as with other antitumor drugs without any risk of inducing cross-resistance. Being miner invasive and selective in tumor targeting, and having no risk of complications, the technique is attractive for application in oncologic pediatrics as an innovation capable of expanding the range of therapeutic techniques. The aim of the study was to investigate the effectiveness of intraoperative photodynamic therapy in children with stage III–IV nephroblastoma. The study included 66 patients aged 0–11 years with stage III and IV nephroblastoma. The patients of the control group (35 children) underwent surgical treatment in combination with chemotherapy and radiation therapy according to the SIOP protocol. The patients of the main group (31 children) underwent therapy according to the SIOP protocol, but in combination with intraoperative PDT. The 5-year survival rate in the main group was 90.3%, in the control group – 71.4% ($p = 0.05$). The recurrence rate in the main group was 9.7%, in the control group – 11.4%. Thus, high therapeutic efficacy of PDT during intraoperative irradiation of the tumor bed after its removal has been demonstrated. The technique contributes to the increased survival rate of patients with retroperitoneal tumors, which is a promising method to be used in pediatric oncological practice.

Key words: pediatric surgery, photodynamic therapy, nephroblastoma, radachlorin.

Contacts: Rostovtsev N.M., e-mail: rostovcevnm@mail.ru

For citations: Rostovtsev N.M., Polyakov V.G., Kuzmina N.E., Neizvestnykh E.A., Kuzmina A.V. The effectiveness of intraoperative photodynamic therapy in the complex treatment of stage III and IV nephroblastoma in children, *Biomedical Photonics*, 2025, vol. 14, no. 4, pp. 34–42. doi: 10.24931/2413–9432–2025–14-4-34-42

ЭФФЕКТИВНОСТЬ ИНТРАОПЕРАЦИОННОГО ПРИМЕНЕНИЯ ФОТОДИНАМИЧЕСКОЙ ТЕРАПИИ В КОМПЛЕКСНОМ ЛЕЧЕНИИ НЕФРОБЛАСТОМЫ III, IV СТАДИИ У ДЕТЕЙ

Н.М. Ростовцев[1,2], **В.Г. Поляков**[3], **Н.Е. Кузьмина**[1,2], **Е.А. Неизвестных**[1,2], **А.В. Кузьмина**[2]
[1]Челябинская областная детская клиническая больница, Челябинск, Россия
[2]Южно-Уральский государственный медицинский университет, Челябинск, Россия
[3]Национальный медицинский исследовательский центр онкологии имени Н. Н. Блохина, Москва, Россия

Резюме

Проблема борьбы со злокачественными новообразованиями остается приоритетной для современного общества. Для достижения дальнейшего прогресса в лечении онкологических заболеваний необходимо акцентировать внимание на существующих, но все еще недооцененных методиках. Одной из таких технологий является фотодинамическая терапия (ФДТ), которая может использоваться в сочетании с хирургическим вмешательством, применяться с другими противоопухолевыми препаратами без риска индукции перекрестной резистентности. Малая инвазивность, избирательность в поражении опухоли, отсутствие риска осложнений делают методику привлекательной для применения в онкопедиатрии как инновации, способной расширить диапазон используемых тера-

певтических методик. Целью исследования стало изучение эффективности ФДТ у детей с нефробластомой III-IV стадии при интраоперационном применении. В исследование включены 66 пациентов в возрасте от 0 до 11 лет с нефробластомой III-IV стадии. Пациентам контрольной группы, включавшей 35 детей, проведено хирургическое лечение в комплексе с химиотерапией и лучевой терапией по протоколу SIOP. Пациентам основной группы, включавшей 31 ребенка, проведена терапия по протоколу SIOP, но в комбинации с интраоперационной ФДТ. 5-летняя общая выживаемость в основной группе составила 90,3%, в контрольной – 71,4% (p = 0,05). Частота рецидивов в основной группе составила 9,7%, в контрольной – 11,4%. Предложенная методика комплексного лечения забрюшинных опухолей по протоколу SIOP в комбинации с интраоперационным фотодинамическим воздействием на ложе удаленной опухоли у детей позволяет улучшить результаты оперативного лечения и увеличивает выживаемость пациентов с забрюшинными опухолями. Полученные данные об эффективности делают методику перспективной для применения в детской онкологической практике.

Ключевые слова: детская хирургия, фотодинамическая терапия, нефробластома, радахлорин.

Контакты: Ростовцев Н.М., e-mail: rostovcevnm@mail.ru

Для цитирования: Ростовцев Н.М., Поляков В.Г., Кузьмина Н.Е., Неизвестных Е.А., Кузьмина А.В. Эффективность интраоперационного применения фотодинамической терапии в комплексном лечении нефробластомы III, IV стадии у детей // Biomedical Photonics. – 2025. – Т. 14, № 4. – С. 34–42. doi: 10.24931/2413–9432–2025–14-4-34-42

Introduction

Even with all the latest technological advances, childhood cancer remains a major global problem: malignant neoplasms remain the leading cause of childhood mortality, second only to external causes. Approximately 3,500 children in Russia are diagnosed with malignant neoplasms annually, which is approximately 14–15 per 100,000 children [1,2]. Of particular importance in solving the problems of pediatric oncology is the search for ways to improve specialized medical care for children with malignant neoplasms. The development and implementation of high–tech innovations for the diagnosis and treatment of cancer is a key task of modern medical research.

Wilms' tumor (nephroblastoma), a well-studied and treatable childhood tumor, is a malignant embryonic neoplasm of the kidney and the second most common malignant tumor of the retroperitoneum [3]. Nephroblastoma accounts for 6% of all childhood cancers and is the most common kidney cancer in the pediatric age group, occurring in 1 in 10,000 children under 15 years of age [4–6].

Nephroblastoma can often remain asymptomatic for a long time, with no specific symptoms. Nonspecific symptoms such as loss of appetite, weight loss, lethargy, weakness, fatigue, and abdominal pain are frequently observed. Parents may not attach significant importance to these symptoms, and the first clinical manifestation is usually a palpable abdominal mass, which is discovered incidentally [7]. With prolonged tumor development, the tumor can reach large sizes, which can include invasion of intrarenal blood and lymphatic vessels, penetration of the renal capsule, and invasion of the perirenal tissue, and can also lead to tumor rupture [8,9]. These factors significantly worsen the prognosis and reduce patient survival. In this regard, the search for methods that increase the radicalism of surgical intervention and reduce the frequency of relapses and metastatic lesions remains relevant.

One such method is photodynamic therapy (PDT), which involves the administration of photosensitizers (PS) capable of selectively accumulating in tumor tissue. With specific laser exposure, PDT exerts its antitumor effects, which are associated with a direct cytotoxic effect on tumor cells, destruction of the tumor's vascular stroma, and tumor elimination under the influence of immune cells due to the induction of an inflammatory reaction and the development of a systemic immune response [10–12]. Numerous studies have demonstrated that PDT can be used both before and after chemotherapy, radiation therapy, or surgery without compromising these treatment modalities. None of the clinically approved PS accumulates in cell nuclei (which could cause DNA damage and, therefore, lead to carcinogenic effects), and they have no serious side effects [13–15].

Most of the studies analyzing the therapeutic efficacy and scope of PDT have been conducted in adult oncological practice. Studies of domestic PS devoted to the study of the kinetics of their interstitial distribution have been performed to identify optimal treatment regimens that allowed optimizing techniques and setting PDT targets [16-19]. A significant advantage of PDT as an adjuvant therapy and for intraoperative intervention is its effective use in patients with a high risk of local tumor recurrence after surgery [14].

However, despite the interest of researchers in PDT and the active introduction of the method in adult patients, data on the use of PDT in pediatric practice are sparse. There are only isolated studies indicating the high effectiveness of PDT use in pediatric oncology, dentistry, ophthalmology, and dermatology [20-24].

Clearly, the anatomical and physiological characteristics of children require the development of

unique therapeutic methods, regimens, and schedules tailored to their age and disease severity. We found no literature on the use of PDT with radachlorin in the combination therapy of retroperitoneal tumors in children. Therefore, the aim of our study was to evaluate the clinical efficacy of intraoperative PDT with radachlorin in the treatment of nephroblastoma, addressing the challenges of preventing metastasis and improving survival in children with solid retroperitoneal tumors.

Materials and Methods

The study was conducted at the Surgical Department and the V.I. Gerain Regional Oncohematology Center for Children and Adolescents of the State Autonomous Healthcare Institution "Chelyabinsk Regional Children's Clinical Hospital."

The study was approved by the local Ethics Committee of the Chelyabinsk Regional Children's Clinical Hospital (Protocol No. 17 dated March 20, 2015) and the Ethics Committee of the South Ural State Medical University (Protocol No. 6 dated September 9, 2024). Patient participation in the study was voluntary. The clinical study was conducted in accordance with the scientific and ethical principles set out in the Helsinki Declaration of the World Medical Association and reflected in OST 42-511-99 "Rules for Conducting Quality Clinical Trials in the Russian Federation", ICH GCP guidelines, and current regulatory documents. All patients and their legal representatives were provided with written information about the PDT technique prior to the study. The physician conducting the study provided detailed information on the PS administration procedure to patients and their legal representatives. Before the study, the legal representatives signed an informed consent form confirming the patient's voluntary participation in the study.

The inclusion criteria for the study evaluating the efficacy of PDT for retroperitoneal tumors in children were:

1) a diagnosed retroperitoneal tumor as an initial condition;

2) a guaranteed voluntary, uninterrupted follow-up period of 60 months (5 years) after surgery and PDT;

3) the presence of complete medical documentation, including medical history, laboratory, and diagnostic data.

The complete medical history, laboratory, and diagnostic data were recorded in the patient's individual medical record.

In order to ensure safety, the participants (doctors and patients) used safety glasses with a light filter during laser exposure. The procedure was performed intraoperatively under anesthesia.

Statistical data processing was performed using IBM SPSS Statistics 19. Qualitative analysis of the study groups was performed using cross-tabulation tables and Pearson's χ^2 test for significance. Differences were considered statistically significant at $p < 0.05$, which corresponds to a 95% probability of an accurate prediction.

To analyze 5-year overall and relapse-free survival data, Kaplan-Meier curves were constructed, calculating the mean survival time, its standard error, and the 95% confidence interval. The log-rank test was used to identify statistical differences in the survival curves; differences were considered statistically significant at $p < 0.05$.

The study involved 66 patients with nephroblastoma: 35 boys and 31 girls. The control group, which included 35 children, underwent surgery in combination with chemotherapy and radiation therapy according to the SIOP protocol. The study group, which included 31 children with stage III and IV disease, regional lymph node metastases, and tumor pseudocapsule invasion, received therapy according to the SIOP protocol in combination with photodynamic therapy. The distribution of patients into groups based on gender and age is presented in Table 1.

The vast majority of patients in the study group were young children, aged 0 to 3 years: 43 children (65.2%). The proportion of preschool-age children, aged 4 to 6 years, was 18 people (27.3%). Only 5 cases (7.6%) of nephroblastoma were noted in patients aged 7 years and older. The ratio of boys to girls in the study group of patients was 1.1: 1 – 35 boys (53.0%) and 31 girls (47.0%). Our data are consistent with the literature [26–28], according to which retroperitoneal tumors develop more often in children aged 1 to 3 years, and in 90% of cases the diagnosis is established before the age of 7; without gender predominance.

As noted above, retroperitoneal tumors can be hidden for a long time, during this period there is a slow increase in the tumor. The primary tumor

Таблица 1
Характеристики пациентов, включенных в исследование

Table 1
Characteristics of the patients included in the study

Характеристики пациентов Characteristics of the patients	Контрольная группа (n = 35) Control group (n = 35)	Основная группа (n = 31) Main group (n = 31)
Пол, n: Gender, n:		
мужской/male	20	15
женский/female	15	16
Возраст, n: Age, n:		
0-3 года/years	24	19
4-6 лет/years	10	8
7-12 лет/years	1	4

symptom complex is diverse in its manifestations, associated with the influence of the tumor process on the metabolism and immunity of the child. Often, in patients with nephroblastoma, the only symptom is the presence of a palpable tumor in the abdomen, which is detected by chance. The neoplasm was palpable in the abdominal cavity, causing an increase in abdominal size and its asymmetry in the majority of children - 59 (89.4%). Intoxication syndrome was also noted in patients: weakness, lethargy, decreased appetite were experienced by 50 children (75.8% of the entire analyzed group). Blood changes (hypochromic anemia, leukocytosis, neutrophilia) were noted in 47 patients (71.2%). Complaints of abdominal pain were presented by more than half of the children - 37 (56.1%). Subfebrile temperature was recorded in 21 children, which amounted to 31.8%, and weight loss - in 9 children (13.6%). Urine analysis changes, such as hematuria, associated with tumor invasion into the renal pelvis and subcapsular rupture of nephroblastoma, were detected in 29 children (43.9%). Half of these children were considered critically ill upon admission. Developmental delays were observed in 16 patients (24.2%). Table 2 presents the pattern of primary clinical symptoms in the study group.

All children included in the study group underwent a series of mandatory diagnostic tests in accordance with the clinical guidelines of the Russian Ministry of Health.

To determine subsequent treatment strategies, risk groups and disease stage were taken into account, classifying tumors from stages I to V in accordance with the recommendations of the International Society of Pediatric Oncology (SIOP, 2001) [4]. The study group included patients with stages III and IV, while the control group included patients with stages III, IV, and V. PDT was performed in patients with stage III and IV nephroblastoma (unilateral tumor, with metastases in regional lymph nodes, and with tumor pseudocapsule invasion).

Focal lung lesions, rounded solid lesions measuring 3–5 mm in size, classified as metastases, were detected in 7 patients in the study and control groups (22.6% and 20.0%, respectively). Table 3 presents the distribution of patients by disease stage according to the TNM classification.

The treatment sequence for all patients was as follows: neoadjuvant chemotherapy – surgery – adjuvant chemotherapy. Patients were divided into two groups based on the surgical treatment regimen. Patients in the control group underwent surgery in combination with chemotherapy and radiation therapy according to the SIOP protocol. Patients in the study group received therapy according to the SIOP protocol, but in combination with PDT. This was modified by adding postoperative photodynamic therapy to the standard therapy, targeting residual tumor and metastatic regional lymph nodes, as confirmed by intraoperative imaging.

Thirty minutes before surgery, the patient, who was in a darkened room, received an intravenous injection of a chlorin e6-based PS solution (radachlorin) at a dose of 1 mg/kg of body weight. The accumulation of chlorin e6 in the patient's tissues was monitored using the LESA-01-Biospec laser electron-spectral system. Intraoperative PDT was performed using a Lakhta-Milon high-intensity laser (Russia): laser radiation in the range of 0.1 to 0.8 W/cm^2, light energy dose of 400 J/cm^2, wavelength of 662 nm. The irradiation duration depended on the tumor size and averaged 20 minutes. A midline laparotomy was used as the

Таблица 2
Структура основных клинических симптомов у пациентов исследуемой группы

Table 2
The structure of the main clinical symptoms in patients of the study group

Клинические симптомы Clinical symptoms	Частота встречаемости, n (%)
Пальпируемая опухоль в животе Palpable abdominal mass	59 (89,4)
Интоксикационный синдром Intoxication syndrome	50 (75,8)
Болевой синдром Pain syndrome	37 (56,1)
Изменения в анализах крови Changes in blood tests	47 (71,2)
Повышение температуры тела Increased body temperature	21 (31,8)
Изменения в анализах мочи (гематурия) Changes in urine tests (hematuria)	29 (43,9)
Снижение веса Weight loss	9 (13,6)

Таблица 3
Распределение пациентов по стадиям TNM

Table 3
Distribution of patients by TNM stage

Параметр	Контрольная группа (n = 35) Control group (n = 35)	Основная группа (n = 31) Main group (n = 31)
T3N1M0, n (%)	28 (80,0)	24 (77,4)
T4N1M1, n (%)	6 (17,1)	7 (22,6)
T5N1M1, n (%)	1 (2,9)	-

surgical approach. Following abdominal exploration, a tumor nephroureterectomy was performed, and the renal and inferior vena cava were examined for tumor thrombosis. For disease staging, regional lymph nodes were removed and sent for pathological examination. After tumor removal, patients in the main group underwent PDT on the resected tumor bed. Postoperative 24-hour monitoring was conducted in the oncology intensive care unit. Further treatment of nephroblastoma depended on the stage, histological type, and tumor volume, based on SIOP guidelines. The individual stages of treatment are presented in Fig. 1–4.

Results

To evaluate the effectiveness of PDT, a Kaplan-Meier analysis of patient survival in the study groups was conducted based on the proportion of surviving patients. The follow-up period was 5 years, during which time examinations by a pediatric oncologist were performed, laboratory parameters were monitored, and imaging data were analyzed to rule out continued growth and metastatic lesions, according to the clinical guidelines of the Russian Ministry of Health. Based on the data obtained, the mean survival times to death and relapse were determined for patients in the control and study groups (Table 4).

The graphical representation of the Kaplan-Meier method were the overall 5-year and relapse-free survival curves shown in Fig. 5-6.

A comparison of the study and control groups revealed a significant difference in overall patient survival. In the group receiving protocol-based therapy without additional PDT, the number of deaths over 5 years of follow-up was 10, with a 5-year overall survival rate of 71.4%. In the group of patients who received PDT in addition to the main therapy, the number of deaths over the 5-year follow-up period was lower (3 cases), with an overall survival rate of 90.3% ($p = 0.05$).

No significant differences were found in relapse-free survival of patients with nephroblastoma depending on the use of PDT: relapse was diagnosed in 3 children (9.7%) in the study group and 4 children (11.4%) in the control group ($p = 0.82$).

In the study group, relapse was detected in 3 patients, requiring repeat surgeries. Relapses were associated with unfavorable tumor histology, severe disease stage, and parental noncompliance with the treatment regimen due to social problems. Analysis of

Рис. 1. Мультиспиральная компьютерная томография органов брюшной полости и забрюшинного пространства, нефробластома левой почки.
Fig. 1. Multislice computed tomography of the abdominal organs and retroperitoneal space, nephroblastoma of the left kidney.

Рис. 2. Внешний вид ребенка с нефробластомой: асимметрия живота в связи с наличием крупной опухоли.
Fig. 2. The appearance of a child with nephroblastoma: abdominal asymmetry due to the presence of a large tumor.

Рис. 3. Ревизия брюшной полости с опухолью во фланке.
Fig. 3. Revision of the abdominal cavity with a tumor in the flank.

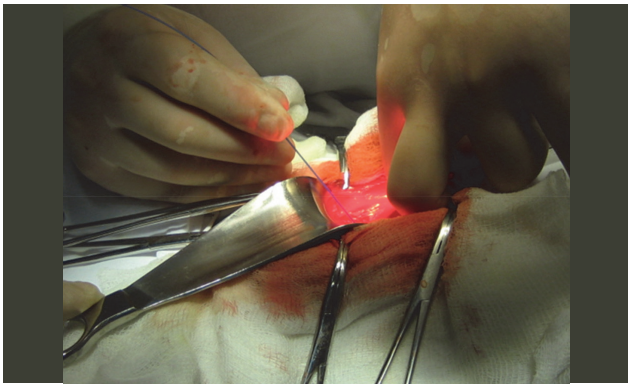

Рис. 4. Фотодинамическая терапия ложа опухоли.
Fig. 4. Photodynamic therapy of the tumor bed.

Таблица 4
Эффективность терапии в основной и контрольной группах (5-летнее наблюдение)

Table 4
Therapy effectiveness in the main and control groups (5-year follow-up)

Показатели эффективности Efficacy indicators	Контрольная группа (n = 35) Control group (n = 35)	Основная группа (n = 31) Main group (n = 31)
5-летняя общая выживаемость, % 5-year overall survival, %	71,4	90,3
Число летальных случаев, n (%) Number of deaths, n (%)	10 (28,3)	3 (9,7)
Среднее время дожития до летального исхода (m±SD), мес Mean survival time to death (m±SD), months 95% ДИ 95% CI	54,7±2,9 49,1-60,4	57,1±2,9 53,0-61,2
5-летняя безрецидивная выживаемость, % 5-year relapse-free survival, %	88,6	90,3
Среднее время дожития до рецидива (m±SD), мес Mean survival time to relapse (m±SD), months 95% ДИ 95% CI	54,1±2,8 48,6-59,6	54,7±2,9 49,1-60,4

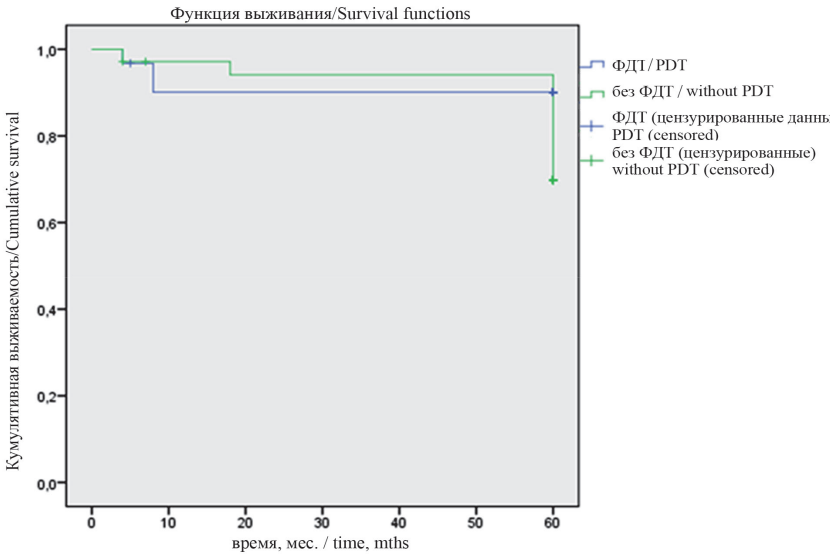

Рис. 5. Общая 5-летняя выживаемость пациентов исследуемых групп с нефробластомой (мес)
Fig. 5. Overall 5-year survival of patients in the study groups with nephroblastoma (months)

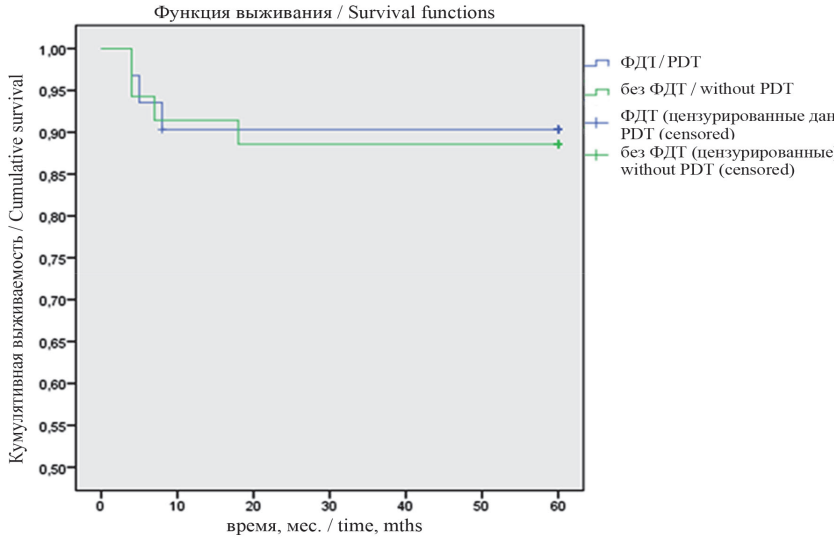

Рис. 6. Безрецидивная выживаемость пациентов с нефробластомой (мес)
Fig. 6. Recurrence-free survival of patients with nephroblastoma (months)

relapse rates prompted a more thorough assessment and monitoring of the child's outpatient care.

Discussion

As previously reported, there are isolated studies on the use of PDT in pediatric practice [20–24]. No reports on the use of PDT in the treatment of retroperitoneal tumors in children were found. In our study, we relied on the results of a preliminary experiment, during which a PDT regimen and protocol were developed [29]. Radachlorin, a second-generation chlorin e6-based photosynthesis agent, was used as the photosynthesis agent. This agent exhibits greater selectivity for accumulation (compared to first-generation photosynthesis agents), resulting in greater tumor penetration depth, preservation of surrounding tissue during irradiation, and low cutaneous phototoxicity. Publications by a number of authors demonstrate good clinical efficacy of PDT using chlorin e6-based PS in the treatment of tumors of various localizations. Thus, in the work of T.E. Sukhova [30], the response of basal cell skin cancer in its various clinical forms, stages, histological types, course and localization to PDT with intralesional administration of radachlorin and photoditazine was studied. At the same time, PDT with radachlorin allowed to significantly improve the results of treatment of the ulcerative form of the tumor compared to PDT carried out using photoditazine (92.8% and 77.8%, respectively, $p < 0.05$). Another research group: E.V. Filonenko et al. [31] used radachlorin in the treatment of precancerous and tumor diseases of the cervix with good clinical results: complete tumor regression was achieved in 86.7% of patients. It is important that no adverse reactions to the administration of the drug radachlorin and PDT were detected during or after treatment.

L.A. Vashakmadze *et al.* reported the intraoperative use of radachlorin in patients with a high risk of local tumor recurrence after surgical treatment [32]. Intraoperative photodynamic therapy with photohem, radachlorin, and photoditazine was performed in 17 patients with morphologically confirmed resectable primary or recurrent retroperitoneal tumors. The tumor bed was irradiated after its complete removal within the healthy tissues from one or more positions, depending on the location of the tumor foci. The researchers noted a relapse of the disease after intraoperative PDT in 6 of 17 patients within 2 to 6 months. Importantly, the authors noted the development of local relapses in patients who received intraoperative PDT at the stage of practicing the technique, selecting modes, and the radiation dose. The researchers drew conclusions about the safety of PDT and the affinity of the used PS for the tissue of retroperitoneal sarcomas. The work of this research group was the most interesting and similar in structure to our study.

Conclusion

The proposed method of comprehensive treatment of retroperitoneal tumors using the SIOP protocol in combination with intraoperative photodynamic therapy at the tumor bed in children improves surgical outcomes and increases survival in patients with retroperitoneal tumors. The obtained efficacy data make this method promising for use in pediatric oncology.

REFERENCES

1. Rykov M.Yu., Baibarina E.N., Chumakova O.V., Polyakov V.G. Epidemiology of cancer in children in the Russian Federation: analysis of key indicators and ways to overcome the defects of statistical data. *Onkopediatria*, 2017, vol. 4, no. 3, pp. 159–176. (In Russ.) doi: 10.15690/onco.v4i3.1747.
2. Rykov M.Yu., Manerova O.A., Turabov I.A., Kozlov V.V., Reshetnikov V.A. The role of the pediatrician in the early diagnosis of malignant neoplasms in children. *Rossiyskiy Vestnik Perinatologii i Pediatrii (Russian Bulletin of Perinatology and Pediatrics)*, 2020, vol. 65, no. 1, pp. 94–99. (In Russ.) doi: 10.21508/1027-4065-2020-65-1-94-99.
3. Graf N., Rübe C., Gessler M. Kidney tumors. In: Gadner H., Gaedicke G., Niemeyer C., Ritter J. (eds.). *Pediatric hematology and oncology*. Berlin, Heidelberg: Springer-Verlag; 2006, pp. 847–864. (In German.) doi: 10.1007/3-540-29036-2.
4. Illade L., Hernandez-Marques C., Cormenzana M., Lassaletta Á., Andión Catalán M., Ruano D., et al. Wilms' tumour: A review of 15 years recent experience. *An. Pediatr. (Engl. Ed)*, 2018, vol. 88, no. 3, pp. 140–149. (In Spanish.) doi: 10.1016/j.anpedi.2017.03.019.
5. Kim S., Chung D.H. Pediatric solid malignancies: neuroblastoma and Wilms' tumor. *Surg. Clin. North Am*, 2006, vol. 86, no. 2, pp. 469–487, xi. doi: 10.1016/j.suc.2005.12.008.
6. Miniati D., Gay A.N., Parks K.V., Naik-Mathuria B.J., Hicks J., Nuchtern J.G., et al. Imaging accuracy and incidence of Wilms' and non-Wilms' renal tumors in children. *J. Pediatr. Surg*, 2008, vol. 43, no. 7, pp. 1301–1307. doi: 10.1016/j.jpedsurg.2008.02.077.

ЛИТЕРАТУРА

1. Рыков М.Ю., Байбарина Е.Н., Чумакова О.В., Поляков В.Г. Эпидемиология злокачественных новообразований у детей в Российской Федерации: анализ основных показателей и пути преодоления дефектов статистических данных // Онкопедиатрия. – 2017. – Т. 4, № 3. – С. 159–176. doi: 10.15690/onco.v4i3.1747.
2. Рыков М.Ю., Манерова О.А., Турабов И.А., Козлов В.В., Решетников В.А. Роль педиатров в ранней диагностике злокачественных новообразований у детей // Российский вестник перинатологии и педиатрии. – 2020. – Т. 65, № 1. – С. 94–99. doi: 10.21508/1027-4065-2020-65-1-94-99.
3. Graf N., Rübe C., Gessler M. Nierentumoren // Gadner H., Gaedicke G., Niemeyer C., Ritter J. (eds.). Pädiatrische Hämatologie und Onkologie. – Berlin, Heidelberg: Springer-Verlag, 2006. – P. 847–864. doi.org/10.1007/3-540-29036-2.
4. Illade L., Hernandez-Marques C., Cormenzana M., Lassaletta Á., Andión Catalán M., Ruano D., et al. Tumor de Wilms: revisión de nuestra experiencia en los últimos 15 años // An. Pediatr. (Engl. Ed.). – 2018. – Vol. 88, № 3. – P. 140–149. doi: 10.1016/j.anpedi.2017.03.019.
5. Kim S., Chung D.H. Pediatric solid malignancies: neuroblastoma and Wilms' tumor // Surg. Clin. North Am. – 2006. – Vol. 86, № 2. – P. 469–487, xi. doi: 10.1016/j.suc.2005.12.008.
6. Miniati D., Gay A.N., Parks K.V., Naik-Mathuria B.J., Hicks J., Nuchtern J.G., et al. Imaging accuracy and incidence of Wilms' and non-Wilms' renal tumors in children // J. Pediatr. Surg. – 2008. – Vol. 43, № 7. – P. 1301–1307. doi: 10.1016/j.jpedsurg.2008.02.077.

7. Rykov M.Yu., Polyakov V.G. Clinical manifestations and diagnosis of malignant neoplasms in children: what do pediatricians need to know? *Rossiyskiy Vestnik Perinatologii i Pediatrii (Russian Bulletin of Perinatology and Pediatrics)*, 2017, vol. 62, no. 5, pp. 69–79. (In Russ.) doi: 10.21508/1027-4065-2017-62-5-69-79.
8. Fedorova D.V. The differential diagnosis of neuroblastoma and Wilms' tumor: a clinical observation and review of the literature. *Russian Journal of Pediatric Hematology and Oncology*, 2015, vol. 2, no. 4, pp. 91–97. (In Russ.) doi: 10.17650/2311-1267-2015-2-4-91-97.
9. Meyer J.S., Harty M.P., Khademian Z. Imaging of neuroblastoma and Wilms' tumor. *Magn. Reson. Imaging Clin. N. Am*, 2002, vol. 10, no. 2, pp. 275–302. doi: 10.1016/s1064-9689(01)00010-1.
10. Bacellar I.O., Tsubone T.M., Pavani C., Baptista M.S. Photodynamic efficiency: from molecular photochemistry to cell death. *Int. J. Mol. Sci*, 2015, vol. 16, no. 9, pp. 20523–20559. doi: 10.3390/ijms160920523.
11. Kessel D. Death pathways associated with photodynamic therapy. *Med. Laser Appl*, 2006, vol. 21, no. 4, pp. 219–224. doi: 10.1016/j.mla.2006.05.006.
12. Mroz P., Hashmi J.T., Huang Y.Y., Lange N., Hamblin M.R. Stimulation of anti-tumor immunity by photodynamic therapy. *Expert Rev. Clin. Immunol*, 2011, vol. 7, no. 1, pp. 75–91. doi: 10.1586/eci.10.81.
13. Filonenko E.V. Fluorescence diagnostics and photodynamic therapy in oncology. *Science in Russia*, 2012, no. 4, pp. 4–9. (In Russ.)
14. Filonenko E.V. Fluorescence diagnostics and photodynamic therapy: justification of applications and opportunities in oncology. *Photodynamic therapy and photodyagnosis*, 2014, vol. 3, no. 1, pp. 3–7. (In Russ.)
15. Filonenko E.V., Serova L.G. Photodynamic therapy in clinical practice. *Biomedical Photonics*, 2016, vol. 5, no. 2, pp. 26–37. (In Russ.)
16. Sokolov V.V., Filonenko E.V. Photodynamic therapy in patients with early central lung cancer. *Photodynamic therapy and photodyagnosis*, 2013, vol. 2, no. 4, pp. 3–6. (In Russ.)
17. Sokolov V.V., Filonenko E.V., Karpova E.S. Long-term palliative treatment of patient with signet ring cell gastric cancer using endoscopic photodynamic therapy. *Photodynamic therapy and photodyagnosis*, 2014, vol. 3, no. 3, pp. 34–36. (In Russ.)
18. Titova V.A. The role of photodynamic therapy in multimodality cancer treatment. *Photodynamic therapy and photodyagnosis*, 2012, vol. 1, no. 1, pp. 3–5. (In Russ.) doi: 10.24931/2413-9432-2012-1-1-3-5.
19. Chernyshev I.V., Altunin D.V., Samsonov Yu.V., Kallaev K.K. Photodynamic methods of diagnostics and treatment of prostate and kidney cancer: new possibilities. *Experimental and clinical urology*, 2011, no. 2–3, pp. 92–94. (In Russ.)
20. Filatova N.V., Sidorenko E.I., Filatov V.V., Ponomarev G.V., Muravyev M.V. The use of photodynamic therapy with Photoditazine for the treatment of corneal neovascularization in children and adolescents. *Russian Journal of Biotherapy*, 2012, vol. 11, no. 2, pp. 56. (In Russ.)
21. Kumar N., Warren C.B. Photodynamic therapy for dermatologic conditions in the pediatric population: a literature review. *Photodermatol. Photoimmunol. Photomed*, 2017, vol. 33, no. 3, pp. 125–134. doi: 10.1111/phpp.12296.
22. Schipmann S., Müther M., Stögbauer L., Zimmer S., Brokinkel B., Holling M., et al. Combination of ALA-induced fluorescence-guided resection and intraoperative open photodynamic therapy for recurrent glioblastoma: case series on a promising dual strategy for local tumor control. *J Neurosurg*, 2020, vol. 134, no. 2, pp. 426–436. doi: 10.3171/2019.11.JNS192443.
23. Schwake M., Nemes A., Dondrop J., Schroeteler J., Schipmann S., Senner V., et al. In-vitro use of 5-ALA for photodynamic therapy in pediatric brain tumors. *Neurosurgery*, 2018, vol. 83, no. 6, pp. 1328–1337. doi: 10.1093/neuros/nyy054.
24. da Silva Barbosa P., Duarte D.A., Leite M.F., de Sant' Anna G.R. Photodynamic therapy in pediatric dentistry. *Case Rep. Dent*, 2014, vol. 2014, pp. 217172. doi: 10.1155/2014/217172.
25. Mazurin A.V., Vorontsov I.M. *Propaedeutics of children diseases*. Moscow: Meditsina; 1985. 432 p.

7. Рыков М.Ю., Поляков В.Г. Клинические проявления и диагностика злокачественных новообразований у детей: что необходимо знать педиатру // Российский вестник перинатологии и педиатрии. – 2017. – Т. 62, № 5. – С. 69–79. doi: 10.21508/1027-4065-2017-62-5-69-79.
8. Федорова Д.В. Дифференциальный диагноз нейробластомы и опухоли Вильмса: клиническое наблюдение и обзор литературы // Российский журнал детской гематологии и онкологии (РЖДГиО). – 2015. – Т. 2, № 4. – С. 91–97. doi: 10.17650/2311-1267-2015-2-4-91-97.
9. Meyer J.S., Harty M.P., Khademian Z. Imaging of neuroblastoma and Wilms' tumor // Magn. Reson. Imaging Clin. N. Am. – 2002. – Vol. 10, № 2. – P. 275–302. doi: 10.1016/s1064-9689(01)00010-1.
10. Bacellar I.O., Tsubone T.M., Pavani C., Baptista M.S. Photodynamic efficiency: from molecular photochemistry to cell death // Int. J. Mol. Sci. – 2015. – Vol. 16, № 9. – P. 20523–20559. doi: 10.3390/ijms160920523.
11. Kessel D. Death pathways associated with photodynamic therapy // Med. Laser Appl. – 2006. – Vol. 21, № 4. – P. 219–224. doi: 10.1016/j.mla.2006.05.006.
12. Mroz P., Hashmi J.T., Huang Y.Y., Lange N., Hamblin M.R. Stimulation of anti-tumor immunity by photodynamic therapy // Expert Rev. Clin. Immunol. – 2011. – Vol. 7, № 1. – P. 75–91. doi: 10.1586/eci.10.81.
13. Филоненко Е.В. Флуоресцентная диагностика и фотодинамическая терапия в онкологии // Наука в России. – 2012. – № 4. – С. 4–9.
14. Филоненко Е.В. Флюоресцентная диагностика и фотодинамическая терапия – обоснование применения и возможности в онкологии // Фотодинамическая терапия и фотодиагностика. – 2014. – Т. 3, № 1. – С. 3–7.
15. Филоненко Е.В., Серова Л.Г. Фотодинамическая терапия в клинической практике // Biomedical Photonics. – 2016. – Т. 5, № 2. – С. 26–37.
16. Соколов В.В., Филоненко Е.В. Фотодинамическая терапия больных ранним центральным раком легкого // Фотодинамическая терапия и фотодиагностика. – 2013. – Т. 2, № 4. – С. 3–6.
17. Соколов В.В., Филоненко Е.В., Карпова Е.С. Длительное паллиативное лечение больной перстневидно-клеточным раком желудка с использованием эндоскопической фотодинамической терапии // Фотодинамическая терапия и фотодиагностика. – 2014. – Т. 3, № 3. – С. 34–36.
18. Титова В.А. Роль и место фотодинамической терапии в мультимодальных программах лечения злокачественных опухолей // Фотодинамическая терапия и фотодиагностика. – 2012. – Т. 1, № 1. – С. 3–5. doi: 10.24931/2413-9432-2012-1-1-3-5.
19. Чернышев И.В., Алтунин Д.В., Самсонов Ю.В., Каллаев К.К. Новые возможности фотодинамической диагностики и лечения рака предстательной железы и почки // Экспериментальная и клиническая урология. – 2011. – № 2–3. – С. 92–94.
20. Филатова Н.В., Сидоренко Е.И., Филатов В.В., Пономарёв Г.В., Муравьев М.В. Применение фотодинамической терапии с препаратом Фотодитазин для лечения неоваскуляризации роговицы у детей и подростков // Российский биотерапевтический журнал. – 2012. – Т. 11, № 2. – С. 56.
21. Kumar N., Warren C.B. Photodynamic therapy for dermatologic conditions in the pediatric population: a literature review // Photodermatol. Photoimmunol. Photomed. – 2017. – Vol. 33, № 3. – P. 125–134. doi: 10.1111/phpp.12296.
22. Schipmann S., Müther M., Stögbauer L., Zimmer S., Brokinkel B., Holling M., et al. Combination of ALA-induced fluorescence-guided resection and intraoperative open photodynamic therapy for recurrent glioblastoma: case series on a promising dual strategy for local tumor control // J. Neurosurg. – 2020. – Vol. 134, № 2. – P. 426–436. doi: 10.3171/2019.11.JNS192443.
23. Schwake M., Nemes A., Dondrop J., Schroeteler J., Schipmann S., Senner V., et al. In-vitro use of 5-ALA for photodynamic therapy in pediatric brain tumors // Neurosurgery. – 2018. – Vol. 83, № 6. – P. 1328–1337. doi: 10.1093/neuros/nyy054.
24. da Silva Barbosa P., Duarte D.A., Leite M.F., de Sant' Anna G.R. Photodynamic therapy in pediatric dentistry // Case Rep. Dent. – 2014. – Vol. 2014. – P. 217172. doi: 10.1155/2014/217172.
25. Мазурин А.В., Воронцов И.М. Пропедевтика детских болезней. – Москва: Медицина, 1985. – 432 с.

26. Breslow N.E., Collins A.J., Ritchey M.L., Grigoriev Y.A., Peterson S.M., Green D.M. End stage renal disease in patients with Wilms tumor: results from the National Wilms Tumor Study Group and the United States Renal Data System. *J. Urol*, 2005, vol. 174, no. 5, pp. 1972–1975. doi: 10.1097/01.ju.0000176800.00994.3a.
27. Metzger M.L., Dome J.S. Current therapy for Wilms' tumor. *Oncologist*, 2005, vol. 10, no. 10, pp. 815–826. doi: 10.1634/theoncologist.10-10-815.
28. Wang J., Li M., Tang D., Gu W., Mao J., Shu Q. Current treatment for Wilms tumor: COG and SIOP standards. *World J. Pediatr. Surg*, 2019, vol. 2, pp. e000038. doi: 10.1136/wjps-2019-000038.
29. Rostovtsev N., Zhukovskaya E., Pasternak A., Kotlyarov A., Mustakimov B. Morphological study of the combined laser and photodynamic effect with radachlorin on the structure of experimental Ehrlich sarcoma. *Revista Inclusiones*, 2020, vol. 7, spec. nr, pp. 507–524.
30. Sukhova T.E. Comparative assessment of the efficacy of photodynamic therapy of basal cell skin cancer with the intralesional administration of Radachlorin and Fotoditazin. *Almanac of Clinical Medicine*, 2016, vol. 44, no. 1, pp. 78–87. (In Russ.) doi: 10.18786/2072-0505-2016-44-1-78-87.
31. Filonenko E.V., Serova L.G., Ivanova-Radkevich V.I. Results from phase III clinical trials with radachlorine for photodynamic therapy of pre-cancer and early cancer of cervix. *Biomedical Photonics*, 2015, vol. 4, no. 3, pp. 36–42. (In Russ.) doi: 10.24931/2413-9432-2015-4-3-36-42.
32. Vashakmadze L.A., Filonenko E.V., Cheremisov V.V., Khomyakov V.M. Intraoperative photodynamic therapy for nonorgan retroperitoneal tumors. *Photodynamic therapy and photodyagnosis*, 2013, vol. 2, no. 2, pp. 8–12. (In Russ.)

26. Breslow N.E., Collins A.J., Ritchey M.L., Grigoriev Y.A., Peterson S.M., Green D.M. End stage renal disease in patients with Wilms tumor: results from the National Wilms Tumor Study Group and the United States Renal Data System // J. Urol. – 2005. – Vol. 174, № 5. – P. 1972–1975. doi: 10.1097/01.ju.0000176800.00994.3a.
27. Metzger M.L., Dome J.S. Current therapy for Wilms' tumor // Oncologist. – 2005. – Vol. 10, № 10. – P. 815–826. doi: 10.1634/theoncologist.10-10-815.
28. Wang J., Li M., Tang D., Gu W., Mao J., Shu Q. Current treatment for Wilms tumor: COG and SIOP standards // World J. Pediatr. Surg. – 2019. – Vol. 2. – P. e000038. doi: 10.1136/wjps-2019-000038.
29. Rostovtsev N., Zhukovskaya E., Pasternak A., Kotlyarov A., Mustakimov B. Morphological study of the combined laser and photodynamic effect with radachlorin on the structure of experimental Ehrlich sarcoma // Revista Inclusiones. – 2020. – Vol. 7, spec. nr. – P. 507–524.
30. Сухова Т.Е. Сравнительная оценка эффективности фотодинамической терапии базальноклеточного рака с внутриочаговым введением Радахлорина и Фотодитазина // Альманах клинической медицины. – 2016. – Т. 44, № 1. – С. 78–87. doi: 10.18786/2072-0505-2016-44-1-78-87.
31. Филоненко Е.В., Серова Л.Г., Иванова-Радкевич В.И. Результаты III фазы клинических исследований препарата радахлорин для фотодинамической терапии предрака и начального рака райки матки // Biomedical Photonics. – 2015. – Т. 4, № 3. – С. 36–42. doi: 10.24931/2413-9432-2015-4-3-36-42.
32. Вашакмадзе Л.А., Филоненко Е.В., Черемисов В.В., Хомяков В.М. Интраоперационная фотодинамическая терапия при неорганных забрюшинных опухолях // Фотодинамическая терапия и фотодиагностика. – 2013. – Т. 2, № 2. – С. 8–12.

EFFECTIVENESS OF PHOTODYNAMIC THERAPY IN THE CORRECTION OF POSTACNE SCARS AND MORPHOFUNCTIONAL CHANGES IN THE SKIN

Dubenskiy V.V., Aleksandrova O.A., Chervinets Y.V., Nekrasova E.G.
Federal State Budgetary Educational Institution of Higher Education "Tver State Medical University" of the Ministry of Health of the Russian Federation, Tver, Russia

Abstract

Acne is one of the most common dermatosis in young people. 85% of cases occur in patients between 12 and 24 years old. Duration of the disease, severe form, frequent recurrences of acne, autotraumatization lead to development of symptoms complex postural, manifested in the form of scarring changes, dyschromia, reduced elasticity, increased porosity and mildew. Acne complications occur in 95% of patients. Development of an effective method for the correction of acne complications is a topical problem of modern dermatology and cosmetology. The article describes the method of application of photodynamic therapy with an outer gel photosensitizer based on E6 chloride in patients with severe form of acne after prior treatment with systemic retinoids. The morphofunctional indicators of the skin and the composition of the microbiome in the dynamics were studied. As a result of the course of photodynamic therapy, resolution of scarring was observed in 97,2% of patients, disappearance of pigmentation on cheeks and skin on the forehead in 89,1% and 91,9% of patients respectively, restoration of elasticity in 100% of subjects, decrease in oiliness on the cheeks and skin in 91% and 94,5 % of patients respectively.
The exact exposure of the photosensitizing gel when applied externally to the scar tissue, the time range of its highest concentration and optimal duration of the procedure were determined. As a result of the application of photodynamic therapy, the skin relief was leveled, its oiliness decreased, the pigmentation disappeared and the elasticity was restored. In the microbiota of seborrheic sites, normal flora predominated over pathogenic. This method proved to be effective in the correction of the postural.

Keywords: photodynamic therapy, photosensitizer, chlorin e6, acne, retinoid, scar, microbium.

Contacts: Aleksandrova O.A., e-mail: oaalexandrova@bk.ru

For citations: Dubenskiy V.V., Aleksandrova O.A., Chervinets Y.U., Nekrasova E.G. Efficiency of photodynamic therapy in the correction of postacne scars and morphofunctional changes in the skin, *Biomedical Photonics*, 2025, vol. 14, no. 4, pp. 43–48. doi: 10.24931/2413–9432–2025–14-4-43-48.

ЭФФЕКТИВНОСТЬ ФОТОДИНАМИЧЕСКОЙ ТЕРАПИИ В КОРРЕКЦИИ РУБЦОВ ПОСТАКНЕ И МОРФОФУНКЦИОНАЛЬНЫХ ИЗМЕНЕНИЙ КОЖИ

В.В. Дубенский, О.А. Александрова, Ю.В. Червинец, Е.Г. Некрасова
Федеральное государственное бюджетное образовательное учреждение высшего образования «Тверской государственный медицинский университет» Министерства здравоохранения Российской Федерации, Тверь, Россия

Резюме

Акне является одним из самых распространённых дерматозов у лиц молодого возраста. В 85% случаев встречается у пациентов в возрасте от 12 до 24 лет. Длительность заболевания, тяжелая форма, частые рецидивы угревой болезни, аутотравматизация приводят к развитию симптомокомплекса постакне, проявляющегося в виде рубцовых изменений, дисхромии, сниженной эластичности, повышенного порообразования и милиумов. Осложнения акне встречаются у 95% больных. Разработка эффективного метода для коррекции осложнений акне является актуальной задачей современной дерматологии и косметологии. В статье описана методика применения фотодинамической терапии с наружным гелем фотосенсибилизатором на основе хлорина е6 у пациентов с тяжелой формой угревой болезни после предварительно проведенного лечения системными ретиноидами. Изучались морфофункциональные показатели кожи и состав микробиома в динамике. В результате проведенного курса фотодинамической терапии разрешение рубцов наблюдалось у 97,2% больных, исчезновение пигментации на щеках и на коже лба у 89,1% и 91,9% пациентов соответственно, восстановление эластичности у 100% исследуемых, уменьшение жирности на щеках и коже лба у 91% и 94,5% больных соответственно.

Была установлена точная экспозиция геля фотосенсибилизатора при наружном нанесении на рубцовую ткань, диапазон времени его наибольшей концентрации и оптимальной продолжительности процедуры. В результате применения фотодинамической терапии выровнялся рельеф кожи, уменьшилась ее жирность, исчезла пигментация, а эластичность восстановилась. В составе микробиома себорейных участков преобладала нормальная флора над патогенной. Данный метод оказался эффективным в коррекции постакне.

Ключевые слова: фотодинамическая терапия, фотосенсибилизатор, хлорин е6, акне, ретиноид, рубец постакне, микробиом.

Контакты: Александрова О.А., e-mail: oaalexandrova@bk.ru

Для цитирования: Дубенский В.В., Александрова О.А., Червинец Ю.В., Некрасова Е.Г. Эффективность фотодинамической терапии в коррекции рубцов постакне и морфофункциональных изменений кожи // Biomedical Photonics. – 2025. –Т. 14, № 4. – С. 43–48. doi: 10.24931/2413–9432–2025–14-4-43-48

Introduction

Acne is a chronic, recurring disease of the sebaceous glands and hair follicles, characterized by comedones, pustules, and inflammatory infiltrates, most commonly occurring in young adults [1]. Antibacterial drugs (doxycycline), isotretinoin, and androgen receptor blockers (cyproterone acetate in combination with ethinyl estradiol as part of an oral contraceptive) are used to treat acne. For severe inflammatory acne in women, short courses of systemic glucocorticosteroids are used [1,2,3]. Topical retinoids (adapalene), benzoyl peroxide, antibacterial drugs (clindamycin phosphate), and combination medications are prescribed for topical therapy [1,4].

For severe acne and ineffective topical therapy, isotretinoin, a vitamin A derivative, is widely used. The drug suppresses sebaceous gland function, normalizes keratinization processes, has a pronounced anti-inflammatory effect, and reduces the appearance of post-acne scars. Isotretinoin is prescribed at an initial dose of 0.5 mg/kg of body weight per day, with a possible increase to 1.0 mg/kg. A cumulative dose of 120–150 mg/kg is required to achieve sustained remission. Dry skin and mucous membranes, reversible lipid metabolism disorders, and liver enzyme abnormalities often occur during treatment. Systemic retinoids, if necessary, are combined with antibiotics or hormonal drugs, which increases the overall effectiveness of treatment [1,3].

However, after a course of therapy, post-acne manifestations often remain in the form of post-inflammatory changes in the dermis, dyschromia, scars, enlarged pores, decreased skin elasticity, milia and atheromas, the severity of which depends on the severity and duration of acne [5].

Acne complications occur in 95% of patients, with 30% experiencing significant cosmetic defects, which can lead to psychological and social problems leading to social maladjustment [6]. Post-acne scars also often arise from auto-traumatization of the skin, untimely and/or inadequate treatment [7]. The main risk factors for the development of cicatricial changes include the severity of the pathological process, the duration of the disease, and recurrence. Thus, patients with severe acne are 3.4–6.8 times more likely to develop scars than those with mild to moderate acne [8].

Atrophic scars arise from collagen breakdown in 80–90% of patients, while keloid and/or hypertrophic scars (due to decreased collagenase activity and excessive deposition of collagen types I and III) occur in 10–20% of patients [9]. Post-inflammatory hyperpigmentation is equally common in men and women at any age and results from melanin deposition in the epidermis or dermis following inflammation and skin trauma. It most often develops in individuals with Fitzpatrick phototypes IV–VI. Ultraviolet radiation increases the severity of hyperpigmentation [10].

The composition of the skin microbiome significantly influences the development of acne. High bacterial counts often cause acne recurrence [11].

Bacteria belonging to 4 types have been mainly identified on human skin: *Actinobacteria* (for example, *Corynebacterineae, Propionibacterineae*), *Firmicutes* (for example, *Staphylococcaceae*), *Proteobacteria* and *Bacteroidetes* [11]. The bacterial composition varies depending on age, body region, and microenvironment [12]. In seborrheic areas of the skin (face, scalp, chest, interscapular region), propionibacteria, which survive in anaerobic conditions, predominate [13]. Staphylococci and corynebacteria are more common on the moist skin of the armpits, groin, and popliteal fossa. Gram-negative bacteria predominantly colonize dry skin [14]. *Malassezia spp.* are distributed over the entire surface of the skin [15]. *Cutibacterium acnes (C. acnes)* accounts for approximately 85-90% of all identifiable microorganisms, dominates in the sebaceous hair follicle area, and is one of the factors in the pathogenesis of acne [16]. However, the number of *C. acnes* does not affect the development of severe acne [17].

Benzoyl peroxide and clindamycin (for topical therapy), isotretinoin and minocycline (for oral administration) reduce the bacterial load. For example, after 5 months of treatment, isotretinoin has been

shown to increase the number of *C. acnes* ribotypes with bactericidal activity [18,19].

Materials and Methods

A dermatological examination of 847 people aged 18-25 years revealed acne in 61.5%. Severe acne was diagnosed in 102 patients, most commonly in men. All patients with severe acne were treated with isotretinoin for an average of 8 to 10 months. Topical creams containing azelaic acid, adapalene, and benzoyl peroxide were applied. Additionally, skin morphofunctional parameters (moisture, oiliness, elasticity, pigmentation, pore formation) and bacterial count were measured.

The Multiskin Test Center MC 900 software and hardware system (Courage + Khazakaelectronic GmbH, Germany, registration no. 11629994, dated April 17, 2009) was used to evaluate the functional properties of the skin. Measurements were performed on pre-cleansed skin in a well-ventilated room at a temperature of 22°C and 40–60% humidity for 15–20 minutes. Sensors were placed on the medial forehead, the central area of the right cheek (under the zygomatic bone), and the medial chin [20,21].

Skin scrapings from the forehead were used for microbiological analysis. Samples were collected twice: before treatment and after a course of photodynamic therapy (PDT). The microbiome was studied using a classical bacteriological method. Cultivation was performed on enriched nutrient media, followed by colony counting (lg CFU/ml) under standard conditions [14].

To correct acne complications, PDT was used, a treatment method using an external photosensitizer gel (PS) and laser radiation, the wavelength of which corresponds to the peak absorption of PS [22]. The use of topical PS eliminated toxic and irritating effects. After activation of ultra-bright LEDs, cytotoxicity resulting from the photochemical reaction causes necrosis or apoptosis of the pathogenic cell. This results in the growth of young, healthy cellular structures, collagen and elastin synthesis, improved microcirculation, and restored skin pigmentation. The procedure is painless and non-invasive, with no downtime or side effects [23].

For PDT, an external photosensitizer gel was used, the active substance of which is the N-dimethylglucamine salt of chloride e6, obtained by extraction of chlorophyll A from the marine microalgae spirulina and its subsequent chemical transformation using the original technology [24]. Trade name of the drug: gel photoditazine (VETA-GRAND LLC, Russia, registration certificate no. FSR 2012/ 13043 dated June 08, 2017). The facial skin was pre-cleaned with an aqueous solution of chlorhexidine. The gel was applied to dry skin under occlusion and left for 10 minutes, then washed off with water and a gel/foam cleanser, thoroughly cleansing the pores of the photodynamic reaction. To activate the photodynamic reaction, red laser radiation was used for 10 minutes in the range of 660 ± 2 nm. To irradiate the entire surface to be treated, a laser device (Latus-T, registration No. FSR 2010/09207, Russia) with a power of 1-1.5 mW/cm^2, cumulative energy of 100-180 J/cm^2 was used. The procedure was carried out once a week, with a total of 10 courses [22].

Results

Clinical cure of acne with the use of systemic retinoids was achieved in 97% of patients. However, when examining morphofunctional parameters of the skin, dehydration was detected in 92% of patients, increased oiliness of the cheeks and forehead in 83.7% and 78.3% of patients, respectively, low elasticity in 32.4% of patients, increased pore formation in the nose area in 27.2% of patients, cheeks in 36.3% of patients, forehead in 40.9% of patients, and hyperpigmentation on the cheeks and forehead in 64.8% and 45.9% of patients, respectively. Post-acne scarring was observed as complications in 37.3% of patients.

The following microorganisms were identified in the forehead skin microbiome before photodynamic therapy: *Staphylococcus spp.* (66.7% and 4.2 lg CFU/ml), *Staphylococcus aureus* (33.3% and 2.3 lg CFU/ml), *Micrococcus spp.* (58.3% and 3.3 lg CFU/ml), *Enterobacter spp*. (8.3% and 3.3 lg CFU/ml), *Klebsiella spp.* (8.3% and 2.2 lg CFU/ml), *Bacillus spp.* (8.3% and 1.6 lg CFU/ml), and *Candida spp.* (25% and 3 lg CFU/ml). Hemolytic *Staphylococcus spp.* (75% and 4.1 lg CFU/ml) and *Candida spp.* (25% and 2.6 lg CFU/ml) were also isolated.

After the course of PDT, scar resolution was observed in 97.2% of patients, disappearance of pigmentation on the cheeks and forehead skin in 89.1% and 91.9% of patients, respectively, restoration of elasticity in 100% of patients, and a decrease in oiliness on the cheeks and forehead skin in 91% and 94.5% of patients, respectively.

In the microbiological examination after PDT, the frequency of *Staphylococcus spp.* increased (up to 75% and 3.7 lg CFU/ml), while *Staphylococcus epidermidis* was found in 41.7% of cases in the amount of 4.3 lg CFU/ml, the prevalence of *Enterobacter spp.* increased (16.7% and 3.5 lg CFU/ml), *Candida spp.* (41.7% and 3.6 lg CFU/ml). Also, the frequency of hemolytic *Staphylococcus spp.* decreased (up to 33.3% and 2.8 lg CFU/ml) and *Candida spp.* (up to 8.3% and 2.7 lg CFU/ml), and *Staphylococcus aureus*, *Bacillus spp.,* and *Klebsiella spp.* completely disappeared. *Micrococcus spp.* remained constant (58.3% and 2.7 lg CFU/ml).

To more accurately determine the exposure of the PS gel to the skin and improve the effectiveness of PDT,

individual measurements of chlorin e6 fluorescence in the skin were performed in patients with cicatricial changes within 5-25 minutes, which can indirectly assess the accumulation of the photosensitizer gel (Table, Fig.).

According to the results of fluorimetry, the highest fluorescence intensity was determined in the range of 10-20 minutes, which determines the optimal exposure of the photosensitizer gel based on e6 chloride for 10 minutes, and the exposure time to laser radiation for 10 minutes.

Discussion

Long-term acne, severe acne, frequent acne recurrences, and autotraumatization lead to the development of post-acne symptoms, manifested as scarring, dyschromia, decreased elasticity, increased pore formation, and milia. The development of an effective method for correcting acne complications is an urgent task of modern dermatology and cosmetology. Many post-acne treatments are accompanied by soreness and require a period of rehabilitation. The article describes a technique for using PDT with an external photosensitizer gel based on e6 chloride in patients with severe acne after prior treatment with systemic retinoids. The positive dynamics of the morphofunctional parameters of the skin and the composition of the microbiome under the influence of PDT has been established. The exact exposure of the photosensitizer gel during external application to scar tissue, the time range of its highest concentration and the optimal duration of the procedure were determined. As a result of the application of PDT, the skin's relief was evened out, its oiliness decreased, pigmentation disappeared, and elasticity was restored. This method proved to be effective in correcting post-acne.

Таблица
Динамика интенсивности флуоресценции после местного использования геля фотосенсибилизатора на основе хлорина е6

Table
Dynamics fluorescence intensity after topical application of chlorin e6 photosensitizer gel

Экспозиция геля (мин) Gel exposure (min)	Интенсивность флуоресценции (усл.ед.) Fluorescence intensity (units)
5	0,199
10	0,659
15	0,754
20	0,707
25	0,539

Conclusion

PDT resulted in the correction of scarring, pigmentation resolution, a decrease in oiliness, and restoration of elasticity. Using PDT with a topical gel based on chlorin e6 resulted in the restoration of the microbiome composition of seborrheic areas. The population of opportunistic microorganisms that produce pathogenic enzymes (hemolytic *Staphylococcus spp.* and *Candida spp., Staphylococcus aureus,* and *Klebsiella spp.*) significantly decreased. However, an increase in *Staphylococcus epidermidis*, which adversely affects the development of acne, was observed.

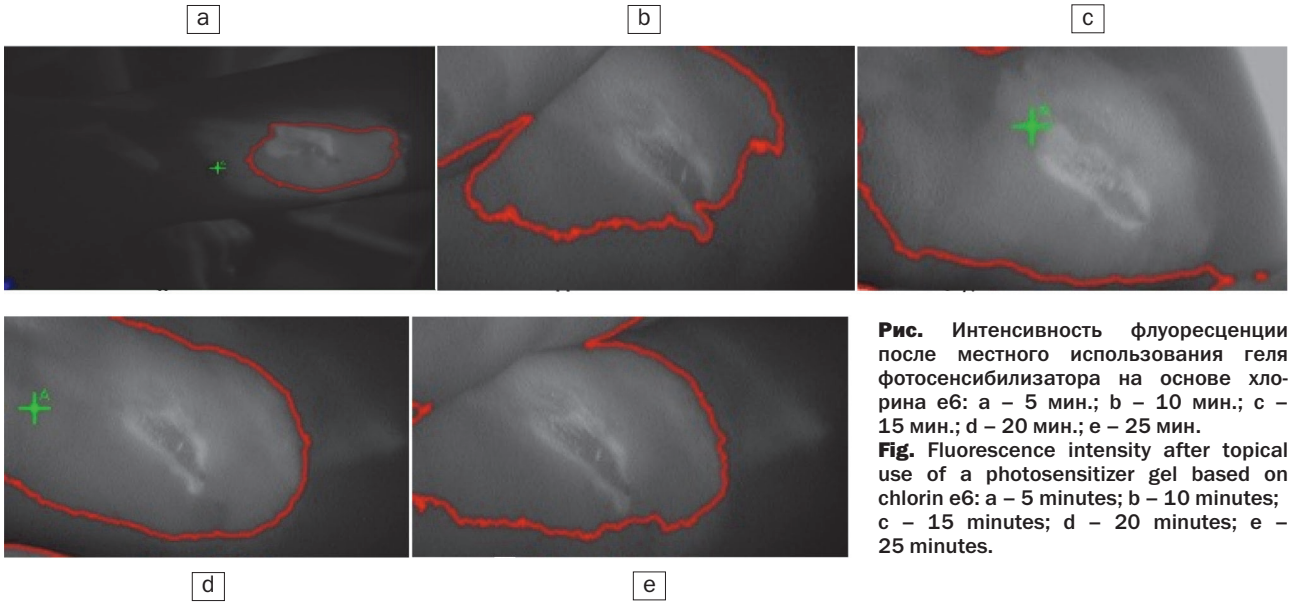

Рис. Интенсивность флуоресценции после местного использования геля фотосенсибилизатора на основе хлорина е6: a – 5 мин.; b – 10 мин.; c – 15 мин.; d – 20 мин.; e – 25 мин.
Fig. Fluorescence intensity after topical use of a photosensitizer gel based on chlorin e6: a – 5 minutes; b – 10 minutes; c – 15 minutes; d – 20 minutes; e – 25 minutes.

REFERENCES

1. Clinical guidelines. Acne vulgaris. Edited by the Russian Society of Dermatovenerologists and Cosmetologists – Moscow, 2020, pp. 4-33.
2. Acne and rosacea: Clinical manifestations, diagnosis, and treatment / L.S. Kruglova, A.G. Stenko, N.V. Gryazeva et al. - Moscow: GEOTAR-Media Publishing Group, Limited Liability Company, 2021, pp. 208. doi 10.33029|9704-6063-4acn-2021-1-208.
3. Kruglova L.S., Gryazeva, N.V., Sidorenko E.V., Use of isotretinoin in moderate to severe acne: current recommendations // Medical alphabet, 2021. doi 10.33667||2078-5631-2021-27-20-25.
4. Acneiform dermatoses and acne in the practice of a dermatovenerologist: a guide for physicians / R. A. Ravodin, K. I. Raznatovsky. - *Moscow: Geotarmedia*, 2022, pp. 192. doi: 10.33029/9704-6288-1-rav-2022-1-192.
5. Monakhov S.A. Acne: Clinic and Therapy. A Methodological Handbook for Physicians. – Moscow, 2013.
6. Kruglova L.S., Samushiya M.A., Talybova A.M. Mental Disorders, Social Maladjustment, and Quality of Life in Patients with Acne and Post-Acne Symptoms. *S.S. Korsakov Journal of Neurology and Psychiatry*, 2018, Vol. 118(12), pp. 4-10.
7. Drozhdina M.B., Bobro V.A., Sennikova Yu.A., Kornilova E.I. Postacne symptomcomplex. Approaches to Therapy. *Bulletin of Dermatology and Venereology*, 2022, Vol. 98 (2), pp. 28-41. doi: 10.25208/vdv1279.
8. Thiboutot D.M., Dréno B., Abanmi A. et al. Practical management of acne for clinicians: An international consensus from the Global Alliance to Improve Outcomes in Acne. *J. Am. Acad. Dermatol*, 2018, Vol. 78 (2, 1), pp. 1-23. doi: 10.1016/j.jaad.2017.09.078.
9. Muzychenko A.P. Acne, postacne: practical aspects. *Medical News*, 2023, Vol. 6, pp. 345.
10. Kruglova L.S., Gryazeva N.V. Therapy of postinflammatory hyperpigmentation post-acne. *Medical Council*, 2022, Vol. 13, pp. 11-16. doi: 10.21518/2079-701x-2022-16-13-11-16.
11. Fitz-Gibbon S., Tomida S., Chiu B.H., et al. Propionibacterium acnes strain populations in the human skin microbiome associated with acne. *J Invest Dermatol*, 2013, Vol. 133(9), pp. 2152-2160. doi: 10.1038/jid.2013.21.
12. Barnard E., Shi B., Kang D., Craft N., Li H. The balance of metagenomic elements shapes the skin microbiome in acne and health. *Sci Rep*, 2016, Vol. 6, pp. 39491. doi: 10.1038/srep39491.
13. Achermann Y., Goldstein E.J., Coenye T., Shirtliff M.E. Propionibacterium acnes: From commensal to opportunistic biofilm associated implant pathogen. *Clin Microbiol Rev*, 2014, Vol. 27(3), pp. 419 440. doi: 10.1128/cmr.00092-13.
14. Ferček I., Lugović-Mihić L., Tambić-Andrašević A. et al. Features of the Skin Microbiota in Common Inflammatory Skin Diseases. *Life (Basel)*, 2021, Vol. 11(9), pp. 962. doi: 10.3390/life11090962.
15. Gaitanis G., Magiatis P., Hantschke M., Bassukas I.D., Velegraki A. The Malassezia genus in skin and systemic diseases. *Clin Microbiol Rev*, 2012, Vol. 25(1), pp. 106-141. doi: 10.1128/cmr.00021-1.
16. Lee Y.B., Byun E.J., Kim H.S. Potential Role of the Microbiome in Acne: A Comprehensive Review. *J Clin Med*, 2019, Vol. 8(7), pp. 987. doi: 10.3390/jcm8070987.
17. Kelhälä HL, Aho VTE, Fyhrquist N et al. Isotretinoin and lymecycline treatments modify the skin microbiota in acne. *Exp Dermatol*, 2018, Vol. 27(1), pp. 30-36. doi: 10.1111/exd.13397.
18. McCoy WH 4th, Otchere E., Rosa B.A., Martin J., Mann C.M., Mitreva M. Skin Ecology during Sebaceous Drought-How Skin Microbes Respond to Isotretinoin. *J Invest Dermatol*, 2019, Vol. 139(3), pp. 732-735. doi: 10.1016/j.jid.2018.09.023.
19. Kruglova L.S., Gryazeva N.V., Tamrazova A.V. Composition of skin microbiota in children and its influence on acne pathogenesis. *Issues of modern pediatrics*, 2021, Vol. 20(5), pp. 430-434. doi: 10.15690/vsp.v.201i5.2319.

ЛИТЕРАТУРА

1. Клинические рекомендации. Акне вульгарные. Под редакцией российского общества дерматовенерологов и косметологов – Москва: 2020. – С. 4-33.
2. Акне и розацеа: Клинические проявления, диагностика и лечение / Л.С. Круглова, А.Г. Стенько, Н.В. Грязева [и др.]. – Москва: Общество с ограниченной ответственностью Издательская группа «ГЭОТАР-Медиа», – 2021. – С. 208. doi: 10.33029|9704-6063-4acn-2021-1-208.
3. Круглова Л.С., Грязева Н.В., Сидоренко Е.В. Применение изотретиноина при среднетяжелых и тяжелых формах акне: актуальные рекомендации // Медицинский алфавит. – 2021. doi: 10.33667||2078-5631-2021-27-20-25.
4. Акнеформные дерматозы и акне в практике врача-дерматовенеролога: руководство для врачей / Р.А. Раводин, К.И. Разнатовский. – Москва: ГЭОТАРМедиа, – 2022. – С. 192. doi: 10.33029/9704-6288-1-rav-2022-1-192.
5. Монахов С.А. Акне: клиника и терапия. Методическое пособие для врачей. – Москва – 2013.
6. Круглова Л.С., Самушия М.А., Талыбова А.М. Психические расстройства, социальная дезадаптация и качество жизни пациентов с акне и симптомами постакне // Журнал неврологии и психиатрии им. С.С. Корсакова. – 2018. – Т. 118. – С. 4-10. doi: 10.17116/jnevro20181181214.
7. Дрождина М.Б., Бобро В.А., Сенникова Ю.А., Корнилова Е.И. Симптомокомплекс постакне. Подходы к терапии // Вестник дерматологии и венерологии. – 2022. – Т. 98 (2). – С. 28-41. doi: 10.25208/vdv1279.
8. Thiboutot D.M., Dréno B., Abanmi A. et al. Practical management of acne for clinicians: An international consensus from the Global Alliance to Improve Outcomes in Acne // J. Am. Acad. Dermatol. – 2018. – Vol. 78 (2, 1). – P. 1-23. doi: 10.1016/j.jaad.2017.09.078.
9. Музыченко А.П. Акне, постакне: практические аспекты // Медицинские новости. – 2023. – Т. 6. – С. 345.
10. Круглова Л.С., Грязева Н.В. Вопросы терапии поствоспалительной гиперпигментации постакне // Медицинский совет. – 2022. – Т. 12. – С. 11-16. doi:10.21518/2079-701x-2022-16-13-11-16.
11. Fitz-Gibbon S, Tomida S, Chiu BH, et al. Propionibacterium acnes strain populations in the human skin microbiome associ ated with acne // J Invest Dermatol. – 2013. – Vol. 133(9). – P. 2152-2160. doi: 10.1038/jid.2013.21.
12. Barnard E., Shi B., Kang D., Craft N., Li H. The balance of metagenomic elements shapes the skin microbiome in acne and health // Sci Rep. – 2016. – Vol. 6. – P. 39491. doi: 10.1038/srep39491
13. Achermann Y., Goldstein E.J., Coenye T., Shirtliff M.E. Propionibacterium acnes: From commensal to opportunistic biofilm associated implant pathogen // Clin Microbiol Rev. – 2014. –Vol. 27(3). – P.419 - 440. doi: 10.1128/cmr.00092-13.
14. Ferček I., Lugović-Mihić L., Tambić-Andrašević A., et al. Features of the Skin Microbiota in Common Inflammatory Skin Diseases // Life (Basel). – 2021. – Vol. 11(9). – P. 962. doi: 10.3390/life11090962.
15. Gaitanis G., Magiatis P., Hantschke M., Bassukas I.D., Velegraki A. The Malassezia genus in skin and systemic diseases // Clin Microbiol Rev. – 2012. – Vol. 25(1). – P.106-141. doi: 10.1128/cmr.00021-1.
16. Lee Y.B., Byun E.J., Kim H.S. Potential Role of the Microbiome in Acne: A Comprehensive Review // J Clin Med. – 2019. – Vol. 8(7). – P. 987. doi: 10.3390/jcm8070987.
17. Kelhälä H.L., Aho V.T.E., Fyhrquist N., et al. Isotretinoin and lymecycline treatments modify the skin microbiota in acne // Exp Dermatol. – 2018. – Vol. 27(1). – P.30-36. doi: 10.1111/exd.13397.
18. McCoy WH 4th, Otchere E, Rosa BA, Martin J, Mann CM, Mitreva M. Skin Ecology during Sebaceous Drought-How Skin Microbes Respond to Isotretinoin // J Invest Dermatol. – 2019. – Vol. 139(3). – P. 732-735. doi: 10.1016/j.jid.2018.09.023.
19. Круглова Л.С., Грязева Н.В., Тамразова А.В. Состав микробиоты кожи у детей и его влияние на патогенез акне // Вопросы современной педиатрии. – 2021. – Том 20(5). – С. 430-434. doi: 10.15690/vsp.v.201i5.2319.

20. Agafonova S.G., Indilova N.I., Ivanova E.V. et al. Non-invasive diagnostic methods in dermatology and dermatocosmetology. *Experimental and clinical dermatocosmetology*, 2010, Vol. 4, pp. 41-5. doi: 10.18821/1560-9588-2018-21-1-51-53-60.
21. Barinova O.A., Galliamova Yu.A. Comparative study of morphofunctional and structural indices of facial skin in women of different age groups. *Experimental and clinical dermatocosmetology*, 2012, Vol. 4, pp. 3-7. udc 616.992.282: [616. 34 + 616.15].
22. Dubenskiy V.V., Alexandrova O.A., Nekrasova E.G. et al. The effectiveness of photodynamic therapy with an external photosensitizer gel based on chlorin e6 in the correction of post-acne scars. *Archiv EuroMedica*, 2023, Vol. 13, pp. 2. doi: 10.35630/2023/13/2.412.
23. Panova O.S., Dubensky V.V., Dubensky V.V. et al. Photodynamic reparative skin regeneration using an external photosensitizer gel based on chlorin E6/O.S. *Biomedical Photonics*, 2021, Vol. 10(3). pp. 5. doi: 10.24931/2413-9432-2021-10-3-4-11.
24. Aleksandrova O.A., Muravyova E.S., Afanasyeva T.A. et al. Use of photodynamic therapy, retinol peeling and type I collagen in the treatment of postacne. - Text: direct. *Tver medical journal*, 2023, Vol. 1, pp. 11-14. id 50156694.

20. Агафонова С.Г., Индилова Н.И., Иванова Е.В. [и др.]. Неинвазивные методы диагностики в дерматологии и дерматокосметологии // Экспериментальная и клиническая дерматокосметология. – 2010. – Том 4. – С. 41-45. doi: 10.18821/1560-9588-2018-21-1-51-53-60.
21. Баринова О.А., Галлямова Ю.А. Сравнительное исследование морфофункциональных и структурных показателей кожи лица женщин разных возрастных групп // Экспериментальная и клиническая дерматокосметология. – 2012. – Т. 4. – С.3-7.
22. Dubensky V.V., Alexandrova O.A., Nekrasova E.G. et al. The effectiveness of photodynamic therapy with an external photosensitizer gel based on chlorin e6 in the correction of post-acne scars // Archiv EuroMedica. – 2023. – Vol.13 (2). doi 10.35630/2023/13/2.412.
23. Панова О.С., Дубенский В.В., Дубенский В.В. [и др.]. Фотодинамическая репаративная регенерация кожи с применением наружного геля- фотосенсибилизатора на основе хлорина е6 // Biomedical Photonics. – 2021. – Том. 10 (3). – С. 5. doi: 10.24931/2413-9432-2021-10-3-4-11.
24. Александрова О. А., Муравьева Е.С., Афанасьева Т.А. [и др.]. Применение фотодинамической терапии, ретинолового пилинга и коллагеном первого типа в лечении постакне. - Текст: директ // Тверской медицинский журнал. – 2023. – Т. 1. – С.11-14. id 50156694.

COMBINED PHOTODYNAMIC THERAPY IN METASTATIC BREAST CANCER: POSSIBILITIES AND OUTCOMES (CLINICAL CASE)

Shanazarov N.A.[1], Kumisbekova R.K.[2], Albaev R.K.[1], Usenbay M.[3], Tashpulatov T.B.[1], Magzamova A.S.[4], Disaenko K.S.[5]

[1]Hospital of the President's Affairs Administration, Astana, Kazakhstan
[2]Multidisciplinary Medical Center, Akimat of Astana, Astana, Kazakhstan
[3]City Polyclinic No. 4, Akimat of Astana, Astana, Kazakhstan
[4]Multidisciplinary Regional Hospital, Health Department of Akmola Region, Astana, Kazakhstan
[5]Kostanay City Multidisciplinary Oncology Hospital, Kostanay, Kazakhstan

Abstract

The Center for Photodynamic Therapy of the Hospital of the Medical Center of the Administrative Department of the President of the Republic of Kazakhstan has clinical experience in treating cutaneous metastases of breast cancer. This paper presents the results of clinical observation of a patient with metastatic breast cancer who underwent combined photodynamic therapy, including systemic photomodification of blood and local irradiation of metastatic lesions. This clinical case is of particular interest since the patient did not receive standard antitumor treatments such as chemotherapy or hormone therapy. This was due to advanced age and decreased tolerance to aggressive treatment regimens associated with comorbidities, which limited the feasibility of conventional therapy. Despite the absence of systemic treatment, the use of combined photodynamic therapy resulted in a pronounced positive clinical response. A reduction in the size and infiltration of cutaneous metastatic lesions, as well as an improvement in the patient's general condition and quality of life, were observed. These findings demonstrate the potential of photodynamic therapy as an effective and safe alternative therapeutic approach for metastatic breast cancer, particularly in clinical situations where the use of standard treatment protocols is impossible or contraindicated.

Key words: photodynamic therapy, breast cancer, palliative care, quality of life.

Contacts: Kumisbekova R.K., e-mail: raushankumisbekova@gmail.com

For citation: Shanazarov N.A., Kumisbekova R.K., Albaev R.K., Usenbay M., Tashpulatov T.B., Magzamova A.S., Disaenko K.S. Combined photodynamic therapy for metastatic breast cancer: possibilities and results (clinical case), *Biomedical Photonics*, 2025, vol. 14, no. 4, pp. 49–55. doi: 10.24931/2413–9432–2025–14-4-49-55

КОМБИНИРОВАННАЯ ФОТОДИНАМИЧЕСКАЯ ТЕРАПИЯ ПРИ МЕТАСТАТИЧЕСКОМ РАКЕ МОЛОЧНОЙ ЖЕЛЕЗЫ: ВОЗМОЖНОСТИ И РЕЗУЛЬТАТЫ (КЛИНИЧЕСКОЕ НАБЛЮДЕНИЕ)

Н.А. Шаназаров[1], Р.К. Кумисбекова[2], Р.К. Албаев[1], М. Усенбай[3], Т.Б. Ташпулатов[1], А.С. Магзамова[4], К.С. Дисаенко[5]

[1]Больница Медицинского центра Управления делами Президента Республики Казахстан, Астана, Казахстан
[2]Многопрофильный медицинский центр акимата г. Астаны, Астана, Казахстан
[3]Городская поликлиника № 4 акимата г. Астана, Астана, Казахстан
[4]Многопрофильная областная больница при Управлении Здравоохранения Акмолинской области, Астана, Казахстан
[5]Костанайская Городская Онкологическая Многопрофильная больница, Костанай, Казахстан

Резюме

Центр фотодинамической терапии Больницы Медицинского центра Управления делами Президента Республики Казахстан имеет клинический опыт лечения кожных метастазов рака молочной железы. В настоящей работе представлены результаты наблюдения за пациенткой с метастатическим раком молочной железы, которой была проведена комбинированная фотодинамическая терапия, включающая системную фотомодификацию крови и локальное воздействие на очаги поражения. Клинический случай представляет особый интерес, поскольку пациентка не получала стандартных методов противоопухолевого лечения, таких как химио- и гормонотерапия. Это обусловлено пожилым возрастом и сниженной переносимостью агрессивных лечебных схем на фоне сопутствующих заболеваний, что ограничивает возможности проведения традиционной терапии. Несмотря на отсутствие системного лечения, применение комбинированной фотодинамической терапии позволило достичь выраженного положительного клинического эффекта. Отмечено уменьшение размеров и инфильтрации кожных метастатических очагов, улучшение общего состояния и качества жизни пациентки. Полученные результаты демонстрируют потенциал фотодинамической терапии как эффективного и безопасного альтернативного метода воздействия при метастатическом раке молочной железы, особенно в клинических ситуациях, когда проведение стандартных схем лечения невозможно или противопоказано.

Ключевые слова: фотодинамическая терапия, рак молочной железы, паллиативное лечение, качество жизни.

Контакты: Кумисбекова Р.К., e-mail: raushankumisbekova@gmail.com

Для цитирования: Шаназаров Н.А., Кумисбекова Р.К., Албаев Р.К., Усенбай М., Ташпулатов Т.Б., Магзамова А.С., Дисаенко К.С. Комбинированная фотодинамическая терапия при метастатическом раке молочной железы: возможности и результаты (клиническое наблюдение) // Biomedical Photonics. – 2025. – Т. 14, № 4. – С. 49–55. doi: 10.24931/2413–9432–2025–14-4-49-55

Introduction

Breast cancer (BC) remains one of the leading causes of morbidity and mortality among women, representing a serious medical and social problem worldwide [1,2]. Despite significant advances in early diagnosis and improved treatment methods, survival rates for common and metastatic forms of the disease remain unsatisfactory.

The modern concept of radical breast cancer treatment is based on the principles of multimodal therapy, including surgery, systemic drug treatment (neoadjuvant and adjuvant chemotherapy), as well as radiation therapy [3]. This comprehensive approach ensures local control of the tumor process and reduces the risk of recurrence. However, with the development of the metastatic form of the disease, systemic antitumor therapy is of primary importance, aimed at slowing the progression, controlling the metastatic process and maintaining a satisfactory quality of life in patients.

Currently, strategies for the systemic treatment of breast cancer include the use of chemotherapy, hormone therapy, targeted and immunotherapeutic drugs. The optimal choice of therapeutic tactics is determined by the molecular biological characteristics of the tumor, including the receptor status (ER, PR, HER2), the general somatic condition of the patient, the presence of concomitant diseases and previous treatment [3]. Individualization of systemic therapy makes it possible to increase its effectiveness, reduce the frequency of adverse events and thereby improve the quality of life of patients with a prolonged course of the metastatic process.

Despite the success of drug treatment, there remains a need to develop new methods aimed at increasing local control and reducing systemic toxicity of therapy. One of these areas is photodynamic therapy (PDT), an innovative method based on the use of a photosensitizer (PS) that selectively accumulates in tumor cells. Under the influence of laser radiation of a certain wavelength, activated PS initiates photochemical reactions that cause damage to tumor cells and blood vessels, which ensures the selective destruction of pathological tissues, including in the postoperative area [5].

We present the results of clinical observation of a patient who received multi-course combined photodynamic therapy (PDT) for metastatic BC.

Materials and methods

The 84-year-old patient has been under medical supervision since 2021 for right breast cancer. After the diagnosis, the patient refused to undergo standard antitumor therapy. In November 2023, the patient complained of an unproductive cough and shortness of breath during exercise. In order to clarify the nature of the process and conduct symptomatic treatment, the patient was admitted to the Hospital of the Medical Center of the Office of the President of the Republic of Kazakhstan.

Computed tomography (CT) of the chest organs revealed multiple nodules in the projection of the right breast, axillary lymph nodes and skin. According to ultrasound examination of the liver, a formation in the right lobe was determined, regarded as a hemangioma or possible metastases. Additionally, a moderate amount of fluid in the pericardial cavity and signs of exudative pleurisy were noted.

For diagnostic purposes, pleurocentesis was performed, in which 220 ml of light yellow exudate was evacuated. Cytological examination of the material revealed mesotheliocytes with marked proliferation and tumor cells with signs of atypia. GeneXpert testing excluded the presence of *Mycobacterium tuberculosis*.

On the background of symptomatic therapy (diuretics, bronchodilators, mucolytics, anticoagulants), repeated accumulation of fluid in the pleural cavity was observed. Repeated pleurocentesis was performed with evacuation of 1100 ml of serous effusion.

Upon examination, the patient's general condition was assessed as moderate, due to respiratory failure. The right mammary gland is almost completely replaced by a tumor infiltrate, and there are 13 × 10 cm ulcers on the skin of the chest on the right. A dense, rounded tumor of 6 × 7.5 × 8 cm in size with signs of skin infiltration was detected in the left mammary gland.

Based on a set of anamnestic, clinical and instrumental data, in 2021, the diagnosis was established: right breast cancer cT4NxM0 (2021). In 2023, the progression of the disease with the collapse of the right breast tumor was revealed. Metastases to the left mammary gland, lymph nodes of the axillary, supraclavicular and cervical regions on both sides, multiple metastases to the lungs, exudative pleurisy on the left were identified.

The patient had the following concomitant diseases: arterial hypertension of the III degree (very high risk of cardiovascular complications), chronic heart failure of the II–III functional class according to NYHA.

Based on the results of an interdisciplinary consultation with oncologists, a biopsy and an immunohistochemical study were recommended to select the optimal drug therapy regimen. The patient refused the proposed treatment.

As part of palliative care, combined PDT was performed at the Photodynamic Therapy Center of the Hospital of the Medical Center of the Office of the President of the Republic of Kazakhstan.

Photodynamic therapy was started in November 2023. The courses were conducted with an interval of 3 weeks.

To carry out PDT, a PS based on e6 chloride was used (photolon, JSC Belmedpreparaty, Republic of Belarus). PS was administered intravenously at a dose of 100 mg diluted in 200 ml of saline solution for 30 minutes. Blood photomodification was performed for 30 minutes (output power of the light fiber is 100 MW). 2.5 hours after intravenous blood photomodification, the affected chest area was irradiated with a "Latus-Fara" device (irradiation from two fields with an output power of 0.20 W for 20 minutes per field, total exposure time of 40 minutes, light dose 200-400 J/cm^2). The tolerability of the procedure was satisfactory.

Results

The patient underwent 28 PDT sessions. According to CT scans of the chest organs performed between January and December 2024 (once every 3 months), stabilization of the tumor process was noted. In a control study in May 2025, an increase in the total size of foci was recorded by more than 20% according to the RECIST 1.1 criteria, which is regarded as disease progression (Table).

Clinically, positive dynamics were noted, including a decrease in the severity of bronchitis syndrome, an improvement in general well-being and a preservation of appetite. At the same time, there was a moderate pain syndrome associated with the presence of a wound surface in the chest wall, as well as shortness of breath due to left-sided exudative pleurisy (Fig.1,2).

During the first year of follow–up (January-December 2024), CT data showed stabilization of the process without the appearance of new metastatic foci. Further progression in 2025 was accompanied by an increase in pleural effusion and the detection of new metastatic changes in the lungs (Fig. 3.4).

PDT demonstrated local efficacy in a patient with metastatic breast cancer, ensuring stabilization of the process for 12 months while maintaining a satisfactory quality of life (Fig. 5,6). Unlike chemo and radiation therapy, PDT did not cause systemic toxicity, as it is a method of selective action on tumor tissues. The introduction of PS into the bloodstream ensures its predominant accumulation in tumor cells, and subsequent laser irradiation activates the process of generation of reactive oxygen species, inducing apoptosis and necrosis of tumor cells and blood vessels [6].

The presented clinical case demonstrates the possibilities of PDT as an effective and clinically significant method of local control in a patient with metastatic breast cancer. Despite the disseminated nature of the disease, PDT made it possible to achieve stabilization of the process during the year, reduce local manifestations and pronounced clinical improvement with a good tolerance profile.

Discussion

In recent years, PDT has been considered as a promising direction in the complex treatment of malignant neoplasms, including breast cancer. The presented clinical case demonstrates the possibility of achieving stabilization of the disease in a patient with a metastatic process when using PDT in a palliative regime. Within a year after the start of treatment, it was possible to maintain the general condition, reduce the

Таблица
Оценка динамики опухолевого процесса по RECIST 1.1 по данным КТ органов грудной клетки
Table
Assessment of tumor dynamics according to RECIST 1.1 based on chest CT data

Дата обследования (КТ органов грудной клетки) Date of examination (Chest CT)	Таргетные очаги Targeted lesions	Нетаргетные очаги Non-targeted lesions	Общая оценка по RECIST Overall RECIST score	Комментарии Comments
18.01.24	Образования в молочных железах, аксиллярные лимфоузлы, множественные очаги в легких Formations in the mammary glands, axillary lymph nodes, multiple foci in the lungs	Плевральные выпоты, лимфогенный канцероматоз Pleural effusions, lymphogenous carcinomatosis	Базовое исследование Basic Study	Установлены исходные очаги для последующей оценки динамики Initial lesions were identified for subsequent progression assessment
30.07.24	Уменьшение опухоли в молочных железах и лимфоузлах Reduction of tumors in the mammary glands and lymph nodes	Прогрессия в легких (увеличение узлов, матовость, канцероматоз), плеврального выпота Progression in the lungs (enlarged nodes, haziness, carcinomatosis), pleural effusion	Относительная стабилизация Relative Stabilization	Частичный ответ по таргетным очагам, но прогрессия по нетаргетным Partial response in targeted lesions, but progression in non-targeted lesions
04.12.24	Без существенной динамики в молочных железах и лимфоузлах No significant changes in the mammary glands and lymph nodes	Стабилизация в легких, без нарастания выпота Stabilization in the lungs, without increasing effusion	Стабилизация Stabilization	Стабилизация Stabilization
27.05.25	Увеличение очагов в правом лёгком молочных железах,появление нового очага в S6 Enlargement of lesions in the right lung and mammary glands, appearance of a new lesion in S6	Нарастание плеврального выпота слева до ~600 мл, стабильность остальных Increase of pleural effusion on the left to ~600 ml, stability of the rest	Прогрессирование Progression	Прогрессия подтверждённых очагов>20%, нарастание плеврального выпота Progression of confirmed lesions >20%, increase in pleural effusion

Примечание: С января по декабрь 2024 года у пациентки наблюдалась стабилизация процесса по данным КТ, без признаков роста или новых метастатических очагов
Note: From January to December 2024, the patient demonstrated disease stabilization according to CT data, with no signs of tumor growth or new metastatic lesions.

severity of symptoms and local control of the tumor process, which is confirmed by CT data and clinical improvement.

Unlike traditional methods of treatment – chemotherapy and radiation therapy – PDT is characterized by minimal systemic toxicity and a gentle effect on healthy tissues, which is especially important for elderly and comorbid patients.

The results of domestic and foreign studies confirm the high effectiveness of PDT in local and recurrent forms of breast cancer. The frequency of complete response in chest wall lesions reaches 60-73%, the overall response is up to 90%, while side effects are limited to mild photosensitivity, pain syndrome, and skin hyperemia [7,8]. These data are consistent with the presented clinical observation, which recorded a long-term stabilization of the tumor process without significant complications.

Of particular interest is the additional mechanism of action of PDT – activation of the antitumor immune response. Under the influence of a photochemical reaction, tumor antigens are released and antigen-presenting cells are activated, which contributes to the development of a secondary immune response

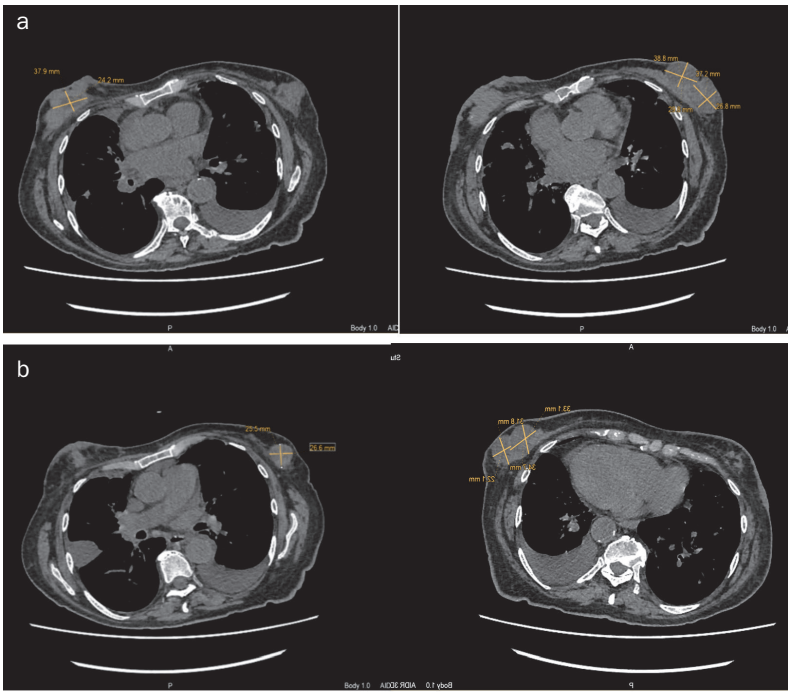

Рис. 1. Результаты КТ органов грудной клетки без контраста от 18.01.24:
а – опухолевое образование в правой молочной железе 3,7х2,4х4,4 см, в структуре левой молочной железы множественные кистозные образования (n~7), размеры наиболее крупного до 3,8х2,9х3,0 см;
b – в плевральной полости слева и вдоль междолевой щели справа визуализируется выпот, с компрессионным субателектазом, толщиной до 3,0 см.
Fig. 1. Results of a chest CT scan without contrast, 18.01.24:
a – a tumor in the right breast measuring 3.7 x 2.4 x 4.4 cm; multiple cystic lesions (n~7) in the left breast, the largest measuring up to 3.8 x 2.9 x 3.0 cm;
b – effusion with compression subatelectasis up to 3.0 cm thick is visible in the pleural cavity on the left and along the interlobar fissure on the right.

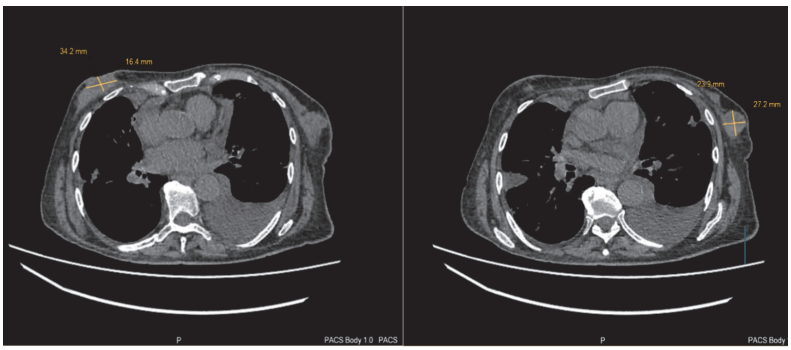

Рис. 2. Результаты КТ органов грудной клетки без контраста от 30.07.24 (уменьшение размеров образований в структуре молочных желез, наиболее крупные уменьшены справа до 3,4х1,6х2,6см (3,7х2,4х4,4 см), слева до 2,7х2,3х3,0см (3,8х2,9х3,0см); уменьшение аксиллярных лимфоузлов; прогрессирование в легких: увеличение количества и размеров узлов, увеличение плеврального выпота слева).
Fig. 2. Results of CT scan of chest organs without contrast from 30.07.24 (decrease in size of formations in the structure of mammary glands, the largest ones have decreased on the right to 3.4x1.6x2.6 cm (3.7x2.4x4.4 cm), on the left to 2.7x2.3x3.0 cm (3.8x2.9x3.0 cm); decrease in axillary lymph nodes; progression in the lungs: increase in the number and size of nodes, increase in pleural effusion on the left).

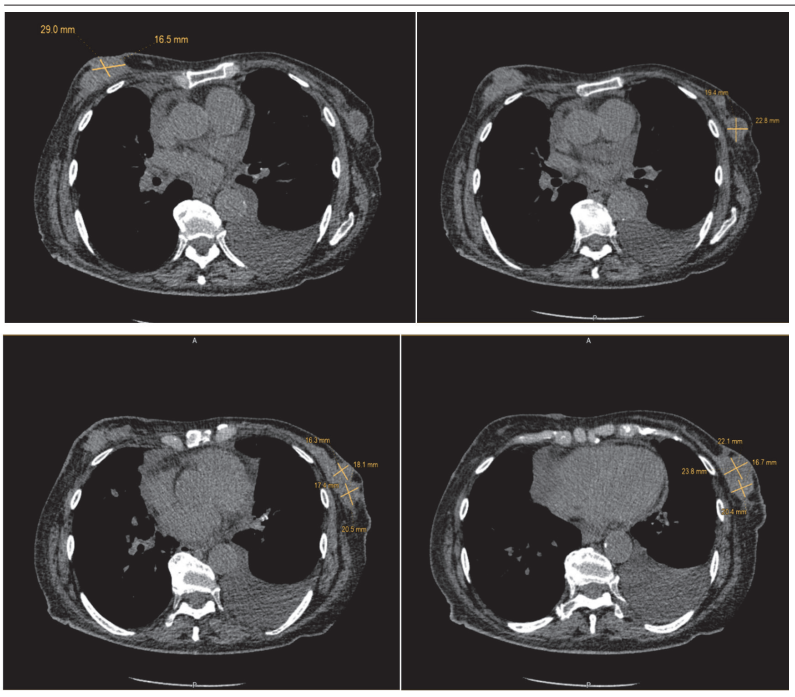

Рис. 3. Результаты КТ органов грудной клетки без контраста 04.12.24 (таргетные очаги (молочные железы, лимфоузлы) – без существенной динамики, некоторые очаги в легких – уменьшение/исчезновение мутности, выпот – без изменений).
Fig. 3. Results of CT scan of the chest organs without contrast 12/04/24 (target lesions (mammary glands, lymph nodes) – no significant dynamics, some lesions in the lungs – decrease/disappearance of haze, effusion – unchanged).

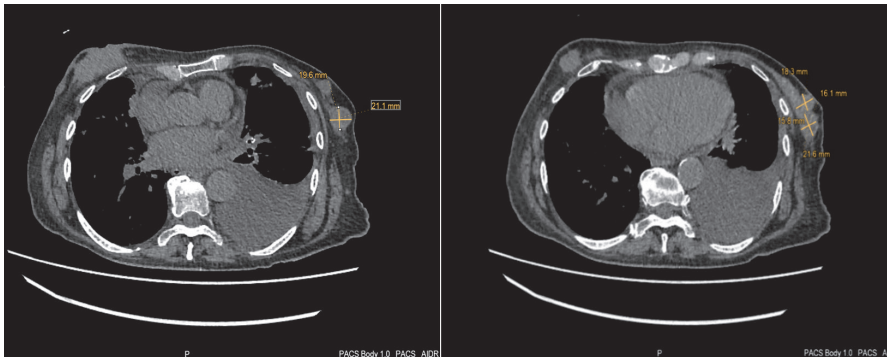

Рис. 4. Результаты КТ органов грудной клетки без контраста от 27.05.25 (несмотря на небольшие изменения по отдельным очагам, общее увеличение подтвержденных метастатических очагов превышает 20% — признак прогрессирования).
Fig. 4. Results of CT scan of the chest organs without contrast from 27.05.25 (despite minor changes in individual lesions, the overall increase in confirmed metastatic lesions exceeds 20% – a sign of progression).

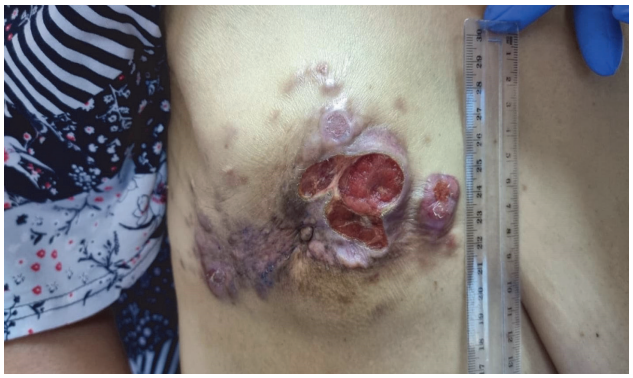

Рис. 5. Опухоль до начала ФДТ: правая молочная железа практически полностью отсутствует за счёт опухолевой инфильтрации, на коже грудной клетки справа изъявления на площади 13x10 см, в левой молочной железе опухолевое образование округлой формы размером 6x75x8 см плотной консистенции с инфильтрацией кожи.
Fig. 5. Tumor before PDT: the right mammary gland is almost completely absent due to tumor infiltration, on the skin of the chest on the right there are lesions on an area of 13x10 cm, in the left mammary gland there is a round tumor formation measuring 6x75x8 cm of dense consistency with skin infiltration.

Рис. 6. Состояние после ФДТ: в верхнебоковом квадранте грудной клетки (правая сторона) визуализируется участок деформированной кожи с выраженными признаками инфильтрации, кожа втянута, с рубцовыми изменениями, пигментными пятнами и следами после сеансов ФДТ.
Fig. 6. Condition after PDT: in the upper lateral quadrant of the chest (right side) an area of deformed skin with pronounced signs of infiltration is visualized, the skin is retracted, with cicatricial changes, pigment spots and traces after PDT sessions.

and reduces the likelihood of local relapses [9-11]. This feature opens up prospects for the combined use of PDT with immunotherapy and targeted agents, which is actively being investigated in modern oncology.

The socio-clinical aspect of the use of PDT should also be noted. For some patients, especially the elderly, the rejection of standard protocols is associated not only with medical contraindications, but also with subjective factors such as fear of side effects, decreased motivation, or previous negative treatment experiences. In such cases, PDT can be considered as a method of choice that provides a balance between the effectiveness and tolerability of therapy. This approach is consistent with the principles of personalized and value-based cancer care, where the therapeutic strategy is adapted to the individual characteristics of the patient.

Thus, the clinical example presented in this study confirms the potential of PDT as an effective and safe method of local exposure in metastatic breast cancer. The use of PDT made it possible to achieve clinical and radiological control while maintaining a high quality of life for the patient, which underlines the importance of the method in palliative practice and the need for further study.

Conclusion

This clinical observation demonstrates that PDT can be considered as an effective and minimally invasive alternative or supplement to standard treatments for metastatic breast cancer. The use of PDT made it possible to achieve lasting stabilization of the disease, clinical improvement and good tolerability of therapy without the development of systemic side effects.

PDT has a number of advantages – selectivity of exposure, the possibility of repeated use, minimal toxicity and the potential for immunostimulating action. These characteristics make the method especially valuable in the treatment of patients with disabilities for standard treatment regimens.

REFERENCES

1. International Agency for Research on Cancer. Absolute numbers, incidence, females, in 2022 [Electronic resource]. Available from: https://gco.iarc.who.int/today/en/dataviz/pie?mode=cancer&group_populations=1&sexes=2.
2. Shanazarov N., Zhapparov Y., Kumisbekova R., Turzhanova D., Zulkhash N. Association of gene polymorphisms with breast cancer risk in the Kazakh population. *Asian Pac. J. Cancer Prev*, 2023, vol. 24, pp. 4195-4207. doi: 10.31557/APJCP.2023.24.12.4195.
3. Tyulyandin S.A., Artamonova E.V., Zhigulev A.N., et al. Breast cancer. Practical recommendations of RUSSCO, part 1.2. *Malig. Tumors*, 2024, vol. 14 (3s2), pp. 32-81. doi: 10. 18027/2224-5057-2024-14-3s2-1.2-01.
4. Zhukova L.G., Andreeva Y.Y., Zavalishina L.E., Zakiriyakhodjaev A.D., Koroleva I.A., Nazarenko A.V., et al. Breast cancer: Clinical guidelines. *Mod. Oncol*, 2021, vol. 23 (1), pp. 5-40. doi: 10.26442/18151434.2021.1.200823.
5. Gelfond M.L., Rogachev M.V. Photodynamic therapy: fundamental and practical aspects. A textbook for students of higher and additional professional education. *St. Petersburg: N.N. Petrov National Medical Research Center of Oncology. Ministry of Health of the Russian Federation*, 2018, pp. 148.
6. Correia J.H., Rodrigues J.A., Pimenta S., Dong T., Yang Z. Photodynamic therapy review: principles, photosensitizers, applications, and future directions. *Pharmaceutics*, 2021, vol. 13 (9), pp. article 1332. doi: 10.3390/pharmaceutics13091332.
7. Banerjee S.M., El-Sheikh S., Malhotra A., Mosse C.A., Parker S., Williams N.R., et al. Photodynamic therapy in primary breast cancer. *J. Clin. Med*, 2020, vol. 9 (2), pp. 483. doi: 10.3390/jcm9020483.
8. Goranskaya E.V., Ragulin Yu.A., Kapinus V.N., et al. Immediate results of photodynamic therapy for intradermal metastases of breast cancer. *Oncosurgery*, 2011, vol. 3 (2), pp. 21-22.
9. Moret F., Reddi E. Strategies for optimizing the delivery to tumors of macrocyclic photosensitizers used in photodynamic therapy (PDT). *J. Porphyr. Phthalocyanines*, 2017, vol. 21, pp. 239-256.
10. Anokhin A.A., et al. Tumor-specific immune response after photodynamic therapy. *Med. J*, 2016, vol. 18 (5), pp. 405-416. doi: 10.15789/1563-0625-2016-5-405-416.
11. Filonenko E.V., Serova L.G. Photodynamic therapy in clinical practice. *Biomedical Photonics*, 2016, vol. 5 (2), pp. 26-37.
12. Rakhimzhanova R.I., Shanazarov N.A., Turzhanova D.E. Photodynamic therapy of intradermal metastases of breast cancer (literature review). *Biomedical Photonics*, 2019, vol. 8 (3), pp. 36-42. doi: 10.24931/2413-9432-2019-8-3-36-42.
13. Shanazarov N., Zinchenko S., Zhapparov E., et al. The clinical case of successful application of photodynamic therapy in the treatment of skin metastases of breast cancer. *BioNanoSci.*, 2021, vol. 11, pp. 957-961. doi: 10.1007/s12668-021-00907-5.
14. Li T., Yan L. Functional polymer nanocarriers for photodynamic therapy. *Pharmaceutics* (*Basel),* 2018, vol. 11 (4), pp. 133

ЛИТЕРАТУРА

1. Absolute numbers, Incidence, Females, in 2022 [Электронный ресурс] // International Agency for Research on Cancer – URL: https://gco.iarc.who.int/today/en/dataviz/pie?mode=cancer&group_populations=1&sexes=2
2. Shanazarov N., Zhapparov Y., Kumisbekova R., Turzhanova D., Zulkhash N. Association of Gene Polymorphisms with Breast Cancer Risk in the Kazakh Population // Asian Pac. J. Cancer Prev. – 2023. – Vol. 24. – P. 4195-4207. doi: 10.31557/APJCP.2023.24.12.4195.
3. Тюляндин С.А., Артамонова Е.В., Жигулев А.Н. и соавт. Рак молочной железы. Практические рекомендации RUSSCO, часть 1.2 // Злокачественные опухоли. – 2024. – Т. 14, № 3s2. – С. 32-81. doi: 10.18027/2224–5057-2024-14-3s2-1.2–01.
4. Жукова Л.Г., Андреева Ю.Ю., Завалишина Л.Э., и др. Рак молочной железы: клинические рекомендации // Современная онкология. – 2021. – Т. 23, № 1. – С. 5-40. doi: 10.26442/18151434.2021.1.200823.
5. Гельфонд М.Л., Рогачёв М.В. Фотодинамическая терапия: фундаментальные и практические аспекты: учебное пособие для обучающихся в системе высшего и дополнительного проф. образования. – Санкт-Петербург: НМИЦ онкологии им. Н.Н. Петрова Минздрава РФ. – 2018. – С. 148.
6. Correia J.H., Rodrigues J.A., Pimenta S., Dong T., Yang Z. Photodynamic Therapy Review: Principles, Photosensitizers, Applications, and Future Directions // Pharmaceutics. – 2021. – Vol. 13(9). – Article 1332. doi: 10.3390/pharmaceutics13091332.
7. Banerjee S.M., El-Sheikh S., Malhotra A., Mosse C.A., Parker S., Williams N.R., MacRobert A.J., Hamoudi R., Bown S.G., Keshtgar M.R. Photodynamic Therapy in Primary Breast Cancer // J. Clin. Med. – 2020. – Vol. 9(2). – P. 483. doi: 10.3390/jcm9020483.
8. Горанская Е.В., Рагулин Ю. А., Капинус В. Н. и др. Непосредственные результаты фотодинамической терапии внутрикожных метастазов рака молочной железы // Онкохирургия. – 2011. – Т. 3, № 2. – С. 21-22.
9. Moret F., Reddi E. Strategies for optimizing the delivery to tumors of macrocyclic photosensitizers used in photodynamic therapy (PDT) // J. Porphyr. Phthalocyanines. – 2017. – Vol. 21. – P. 239-256.
10. Анохин А.А. и др. Опухолеспецифический иммунный ответ после фотодинамической терапии // Медицинский журнал. – 2016. – Т. 18, № 5. – С. 405-416. doi: 10.15789/1563–0625-2016-5-405-416.
11. Филоненко Е. В., Серова Л. Г. Фотодинамическая терапия в клинической практике // Biomedical Photonics. – 2016. – Т. 5, № 2. – С. 26-37.
12. Рахимжанова Р.И., Шаназаров Н.А., Туржанова ДЕ. Фотодинамическая терапия внутрикожных метастазов рака молочной железы (обзор литературы) // Biomedical Photonics. – 2019. – Т. 8, № 3. – С. 36-42. doi: 10.24931/2413–9432-2019-8-3-36–42.
13. Shanazarov N., Zinchenko S., Zhapparov E., et al. The Clinical Case of Successful Application of Photodynamic Therapy in the Skin Metastases Treatment of Breast Cancer // BioNanoSci. – 2021. – Vol. 11. – P. 957-961. doi: 10.1007/s12668-021-00907-5.
14. Li T., Yan L. Functional Polymer Nanocarriers for Photodynamic Therapy // Pharmaceuticals (Basel). – 2018. – Vol. 11(4). – P. 133.

ФОТОСЕНСИБИЛИЗАТОРЫ НОВОГО ПОКОЛЕНИЯ ДЛЯ ФОТОДИНАМИЧЕСКОЙ ТЕРАПИИ

«ФОТОДИТАЗИН®» концентрат для приготовления раствора для инфузий — лекарственное средство (РУ № ЛС 001246 от 18.05.2012 г.)
«ФОТОДИТАЗИН®» гель — изделие медицинского назначения (РУ № ФСР 2012/13043 от 03.02.2012 г.)
«ФОТОДИТАГЕЛЬ®» — косметическое средство (ДС ЕАЭС № RU Д-RU.HB42.B.06108/20 от 24.09.2020 г.)

Препараты применяются для флюоресцентной диагностики и фотодинамической терапии злокачественных новообразований, а также патологий неонкологического характера в следующих областях медицины:

- гинекология
- урология
- нейрохирургия
- торакальная хирургия
- офтальмология
- травматология
- ортопедия
- комбустиология
- гнойная хирургия
- дерматология
- косметология
- стоматология

www.fotoditazin.com
www.фотодитазин.рф

@FOTODITAZIN

@FOTODITAGEL_FDT

ООО «ВЕТА-ГРАНД»
123056, г. Москва, ул. Красина, д. 27, стр. 2
Тел.: +7 (499) 250-40-00, +7 (929) 971-44-46
E-mail: veta-grand@mail.ru